



HAL
open science

Scale dependence of species–area relationships is widespread but generally weak in Palaeartic grasslands

Jinghui Zhang, François Gillet, Sándor Bartha, Juha Mikael Alatalo, Idoia Biurrun, Iwona Dembicz, John-arvid Grytnes, Renaud Jaunatre, Remigiusz Pielech, Koenraad van Meerbeek, et al.

► To cite this version:

Jinghui Zhang, François Gillet, Sándor Bartha, Juha Mikael Alatalo, Idoia Biurrun, et al.. Scale dependence of species–area relationships is widespread but generally weak in Palaeartic grasslands. *Journal of Vegetation Science*, 2021, 32 (3), pp.e13044. 10.1111/jvs.13044. hal-03286001

HAL Id: hal-03286001

<https://univ-fcomte.hal.science/hal-03286001v1>

Submitted on 25 Jun 2024

HAL is a multi-disciplinary open access archive for the deposit and dissemination of scientific research documents, whether they are published or not. The documents may come from teaching and research institutions in France or abroad, or from public or private research centers.

L'archive ouverte pluridisciplinaire **HAL**, est destinée au dépôt et à la diffusion de documents scientifiques de niveau recherche, publiés ou non, émanant des établissements d'enseignement et de recherche français ou étrangers, des laboratoires publics ou privés.

1 Research Article for Special Feature on Macroecology of Vegetation

2 **Scale dependence of species-area relationships is widespread but** 3 **generally weak in Palaeartic grasslands**

4 **Running title:** Scale-dependence of z-values

5 Jinghui Zhang^{1,2,3*}, François Gillet⁴, Sándor Bartha⁵, Juha Mikael Alatalo⁶, Idoia Biurrun⁷, Iwona
6 Dembicz^{8,9,2}, John-Arvid Grytnes¹⁰, Renaud Jaunatre¹¹, Remigiusz Pielech^{12,13}, Koenraad Van
7 Meerbeek¹⁴, Denys Vynokurov¹⁵, Stefan Widmer², Alla Aleksanyan^{16,17}, Kuber Prasad Bhatta¹⁰,
8 Juan Antonio Campos⁷, Patryk Czortek¹⁸, Jiri Dolezal¹⁹, Franz Essl²⁰, Itziar García-Mijangos⁷,
9 Riccardo Guarino²¹, Behlül Güler²², Michal Hájek²³, Anna Kuzemko¹⁵, Frank Yonghong Li^{1,3},
10 Swantje Löbel²⁴, Halime Moradi²⁵, Alireza Naqinezhad²⁶, Vasco Silva²⁷, Eva Šmerdová²², Judit
11 Sonkoly²⁸, Simon Stifter²⁹, Amir Talebi³⁰, Péter Török³¹, Hannah White^{32,33}, Jianshuang Wu³⁴ &
12 Jürgen Dengler^{2,9,35}

13 **Authors' affiliations**

14 ¹School of Ecology and Environment, Inner Mongolia University, Hohhot, China

15 ²Vegetation Ecology Group, Institute of Natural Resource Sciences (IUNR), Zurich University of
16 Applied Sciences (ZHAW), Wädenswil, Switzerland

17 ³Key Laboratory of Ecology and Resource Use of the Mongolian Plateau, Ministry of Education
18 of China, Hohhot, China

19 ⁴UMR Chrono-environnement, Université Bourgogne Franche-Comté, Besançon, France

20 ⁵Institute of Ecology and Botany, Centre for Ecological Research, Vácrátót, Hungary

21 ⁶Environmental Science Center, Qatar University, Doha, Qatar

22 ⁷Plant Biology and Ecology, Faculty of Science and Technology, University of the Basque
23 Country UPV/EHU, Bilbao, Spain

24 ⁸Department of Plant Ecology and Environmental Conservation, Institute of Botany, University
25 of Warsaw, Warsaw, Poland

26 ⁹Plant Ecology, Bayreuth Center of Ecology and Environmental Research (BayCEER), University
27 of Bayreuth, Bayreuth, Germany

28 ¹⁰Department of Biological Sciences, University of Bergen, Bergen, Norway

- 1
2
3
4 29 ¹¹Mountain Ecosystems and Societies Lab (LESSEM), University Grenoble Alpes, INRAE, LESSEM,
5
6 30 St-Martin-d'Hères, France
7
8 31 ¹²Department of Forest Biodiversity, Faculty of Forestry, University of Agriculture in Kraków,
9
10 32 Kraków, Poland
11
12 33 ¹³Foundation for Biodiversity Research, Wrocław, Poland
13
14 34 ¹⁴Department of Earth and Environmental Sciences, KU Leuven, Leuven, Belgium
15
16 35 ¹⁵Geobotany and Ecology Department, M.G. Kholodny Institute of Botany NAS of Ukraine, Kyiv,
17
18 36 Ukraine
19
20 37 ¹⁶Chair of Biology and Biotechnology, Armenian National Agrarian University, Yerevan, Armenia
21
22 38 ¹⁷Department of Geobotany and Plant Eco-Physiology, Institute of Botany after A.L. Takhtajyan
23
24 39 of NAS RA, Yerevan, Armenia
25
26 40 ¹⁸Faculty of Biology, Białowieża Geobotanical Station, University of Warsaw, Białowieża, Poland
27
28 41 ¹⁹Institute of Botany, Czech Academy of Sciences, Pruhonice, Czech Republic
29
30 42 ²⁰BioInvasions, Global Change, Macroecology Group, Department of Botany and Biodiversity
31
32 43 Research, University Vienna, Vienna, Austria
33
34 44 ²¹Department STEBICEF - Botanical Unit, University of Palermo, Palermo, Italy
35
36 45 ²²Biology Education, Dokuz Eylul University, Buca, İzmir, Turkey
37
38 46 ²³Department of Botany and Zoology, Faculty of Science, Masaryk University, Brno, Czech
39
40 47 Republic
41
42 48 ²⁴Landscape Ecology and Environmental Systems Analysis, Institute of Geoecology, Technical
43
44 49 University of Braunschweig, Braunschweig, Germany
45
46 50 ²⁵Department of Plant Science, School of Biology, College of Science, University of Tehran,
47
48 51 Tehran, Iran
49
50 52 ²⁶Department of Plant Biology, Faculty of Basic Sciences, University of Mazandaran, Babolsar,
51
52 53 Iran
53
54 54 ²⁷Centre for Applied Ecology Prof. Baeta Neves, School of Agriculture, University of Lisbon,
55
56 55 Lisbon, Portugal
57
58 56 ²⁸Department of Ecology, University of Debrecen, Debrecen, Hungary
59
60 57 ²⁹Institute for Alpine Environment, Eurac Research, Bolzano, Italy
61
62 58 ³⁰School of Biology and Center of Excellence in Phylogeny of Living Organisms, College of
63
64 59 Science, University of Tehran, Tehran, Iran
65
66 60 ³¹MTA-DE Lendület Functional and Restoration Ecology Research Group, Debrecen, Hungary

61 ³²School of Biology and Environmental Science, Earth Institute, University College Dublin,
62 Dublin, Ireland

63 ³³Zoology, School of Natural Sciences, Trinity College Dublin, Dublin, Ireland

64 ³⁴Institute of Environment and Sustainable Development in Agriculture, Chinese Academy of
65 Agricultural Sciences, Beijing, China

66 ³⁵German Centre for Integrative Biodiversity Research (iDiv) Halle-Jena-Leipzig, Leipzig, Germany

67 **Authors' ORCIDs**

68 Jinghui Zhang: 0000-0002-6217-7376

69 François Gillet: 0000-0002-3334-1069

70 Sándor Bartha: 0000-0001-6331-7521

71 Juha Mikael Alatalo: 0000-0001-5084-850X

72 Idoia Biurrun: 0000-0002-1454-0433

73 Iwona Dembicz: 0000-0002-6162-1519

74 John-Arvid Grytnes: 0000-0002-6365-9676

75 Renaud Jaunatre: 0000-0001-6970-8304

76 Remigiusz Pielech: 0000-0001-8879-3305

77 Koenraad Van Meerbeek: 0000-0002-9260-3815

78 Denys Vynokurov: 0000-0001-7003-6680

79 Stefan Widmer: 0000-0002-4920-5205

80 Alla Aleksanyan: 0000-0003-4073-1812

81 Kuber Prasad Bhatta: 0000-0001-7837-1395

82 Juan Antonio Campos: 0000-0001-5992-2753

83 Patryk Czortek: 0000-0002-4909-8032

84 Jiri Dolezal: 0000-0002-5829-4051

85 Franz Essl: 0000-0001-8253-2112

86 Itziar García-Mijangos: 0000-0002-6642-7782

87 Riccardo Guarino: 0000-0003-0106-9416

88 Behlül Güler: 0000-0003-2638-4340

89 Michal Hájek: 0000-0002-5201-2682

90 Anna Kuzemko: 0000-0002-9425-2756

91 Frank Yonghong Li: 0000-0002-5137-8017

1
2
3
4 92 Swantje Löbel: 0000-0001-9975-263X
5
6 93 Halime Moradi: 0000-0002-3738-9377
7
8 94 Alireza Naqinezhad: 0000-0002-4602-6279
9
10 95 Vasco Silva: 0000-0003-2729-1824
11
12 96 Judit Sonkoly: 0000-0002-4301-5240
13
14 97 Simon Stifter: 0000-0001-5957-9473
15
16 98 Amir Talebi: 0000-0002-5065-1368
17
18 99 Péter Török: 0000-0002-4428-3327
19
20 100 Hannah White: 0000-0002-6793-8613
21
22 101 Jianshuang Wu: 0000-0002-6768-8255
23
24 102 Jürgen Dengler: 0000-0003-3221-660X

103 **Corresponding author**

104 * Corresponding author: 1. School of Ecology and Environment, Inner Mongolia University,
105 Hohhot 010021, China; E-mail: jhzhang1001@126.com; 2. Vegetation Ecology Group, Institute
106 of Natural Resource Sciences (IUNR), Zurich University of Applied Sciences (ZHAW), Grüentalstr.
107 14, Postfach, 8820 Wädenswil, Switzerland.

108 **Funding information**

109 J.Z. was supported by the National Natural Science Foundation of China (grant no. 31960243)
110 and the China Scholarship Council (grant No. JZ. 201908155031). I.B., J.A.C. and I.G.M. were
111 funded by the Basque Government (IT936-16).

Abstract

Questions: Species-area relationships (SARs) are fundamental for understanding biodiversity patterns and are generally well described by a power law with a constant exponent z . However, z -values sometimes vary across spatial scales. We asked whether there is a general scale dependence of z -values at fine spatial grains and which potential drivers influence it.

Location: Palaeartic biogeographic realm.

Methods: We used 6,696 nested-plot series of vascular plants, bryophytes and lichens from the GrassPlot database with two or more grain sizes, ranging from 0.0001 to 1,024 m² and covering diverse open habitats. The plots were recorded with two widespread sampling approaches (rooted presence = species “rooting” inside the plot; shoot presence = species with aerial parts inside). Using GAMs, we tested for scale dependence of z -values by evaluating if the z -values differ with grain size and tested for differences between the sampling approaches. The response shapes of z -values to grain were classified by fitting quadratic GLMs with logit link to each series. We tested whether the grain size where the maximum z -value occurred is driven by taxonomic group, biogeographic or ecological variables.

Results: For rooted presence, we found a strong monotonous increase of z -values with grain sizes for all grain sizes below 1 m². For shoot presence, the scale dependence was much weaker, with hump-shaped curves prevailing. Among the environmental variables studied, latitude, vegetation type, naturalness and land use had strong effects, with z -values of secondary peaking at smaller grain sizes.

Conclusions: The overall weak scale dependence of z -values underlines that the power function generally is appropriate to describe SARs within the studied grain sizes in continuous open vegetation, if recorded with the shoot presence method. When clear peaks of z -values occur, this can be seen as an expression of granularity of species composition, partly driven by abiotic environment.

Keywords: beta diversity, grassland, GrassPlot, heterogeneity, Palaeartic, power law, rooted presence, scale dependence, shoot presence, species-area relationship, z -value, vegetation.

140 Introduction

141 Identifying spatio-temporal patterns in biodiversity is a major challenge in macroecology
142 and biogeography (McGill, 2019; O'Sullivan *et al.*, 2019). The spatial scale is of critical
143 importance in studies of components, patterns, and processes of biodiversity (Chase *et al.*,
144 2018; Schrader *et al.*, 2019). For example, environmental filtering of species, disturbances and
145 biotic interactions drive species richness at fine local scale, while at broader spatial scales the
146 main drivers are speciation, colonization, and extinction dynamics (Shmida and Wilson, 1985;
147 Crawley and Harral, 2001; Drakare *et al.*, 2006). Therefore, when examining the drivers and
148 mechanisms of spatial biodiversity patterns, the scale-sensitivity of these patterns is of
149 paramount importance.

150 Species-area relationships (SARs), which reflect changes in species richness with increasing
151 grain size (Lawton, 1999; Dengler, 2009), are fundamental in comparing diversity patterns
152 across space (Drakare *et al.*, 2006). SARs are among the most widely documented ecological
153 patterns and have long been regarded as a “genuine law” in ecology (MacArthur and Wilson,
154 1967; Schoener, 1976; Tjørve *et al.*, 2018). The shapes of SARs have been described by many
155 mathematical models, including the logarithmic model (Gleason, 1922), power law model
156 (Arrhenius, 1921) and more complex models (for reviews, see Dengler, 2009; Tjørve, 2009;
157 Williams *et al.*, 2009). Based on findings of a wide array of studies on SARs of any kind,
158 including in continuous habitats and on islands, the power law model overall performs best
159 (Triantis *et al.*, 2012; Matthews *et al.*, 2016; Dengler *et al.*, 2020). The power law is
160 conventionally expressed as $S = c A^z$ (Arrhenius, 1921), which in its logarithmic form becomes
161 $\log S = \log c + z \log A$ (where S is species richness, A is area sampled, and c and z are fitted
162 parameters). The exponent z describes the rate of species accumulation with increasing area,
163 and is a suitable measure of multiplicative beta diversity (Koleff *et al.*, 2003; Sreekar *et al.*,
164 2018; Dengler *et al.*, 2020; Dembicz *et al.*, *subm.*).

165 Given the importance and ubiquity of SARs, many biogeographers and ecologists have
166 analysed z -values in detail (Crawley and Harral, 2001; Drakare *et al.*, 2006; Matthews *et al.*,
167 2019). For example, numerous theoretical models and field experiments have attempted to
168 identify a constant value of z for a multitude of different ecosystems and taxa, and have often
169 found values close to 0.25 (Connor and McCoy, 1979; Sugihara, 1980). Other researchers have
170 used the z -value as a fruitful approach for studying how different environmental factors affect

1
2
3
4 171 SARs (Drakare *et al.*, 2006; Patiño *et al.*, 2014). Further, studies have examined the variation in
5
6 172 z-values across spatial and temporal scales, trophic levels and taxonomic groups (Patiño *et al.*,
7
8 173 2014; Roslin *et al.*, 2014; Fattorini *et al.*, 2017; Dembicz *et al.* *subm.*). However, an extensive
9
10 174 review of the literature reveals a lack of consensus regarding the variation in z-values of SARs
11
12 175 across spatial grains.

13
14 176 Many studies assume that the exponent z of the power function (i.e. the slope of the
15
16 177 linearized power function) is relatively constant across spatial grains (Drakare *et al.*, 2006; Qiao
17
18 178 *et al.*, 2012; Dembicz *et al.* *subm.*). However, some detailed studies have revealed significant
19
20 179 changes in z-values with grain size (Crawley and Harral, 2001; Fridley *et al.*, 2005; Polyakova *et*
21
22 180 *al.*, 2016). The concept of ‘local z ’ has been proposed to describe such variation of z-values with
23
24 181 grain size (Williamson, 2003; Dengler, 2009), and can be defined as the local derivative of the
25
26 182 SAR between two subsequent grain sizes in double-log space. Using this approach, Crawley and
27
28 183 Harral (2001: all vegetation types in a landscape in the United Kingdom), Turtureanu *et al.*
29
30 184 (2014: dry grasslands in Romania) and Polyakova *et al.* (2016: dry grasslands in Siberia) found
31
32 185 unimodal relationships, i.e. a peak of local z-values, albeit at quite different grain sizes. By
33
34 186 contrast, Kuzemko *et al.* (2016) and Dembicz *et al.* (2021a) did not find significant scale
35
36 187 dependence in dry grasslands of Ukraine and Bulgaria, respectively.

37
38 188 Finally, also methodological issues can influence small-grain z-values. There are two
39
40 189 contrasting ways how to record a plant species as present in a plot, the any-part system (also
41
42 190 called “shoot presence”: plants are recorded as present when the vertical projection of any
43
44 191 above-ground organ falls inside the plot) and the grid-point system (largely equivalent to
45
46 192 “rooted presence”: plants are recorded as present when they are attached to the soil surface
47
48 193 inside the plot) (Williamson, 2003; Dengler, 2008; Cancellieri *et al.*, 2017). Both methods are
49
50 194 widespread in vegetation ecology, but the majority of researchers seems to be unaware of the
51
52 195 differences, as reflected by the fact that most studies do not report which of the two methods
53
54 196 they applied and standard textbooks like Kent (2012) or van der Maarel and Franklin (2013) do
55
56 197 not even mention that these two options have to be considered. However, rooted vs. shoot
57
58 198 presence sampling can lead to profound differences in results on α - and β -diversity as well as
59
60 199 SAR shapes (Güler *et al.*, 2016; Cancellieri *et al.*, 2017; Dengler *et al.*, 2020). Williamson (2003)
200
201 200 demonstrated theoretically that towards fine grain sizes the difference between rooted and
shoot sampling will override any ecological or taxonomic driver, with local z-values of rooted

202 presence recording always approaching 1 at very fine scales, while those recorded with shoot
203 presence necessarily approaching 0. Thus, taking into account this methodological aspect is
204 essential if one does not wish to misinterpret a mathematical “constraint” as an ecological
205 process that justifies a new theory, as Plotkin *et al.* (2000) did .

206 In conclusion, there is scattered evidence that local z-values sometimes show significant
207 scale-dependence, but there is no general picture how prevalent this is and whether and how
208 this scale dependence is related to taxonomic group or to environmental predictors. While it is
209 evident that rooted vs. shoot recording must influence the results, it is unclear below which
210 grain sizes this difference will become noticeable and how strong it will be in relation to other
211 factors. If there should be peaks of local z-values at certain grain sizes this would indicate how
212 spatial heterogeneity of plant communities is organized spatially. As for fine-grain beta diversity
213 in general (Drakare *et al.*, 2006; Dembicz *et al.*, *subm.*) one should also expect for peak location
214 of local z-values to depend on taxonomic group and various environmental factors.
215 Unfortunately, there are so far no comprehensive macroecological studies to examine the
216 prevalence of peaks in local z-values and which drivers determine their position.

217 The present study thus aims at filling this knowledge gap by using 6,696 nested-plot series
218 from the GrassPlot database (Dengler *et al.*, 2018; Biurrun *et al.*, 2019), covering any type of
219 grasslands and other open habitats of the Palaearctic biogeographic realm. In the absence of
220 extensive prior studies it is premature to formulate specific hypotheses. Instead, we conduct an
221 explorative study including a wide range of predictors that often have been shown to be
222 influential on other facets of fine-grain biodiversity, assuming that they also might play a role in
223 scale-dependence of β -diversity. We aimed to answer the following three questions, which, in
224 turn, might contribute to a better understanding on scale-dependence of β -diversity and thus a
225 future formulation of a theory on that topic:

226 (1) Is there a general pattern of scale dependence of local z-values and does it depend on
227 the recording system (shoot vs. rooted presence)?

228 (2) How does scale dependence differ between taxonomic groups (vascular plants,
229 bryophytes, lichens)?

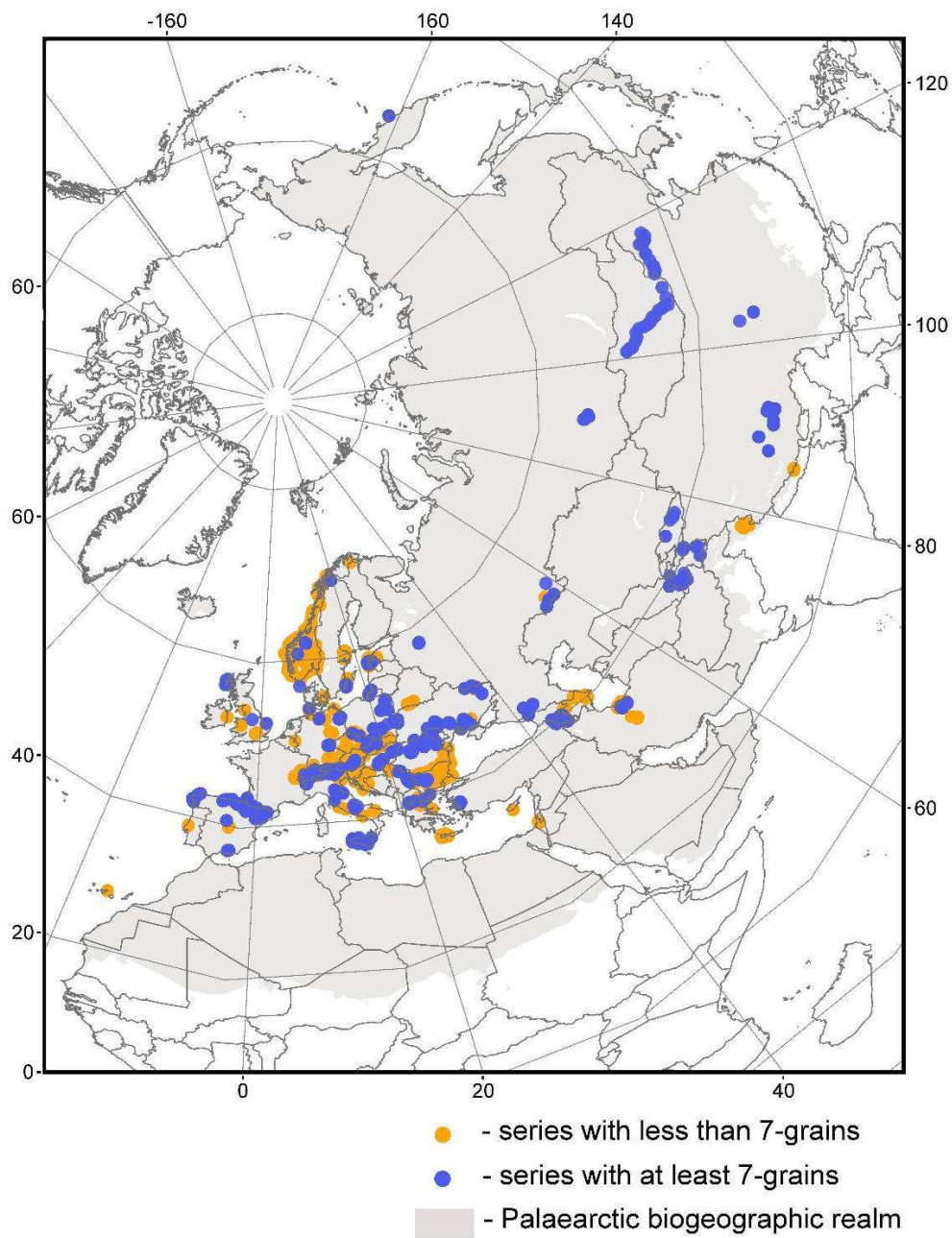
230 (3) How does scale dependence vary in relation to broad-scale biogeographic
231 characteristics (latitude, elevation, climate) and fine-scale ecological characteristics
232 (related to the stress-productivity axis, disturbance and heterogeneity)?

233 **Methods**

234 ***Vegetation-plot data***

235 All plot data used in this paper were taken from the collaborative vegetation-plot database
236 GrassPlot (Dengler *et al.*, 2018; Biurrun *et al.* 2019; <https://edgg.org/databases/GrassPlot>). The
237 GrassPlot database is a compilation of vegetation-plot data, including methodological,
238 environmental, and structural information, from grasslands and other non-forest vegetation
239 types throughout the Palaearctic biogeographic realm. Requirements for inclusion of the data
240 in the database are precise delineation of plots in the field and sampling with the aim of
241 achieving complete species lists. GrassPlot specifically collects multi-scale datasets from nested-
242 plot sampling schemes (e.g. Dengler *et al.*, 2016) with plot (grain) sizes from 0.0001 m² to
243 1,024 m².

244 We extracted all series containing at least two different grain sizes from GrassPlot (v.2.09
245 in August 2020) to form our dataset, altogether 6,696 series and 177,138 individual plots (Fig.
246 1). The plots were distributed across 41 countries, from 28° to 70° N and 16° W to 162°E, and
247 covered an elevational gradient from 0 to 5,680 m a.s.l. All series contained information on
248 vascular plants, while 1,260 series contained information on terricolous bryophytes, 1,353 on
249 terricolous lichens, and 1,212 on all three taxonomic groups (complete vegetation).



250

251 **Figure 1.** Spatial distribution of the 6,696 series in the Palearctic biogeographic realm that were analysed in this
 252 study.

253 **Calculation of local z-values**

254 We first averaged richness values per grain size for the plot series with more than one plot
 255 for a certain grain size. Species richness (S) should increase with area (A) modelled by the
 256 function $S = cA^z$ (Dengler *et al.*, 2020) or its linearized form:

$$257 \log S = z \log A + \log c$$

To account for the possibility that z-values can vary between subsequent grain size transitions of a nested-plot series (Crawley and Harral, 2001; Fridley *et al.*, 2005), we calculated local z ($z_{i \text{ to } i+1}$) (Williamson, 2003) and local grain ($g_{i \text{ to } i+1}$) as:

$$z_{i \text{ to } i+1} = \frac{\log S_{i+1} - \log S_i}{\log A_{i+1} - \log A_i}$$

$$g_{i \text{ to } i+1} = \frac{\log A_{i+1} + \log A_i}{2}$$

where A_i and S_i are the area and the species richness of a particular grain size i , respectively. Note that $z_{i \text{ to } i+1}$ is not defined if one of the two richness values is 0; thus we excluded such grain size transitions from further analyses. We assigned each local z value to the mean of the logarithms of the two successive grain sizes (= logarithm of the geometric mean). In these equations, log denotes base-10 logarithm (\log_{10}).

Statistical analyses

All analyses were conducted in R version 4.0.2 (R Development Core Team, 2016).

Overall scale dependence

To analyse the scale dependence of local z-values in general, we fitted Generalized Additive (Mixed) Models (GAM(M)s) for $z_{local} = f(g_{local})$ separately for nested plots sampled using two widespread methods of presence recording, i.e. shoot presence and rooted presence. GAMMs were analysed with the R package 'mgcv' with series ID as a random factor. Since the results for GAMs and GAMMs were nearly indistinguishable based on AIC, we report only GAMs in the Results. To avoid overfitting, we paid attention to the number of 'knots' (k value) while running GAM(M)s: starting with $k = 0$, we subsequently increased k to find the model that best captures the relationship without overfitting based on AIC and shapes of GAM(M)s. We fitted GAM(M)s for all data and after excluding the very few values of $z_{local} > 1$ and $z_{local} < 0$ (for details see Table S1.3). Such values are theoretically impossible if the richness values of the smaller grain sizes are true spatial averages within the area of the largest plot (Williamson, 2003). However, empirically $z_{local} < 0$ can occur if there is no complete nesting and $z_{local} > 1$ when the smaller grain sizes are not sufficiently replicated and their richness values thus biased.

Individual response curves

For subsequent analyses in this study, we only used the theoretically possible values (Williamson, 2003). Since we had a larger proportion of shoot presence data, all subsequent

analyses were conducted for shoot presence data only. Moreover, we restricted ourselves to nested-plot series with at least seven grain sizes with $S > 0$ (i.e. six local z-values) to allow for a meaningful assessment of the shape of the scale dependence.

To analyse the patterns of scale dependence of local z-values, we fitted to each individual nested-plot series a polynomial GLM with logit link. The underlying model is:

$$y = \frac{1}{1 + \exp(b_0 + b_1x + b_2x^2)}$$

where x is the local grain size g_{local} and y the predicted local z-value. This model has previously been applied to determine the probability of occurrence of a species, in the form of a symmetric Gaussian response curve, based on its presence or absence (binary response) across an environmental gradient (ter Braak and Looman, 1986; Huisman *et al.*, 1993; Oksanen and Minchin, 2002). The same model may be applied to a continuous response in the interval $[0, 1]$, such as local z-values. The choice of this simple parametric model against more complex ones (for instance able to fit skewed or bimodal response curves) was justified by the low number of points in each series (typically six grain size transitions for standard GrassPlot series with seven grain sizes). Therefore, we used the three regression coefficients of the model (b_0 = intercept, b_1 = linear term, b_2 = quadratic term) to classify the response curves into four shapes. In case of a hump-shaped response, parameters of the Gaussian function can be retrieved from b_1 and b_2 . We identified the location of the optimum as $Opt = -b_1/(2b_2)$. We further quantified $Tol = \frac{1}{\sqrt{-2b_2}}$ as the tolerance of the Gaussian curve, which measures the flattening of the curve (equivalent, in statistical terms, to the variance of a normal distribution). To select hump-shaped and U-shaped curves, we identified series in which Opt was within the range of local grain sizes ± 1 order of magnitude. Thus, the shapes of the fitted curves were classified based on the following principles:

Hump-shaped (Gaussian) curves were identified by $Opt \in [\min(g_{local}) - 1, \max(g_{local}) + 1]$, $Tol > 0$.

U-shaped (inverse Gaussian) curves were identified by $Opt \in [\min(g_{local}) - 1, \max(g_{local}) + 1]$, $Tol = NA$.

Monotonic decreasing curves were identified by $Opt \notin [\min(g_{local}) - 1, \max(g_{local}) + 1]$, $b_1 < 0$.

1
2
3
4 316 Monotonic increasing curves were identified by $Opt \notin [\min(g_{local}) - 1, \max(g_{local}) + 1]$
5
6 317 , $b_1 > 0$.

8 318 Methods for determining peak position

10 319 We determined the peak grain size (local grain size where the maximum local z occurred)
11
12 320 with two different approaches: (a) we extracted the local grain size corresponding to the
13
14 321 maximum *observed* local z-value in each series (for explanation, see Fig. S1.1 in Supporting
15
16 322 Information); (b) we extracted the local grain size of the maximum *fitted* local z-value within
17
18 323 the range of local grains ± 1 order of magnitude. In case of fitted hump-shaped curves, we took
19
20 324 *Opt* as the position of the peak of the local z-value (Fig. S1.1, Table S1.1); for monotonic curves
21
22 325 we assigned $\min(g_{local}) - 1$ for decreasing curves, $\max(g_{local}) + 1$ for increasing curves, and
23
24 326 in case of U-shaped curves, we took the local grain one order of magnitude outside the
25
26 327 available data for which the higher value was predicted. We labelled the two methods as (a)
27
28 328 "observed" and (b) "fitted".

30 329 ***Relating peak position to taxonomic and environmental predictors***

32 330 We tested how the position of the peaks, either observed or fitted, depended on
33
34 331 taxonomic group, biogeographic characteristics and ecological characteristics. For continuous
35
36 332 variables, we applied simple linear regressions with both linear and quadratic terms to test
37
38 333 their potential influence on the grain size of the peaks for the four taxonomic groups. Best fit
39
40 334 was assessed with AIC of the contrasting regression models. For categorical predictors, we
41
42 335 applied analysis of variance (ANOVA), followed by Tukey's post-hoc test (R package 'stats').

44 336 Since this is the first broad exploratory study on the phenomenon of scale dependence of
45
46 337 local z-values, we used a wide range of potential predictor variables related to our research
47
48 338 questions. They were mostly determined in the field, but some additionally retrieved via the
49
50 339 plot coordinates (Table S1.2). For simplicity and following a previous paper using the same
51
52 340 dataset (Dembicz *et al.*, *subm.*), we group them into the following categories, acknowledging
53
54 341 that some variables can relate to more than one category: (1) taxonomic group (vascular plants,
55
56 342 bryophytes, lichens, and complete vegetation), (2) macroecological characteristics (climate
57
58 343 variables, latitude and elevation), (3) ecological characteristics at plot-level, subdivided into
59
60 344 those related to (a) productivity, (b) disturbance and (c) heterogeneity, and (4) vegetation

1
2
3
4 345 typologies. In the following, we briefly introduce the variables of categories (2) – (4), while
5
6 346 details are provided in Table S1.2.

7
8 347 (2) As macroecological variables we used two geographic variables (*latitude* and *elevation*)
9
10 348 and four climate variables (*mean annual temperature*, *temperature seasonality*, *mean annual*
11 349 *precipitation*, *precipitation seasonality*). *Latitude* and *elevation* with few exceptions were
12 350 provided by the original dataset collectors, while missing elevation data was derived from
13 351 digital elevation models GTOPO30 (Danielson and Gesch, 2011) and EU-DEM v.1.1 (2020). QGIS
14 352 was used to derive climate data from the CHELSA database (Karger *et al.*, 2017), using plot
15 353 coordinates.

16
17 354 (3a) Here we included variables related to the *stress-productivity gradient* (Grime, 1977;
18 355 Huston, 2014). As plant cover is one of the main predictors of aboveground biomass (Sanaei *et*
19 356 *al.*, 2018), we used *vegetation cover* and *herb layer cover* as rough proxies for productivity and
20 357 for the competition for light (Grytnes, 2000). Changes in soil properties usually affect
21 358 vegetation cover and total biomass production (Emiru and Gebrekidan, 2013). We used *soil pH*
22 359 (assuming maximum productivity at intermediate values) and *mean soil depth* (assuming
23 360 maximum productivity at high values).

24
25 361 (3b) *Disturbance*, in the sense of removal or destruction of accumulated bio- and
26 362 necromass is the other main dimension determining species richness and other diversity facets
27 363 (Grime, 1977; Huston, 2014). Here, we used *litter cover* as a main proxy for the absence of
28 364 disturbance. We used *slope inclination* (°) as another proxy for disturbance, because erosion
29 365 increases with increasing slope (Mangeny *et al.*, 2010). As measures of anthropogenic
30 366 disturbance we included levels of *naturalness* (with five levels) and the presence of *grazing*,
31 367 *mowing* and *fertilizing* (Table S1.2).

32
33 368 (3c) *Heterogeneity* variables are those that describe the small-scale variability of
34 369 productivity and/or disturbance, and they are usually determined within the largest or second-
35 370 largest grain plot of each nested series: *Soil depth CV* (coefficient of variation) indicates the
36 371 variability of soil depth within a plot. From the perspective of herbaceous vegetation, both *rock*
37 372 *and stone cover* and *shrub layer cover* inside the plot can be interpreted as heterogeneity
38 373 measures, assuming maximum variability in within-plot environmental conditions at
39 374 intermediate levels.

(4) We tested three *vegetation typologies*: The *biome* represents the climate-driven potential climax vegetation. It was derived via the plot coordinates, using the classification of Bruehlheide *et al.* (2019), with six biomes: alpine, boreal, continental (dry mid-latitudes), nemoral (temperate mid-latitudes), mediterranean (subtropics with winter rain), and dry tropics and subtropics. Further, we used a coarser and finer typology of the actual vegetation: vegetation group (six classes) is the coarser level, within which vegetation type (20 classes) is nested. This two-level typology was defined to be applicable across the Palaearctic and accessible with the information provided in the individual datasets. It mainly captures aspects of physiognomy (e.g. dwarf shrubs vs. herbs only), naturalness (natural vs. secondary) and stress factors (e.g. drought, flooding, salinity, cold) (for details, see Biurrun *et al.*, 2019).

Results

Pattern of scale dependence of z-values

Local z-values revealed scale dependence and differences between the two ways of recording plant presence (Fig. 2, Fig. S2.1). In the case of complete vegetation, local z-value reached a shallow maximum for \log_{10} (area) at around -1.5 (corresponding to 0.032 m²) for shoot presence, while for rooted presence z-values started to increase strongly and continuously from around 0 (1 m²) towards the smallest grain sizes (Fig. 2). For vascular plants, the situation was similar, except that in rooted presence at grain sizes below -2.5 (0.003 m²) z-values decreased again slightly (Fig. S2.1). Whether recorded as shoot presence or rooted presence, bryophytes hardly showed any scale dependence of local z-values (Fig. S2.1). For lichens recorded as shoot presence, local z-values peaked around -1.75 (0.018 m²), while they decreased over the studied range for rooted presence (Fig. S2.1). The GAMs conducted with data including theoretically impossible values of local $z > 1$ and local $z < 0$ showed similar patterns (Fig. S2.2). Among the shapes of fitted curves to individual nested-plot series, hump-shapes prevailed for all taxonomic groups (Fig. 3, Table S2.1).

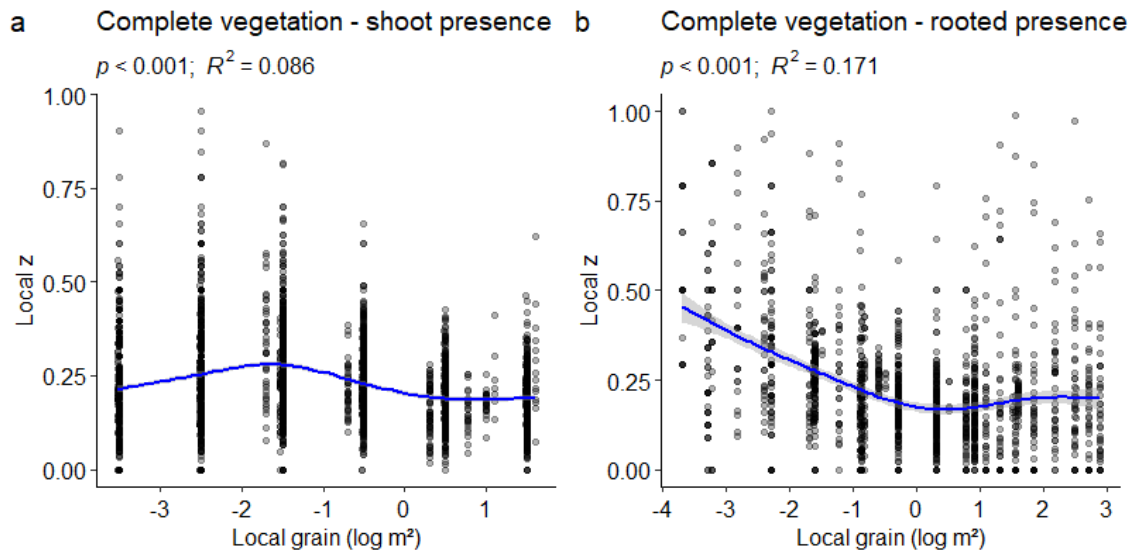


Figure 2. Generalized additive models (GAMs) with 95% confidence intervals (pale blue) for the effect of local grain (on log scale) on local z-value for complete vegetation, in plot series using two different ways of recording species occurrence: a) shoot presence and b) rooted presence.

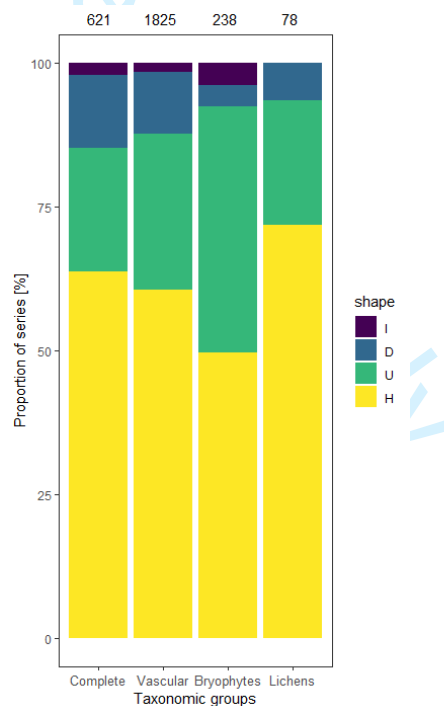


Figure 3. Comparison of the four shapes of fitted curves (hump-shaped (H), U-shaped (U), monotonic decreasing (D), and monotonic increasing (I)) for the complete vegetation and for the taxonomic groups vascular plants, bryophytes, and lichens (series with at least seven grain sizes). Values on top of bars are the number of nested-plot series analyzed.

409 ***Taxonomic groups***

410 The observed peak grain sizes did not differ significantly among taxonomic groups
411 (ANOVA; $p = 0.119$). Mean peak locations were between -1.55 and -1.38 , i.e. 0.03 - 0.04 m^2 (Fig.
412 S2.3). The only discernible difference was that peak position in the case of bryophytes was
413 more variable than for the other two taxonomic groups. By contrast, the fitted peak grain size
414 differed significantly among taxonomic groups (ANOVA with Tukey's HSD test) (Fig. S2.3). Here,
415 the highest fitted peak grain was found for bryophytes (0.06 m^2), followed by lichens (0.05 m^2)
416 and vascular plants (0.02 m^2).

417 ***Observed vs. fitted peaks***

418 We conducted all following analyses for the observed and the fitted peak grain size. As the
419 results were similar, we present only those for observed peaks in the main text, while those for
420 fitted peaks are provided in Supporting Information (Figs. S2.9–S2.12, S2.14, S2.19–S2.22,
421 S2.24, S2.26, S2.31–S2.34).

422 ***Macroecological characteristics***

423 For vascular plants, the observed peak grain size showed a significant U-shaped
424 relationship with latitude (minimum at around 47° N) and an initially flat then increasing
425 relationship with elevation (Fig. 4; see Fig. S2.4 for a map). Also the relationship with mean
426 annual temperature was u-shaped (Fig. 4), while the other macroecological variables only had
427 low explanatory power (Fig. S2.5). Observed peak grain size was not explained by
428 macroecological variables in the case of bryophytes (Fig. S2.6), whereas for lichens it showed a
429 unimodal relationship with latitude and elevation, but a u-shaped relationship with
430 precipitation seasonality (Fig. S2.7). Complete vegetation behaved similarly to vascular plants in
431 the case of elevation (u-shaped to increasing), but showed the opposite pattern (slightly
432 unimodal for latitude and mean annual precipitation (Fig. S2.8).

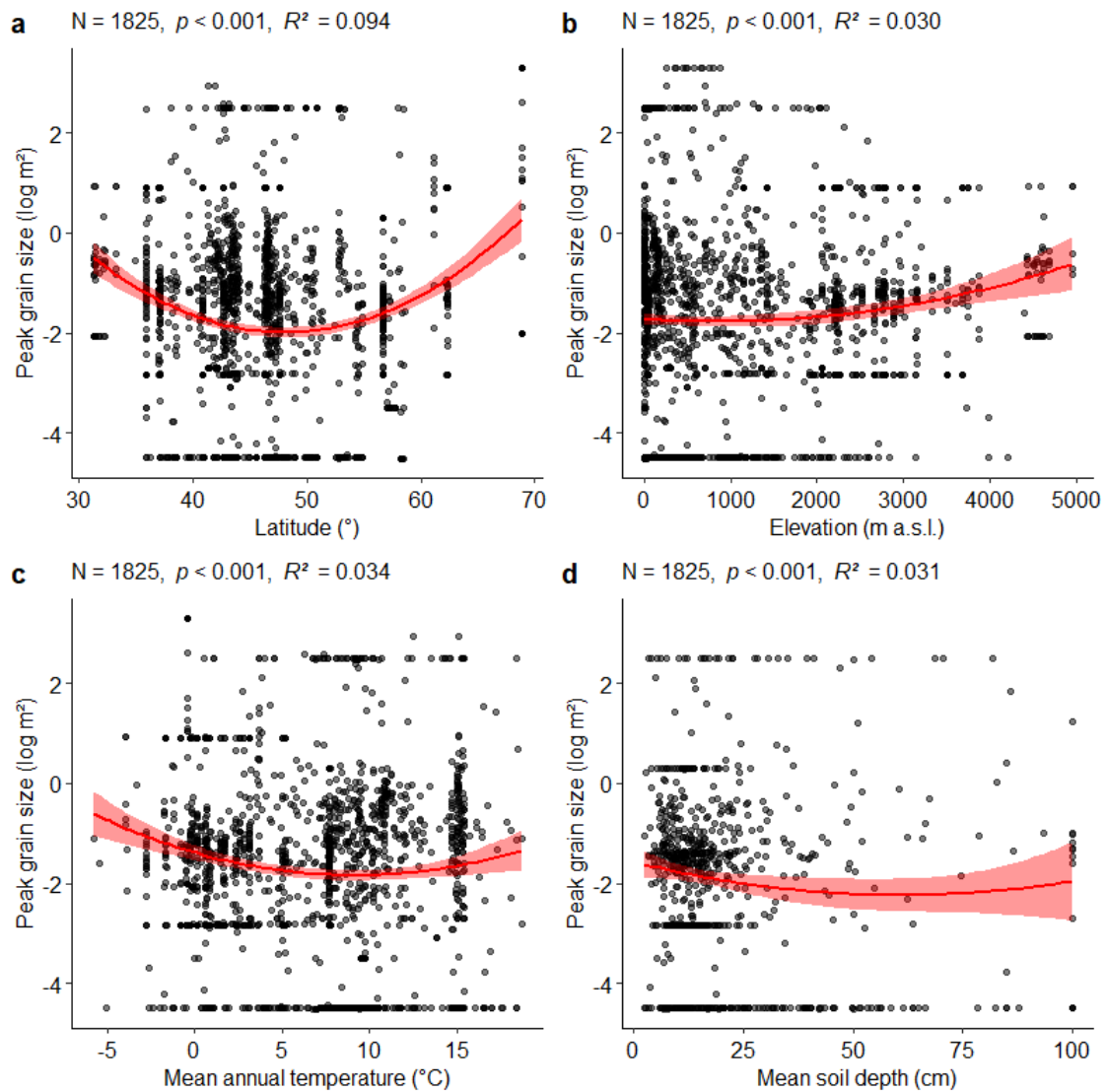


Figure 4. Differences in observed peak grain size (local grain size where the maximum local z occurred) of vascular plants depending on predictor variables. Red lines indicate quadratic relationships ($p < 0.05$) with confidence intervals.

Ecological characteristics related to productivity

From the variables related to the stress-productivity gradient, in vascular plants only mean soil depth had an explanatory power above 3% (u-shaped relationship; Fig. 4) while all others had low explanatory power or were insignificant (Fig. S2.5). The pattern was similar but weaker for complete vegetation (Fig. S2.8), while no relationships for any of the tested variables occurred in bryophytes and lichens (Figs. S2.6–S2.7).

Ecological characteristics related to disturbance

Observed peak grain size of vascular plants and bryophytes increased monotonically with litter cover (Figs. S2.5–S2.6), while there was no relationship for lichens and complete vegetation (Figs. S2.7–S2.8). Slope inclination did not show a pattern for any of the four groups (Figs. S2.5–S2.8).

For vascular plants, observed peak grain size was highest in unused natural grasslands and lowest in semi-intensified secondary grasslands (Fig. 5). Also for complete vegetation there was a tendency of decreasing peak grain size with decreasing naturalness, while for bryophytes there were no differences at all and lichens had a significantly higher peak grain size in extensively managed natural grasslands compared to both unmanaged natural grasslands and semi-natural secondary grasslands (Fig. S2.13). In vascular plants any management consistently decreased peak grain size (Fig. S2.15), but the effect was most pronounced in the case of mowing with a decrease by about one order of magnitude and an explained variance of 3.8% (Fig. 6). While in complete vegetation three of the five management categories also led to a decrease in peak grain size (albeit with very low explained variance; Fig. S2.18), there was no effect in the case of bryophytes (Fig. S2.16) and even an increase for two categories in the case of lichens (Fig. S2.17).

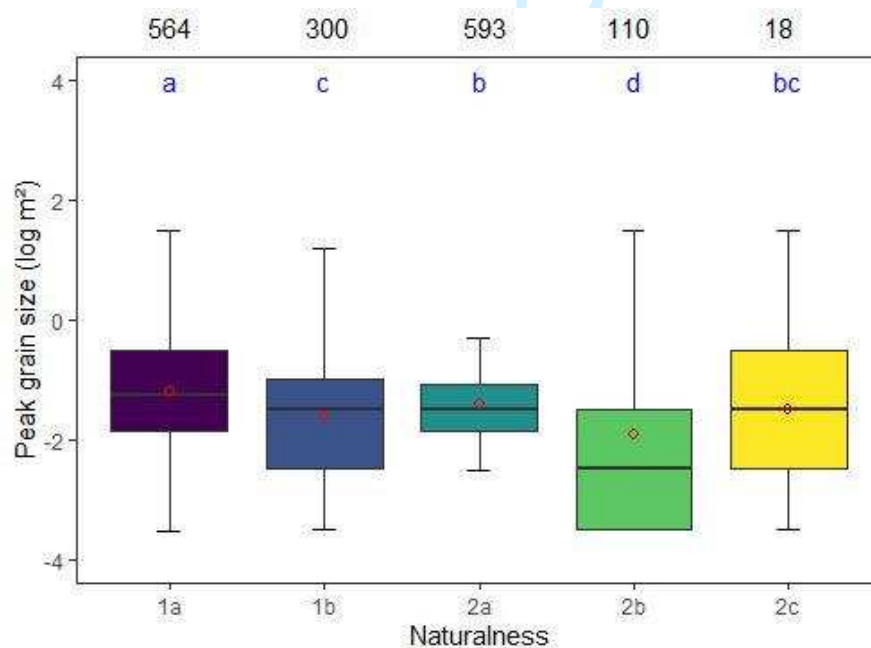
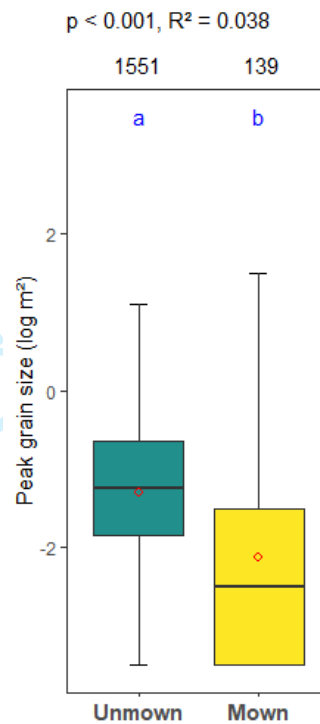


Figure 5. Differences of the observed peak grain size (local grain size where the maximum local z occurred) for vascular plants between the five levels of naturalness present in this study (no series for 1c – natural

1
2
3
4 463 grasslands, overused): 1 – natural grasslands (1a – not managed, 1b – extensively managed); 2 – secondary
5 464 grasslands (2a – semi-natural, 2b – semi-intensified, 2c – intensified) ($p < 0.001$; $R^2_{adj.} = 0.028$). Blue
6
7 465 lowercase letters indicate homogeneous groups ($p < 0.05$) as tested with Tukey's post-hoc test ANOVA, the
8
9 466 figures on top indicate the numbers of data. Box and whisker plots represent the median and quartiles while
10 467 the red dots represent the mean values.



35 468
36
37 469 **Figure 6.** Effect of mowing on observed peak grain size (local grain size where the maximum local z occurred)
38 for vascular plants ($p < 0.001$; $R^2 = 0.038$). Box and whisker plots represent the median and quartiles while the
39 470 red dots represent the mean values for each management type.
40
41 471

42 472 ***Ecological characteristics related to heterogeneity***

43
44 473 We found minimal to no influence of our heterogeneity-related variables on observed
45
46 474 peak position in any of the taxonomic groups (Figs. S2.5–S2.8).
47

48 475 ***Vegetation typologies***

49
50 476 Considering biomes (i.e. broad-scale potential/climax vegetation), for vascular plants the
51
52 477 nemoral biome had the lowest peak grain sizes, the alpine, boreal and dry tropics and
53
54 478 subtropics biomes the highest and the continental biome and the subtropics with winter rain
55
56 479 intermediate peak grain sizes (Fig. S2.23). By contrast for bryophytes and lichens there was no
57
58 480 significant pattern and for complete vegetation it was very weak (Fig. S2.23).
59
60

Among all predictors, in vascular plants the actual vegetation type had the highest predictive power for peak grain size, 13.8% at the fine level (Fig. S2.27) and 6.8% at the coarse level (Fig. 7). Peak grain size was particularly high in all types of dwarf shrublands and particularly low in secondary grasslands and alpine deserts (Figs. 7, S2.27). There was no effect of vegetation type in the case of bryophytes and lichens and only a weak effect in complete vegetation (Figs. S2.25, S2.28–S2.30).

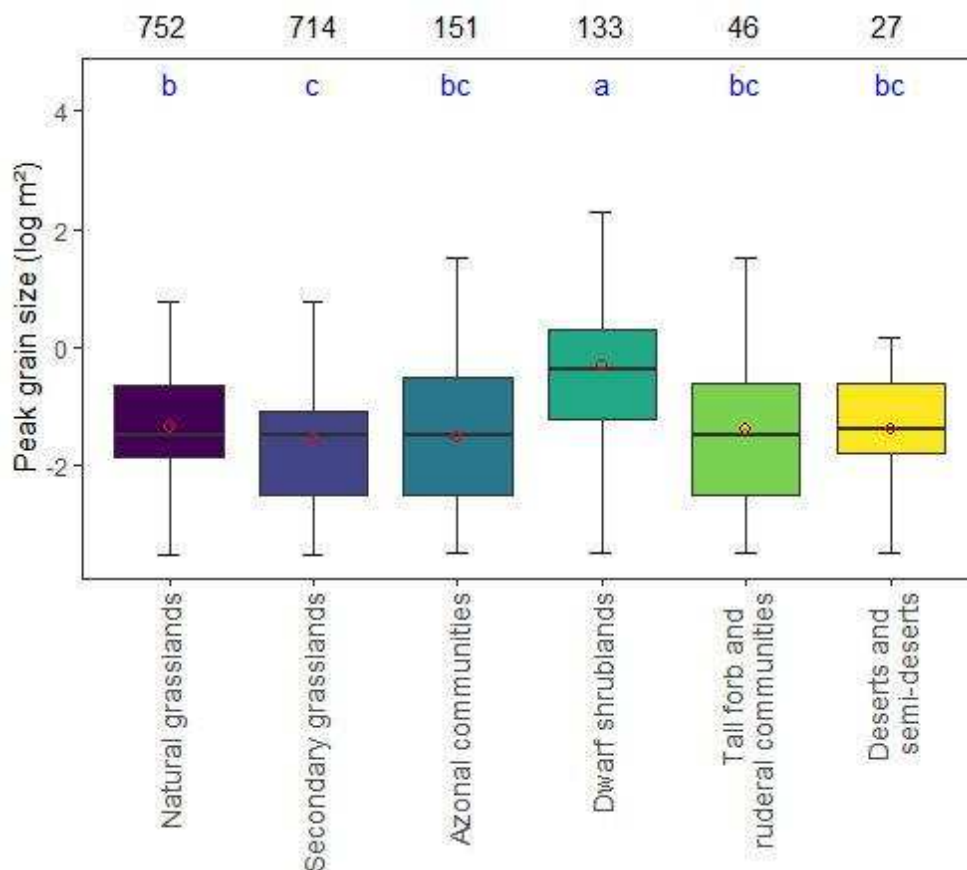


Figure 7. Differences in the observed peak grain size (local grain size where the maximum local z occurred) between the six main vegetation types for the vascular plants ($p < 0.001$, $R^2_{adj.} = 0.068$). A common blue lower-case letter between two boxes indicates homogeneous groups as tested with Tukey's post-hoc test with ANOVA ($p < 0.05$), the figures on top indicate the numbers of data. Box and whisker plots represent the median and quartiles while the red dots represent the mean values for each vegetation type at coarse level.

Explanatory power of different predictors

Overall, for vascular plants, the highest proportion of variance in the observed peak grain size was explained by vegetation types at fine level (0.138), followed by latitude (0.094), vegetation types at coarse level (0.068), mowing (0.038) biomes (0.031) and naturalness

(0.028). The explanatory power of the bivariate regressions for the fitted peaks on average was lower than for the observed peaks. For bryophytes, lichens and complete vegetation, there were much fewer significant relationships and they generally were also weaker.

Discussion

Differences between records of shoot and rooted presence

At fine grain sizes, the scale dependence of local z-values differed depending on whether plants were recorded with shoot presence or rooted presence. These differences were best visible for our big datasets of complete vegetation and vascular plants and somehow less pronounced in our smaller (and thus potentially less balanced) datasets of bryophytes and lichens. In all four groups, z-values of rooted presence recorded data started to increase more or less monotonously below a threshold somewhere between 1 and 10 m², while for shoot presence there was either a shallow peak around 0.01 m² or no systematic scale dependence. This is in agreement with Williamson (2003) who demonstrated mathematically that z-values at very small grain sizes must approach a value of zero in the case of the “any-part system” and a value of one in the case of the “grid-point system”. His “any-part system” is equivalent to shoot presence, while his “grid-point system” is very similar to rooted presence in our study (for details, see Dengler, 2008). These deviations from the “normal” shape of the species-area relationships to the far left of the graph are “mathematical artefacts” caused by the way in which plant presence is recorded, and thus should not be interpreted ecologically. For a tree-only dataset of a tropical rainforest recorded with the grid-point system, Williamson (2003) found that local z-values started to increase from below approx. 10⁵ m² (10 ha) and reached one at around 1 m². For the non-forest communities in our study, we found that for complete vegetation the increase in z-values started below approx. 1 m², and values reached nearly 0.5 at 1 cm². The diverging peak positions can easily be explained by the size difference in the organisms studied (herbs, dwarf shrubs, bryophytes and lichens vs. tropical trees). We did not actually reach a local z-value close to one, possibly because our smallest grain size was not small enough and because rooted presence is similar, but not identical, to the grid-point system. For the any-part (shoot presence) system, Williamson (2003) predicted a decrease in local z-values at small grain sizes towards zero. We found no indication of this effect, since at the smallest grain size we still had a mean local z-value of around 0.22, which was only slightly different from the overall average. This apparent deviation from the theoretical pattern can be

1
2
3
4 528 explained: in a species-area study in dry grasslands with grain sizes down to 1 mm², Dengler *et*
5 529 *al.* (2004) observed “flattening” of the species-area curves towards small grain sizes, equivalent
6
7 530 to a decrease in local z towards zero, but only at grain sizes smaller than 1 cm².

531 ***Overall scale dependence of local z-values***

532 When removing the strong methodological effect of rooted presence sampling and
533 concentrating on shoot presence data, we found only a weak overall scale dependence of local
534 z -values for vascular plants and complete vegetation (8.6% and 10.8% explained variance,
535 respectively). For lichens, the effect was slightly stronger (13.1%), while local z -values of
536 bryophytes hardly showed any systematic scale dependence (1.9%). These relatively weak
537 effects when combining all nested-plot series could either mean that the scale dependence in
538 individual nested-plot series is also low or that it is stronger, but the shape of the response
539 varies idiosyncratically among the series. Our shape analysis of the fitted response curves of
540 local z -values vs. local grain revealed a prevalence of hump-shaped curves (Fig. 3), meaning a
541 peak within the observed range of areas, irrespective of taxonomic group. As for most of the
542 nested-plot series we had only six grain size transitions, we could not conduct a meaningful test
543 on statistical superiority of quadratic vs. linear vs. no scale dependence. Thus, we have to
544 acknowledge that among the four distinguished response types of Figure 3 an unknown
545 fraction of a fifth type of “no significant scale dependence” is hidden, so the prevalence of
546 hump-shaped curves is probably lower than Figure 3 suggests. This coincides with the fact that
547 two studies that analyzed relatively small regional subsets of the GrassPlot data did not either
548 find a significant scale dependence (Kuzemko *et al.*, 2016; Dembicz *et al.*, 2021a). However, as
549 already the combined data of all nested-plot series (Fig. 2, Fig. S2.1) show clear peaks for
550 complete vegetation, vascular plants and lichens, it is evident that among those nested plots
551 that actually show a scale dependence, unimodal relationships with peaks inside the fitted
552 range will prevail.

553 ***Position and meaning of peaks***

554 Assuming a unimodal response, we found that peak grain generally varied across the
555 whole analyzed grain size range (Figs. 2). For all three groups as well as for complete vegetation
556 it was around -1.6 to -1.4, corresponding to 0.03–0.04 m², in the analyses of individual nested-
557 plot series. This coincides to the overall peaks derived for all grain-size transitions with the

1
2
3
4 558 GAMs, except for bryophytes that did not show any peak there (which corresponds to a much
5
6 559 larger variability of the peak location for bryophytes than for the two other taxonomic groups
7
8 560 in case of the series-based analyses). Not to find any systematic difference in the peak location
9
10 561 of the three contrasting taxonomic groups was unexpected as both their sizes and their spatial
11
12 562 distribution patterns seem to be quite different. However, it might be that our prior assumption
13
14 563 that bryophytes and lichens are smaller than vascular plants is not necessarily true in the two-
15
16 564 dimensional projection to the ground which is quantified with shoot presence. Indeed, there
17
18 565 are also quite extensive thalli of some carpet-forming mosses or reindeer lichens.

19 566 The mean peak positions found in this study for vascular plants and complete vegetation
20
21 567 (mostly 0.01 – 0.1 m²) are quite similar to those reported for Palaeartic grasslands in regional
22
23 568 studies (Turtureanu *et al.*, 2014; Polyakova *et al.*, 2016). In contrast, Crawley & Harral (2001)
24
25 569 found a very different peak (at around 40,000 m²) in a study of species richness of vascular
26
27 570 plants in a landscape in England including a wide range of different habitats (grasslands, forest
28
29 571 patches, riparian vegetation, heathlands, etc.). The much larger peak grain size probably
30
31 572 reflects the granularity of habitats in the British landscape, inducing a steep increase of species-
32
33 573 richness when new habitats with ecologically different species are included in the samples. By
34
35 574 contrast, the data in GrassPlot refer to the internal organization of plant communities within
36
37 575 100 m² (or rarely up to 1024 m²) of a patch selected in most of the cases for relative
38
39 576 homogeneity (Dengler *et al.*, 2018; Biurrun *et al.* 2019).

40 577 What is the meaning of such a peak in the relationship of local z-values vs. local grain? A
41
42 578 peak refers to a local maximum in the rate of species accumulation, i.e. it indicates a spatial
43
44 579 grain (sampling unit size) where more new species appear in a sampling unit than expected
45
46 580 from the overall “global” z-value of the power law SAR. These irregularities in the rate of
47
48 581 species accumulation reflect variability of species occupancy due to differences of abundances
49
50 582 and the spatial heterogeneity of vegetation. Let us consider that a plant community is
51
52 583 composed of “granules” or floristically rather homogenous patches: increasing the recording
53
54 584 area within a granule would lead to a slow increase in richness, while moving from one
55
56 585 “granule” to another would give a steep increase. If granules show a wide variation in their
57
58 586 sizes, then likely no or only a weak peak is found, while a strong prevalence of a certain granule
59
60 587 size should cause a visible peak in the curve. The smaller the “granules”, the finer the spatial
588 grain where the position of the maximum local z- value appears. Theoretically, there could also

1
2
3
4 589 be multiple peaks if there are two or more nested granule sizes (cf. the concepts of hierarchical
5 590 patch dynamics; Kotliar and Wiens, 1990; Wu and Loucks, 1995). Unfortunately, the limited
6 591 number of grain-size transitions in our dataset (mostly only six) did not allow us to detect such
7 592 multiple peaks. Generally, the peaks observed were not very pronounced and their position
8 593 varied, indicating a high idiosyncrasy in granule-size distributions in vegetation. Knowledge on
9 594 peak grain size can be useful to explore the relationship between β -diversity and the
10 595 environmental drivers shaping the compositional heterogeneity at different spatial scales.

17 596 ***Drivers of the peak position***

19
20 597 Among the predictors studied for vascular plants, vegetation type had the relatively
21 598 strongest effect, with dwarf shrublands having particularly high peak grain sizes and secondary
22 599 grasslands particularly low ones. This makes sense given that heathlands have dwarf shrubs as
23 600 main structural elements, whose size is larger on average than that of herbs, while secondary
24 601 grasslands are subject to some type of management/land use, which might reduce the average
25 602 size of plant individuals and thus granules. This interpretation coincides with the fact that also
26 603 naturalness and land management were among the variables with relatively strong impact.
27 604 Generally, peak position decreased from natural to secondary grasslands and within each of the
28 605 two groups with increasing land use intensity – with the exception of intensively used
29 606 secondary grasslands, for which, however only a very small locally clustered sample was
30 607 available. Any type of land management (mowing, burning, livestock grazing, fertilization)
31 608 decreased the peak grain size, but the effect of mowing was strongest. This could be explained
32 609 by the fact that mowing is the less discriminant land use (i.e. all the stems of all species are cut).
33 610 Generally, management prevents litter accumulation and limits growth of the strongest
34 611 competitors, thus maintaining species coexistence through reducing competition and increasing
35 612 availability of establishment microsites (Tilman, 1994; Questad and Foster, 2008), so
36 613 (particularly with the shoot presence approach) the smaller “spatial granules” can hold more
37 614 species, thus lead to fine “granule” and cause a z-value peak at smaller grains.

38
39
40
41
42
43
44
45
46
47
48
49
50
51
52
53 615 Among the biogeographic variables, latitude showed the strongest effect on observed
54 616 peak position (9.4% explained variance), with a U-shaped response and a minimum at around
55 617 47° N (Fig. 4). This was also reflected in the comparison of biomes, where we found a minimum
56 618 of the peak position in the nemoral biome and particularly high values in the alpine, boreal and
57 619 dry subtropical biomes (Fig. 7). The fact that local z-values peak at particularly fine grain sizes

1
2
3
4 620 for plots from between 45 and 50 °N latitude and/or the nemoral biome might not be a
5
6 621 consequence of latitude/biome *per se*, but of higher land use intensity driven by the rather
7
8 622 benign environment of this latitude/biome. Interestingly, in the same region also the total z-
9
10 623 values (i.e. assuming a constant z) were lowest, as Dembicz *et al.* (subm.) found and attributed
11 624 this to the same likely reason.

14 625 **Conclusions and outlook**

16 626 The overall weak scale dependence of local z-values within the range 0.0001–1024 m²
17
18 627 questions the widespread search for SAR models that are more complicated than the power
19
20 628 function (see reviews by Tjørve, 2003; 2009). Instead it supports conclusions of two previous
21
22 629 GrassPlot publications (Dengler *et al.*, 2020; Dembicz *et al.*, subm.) that: (i) the power function
23
24 630 is an appropriate model to describe SARs at these scales in continuous vegetation in open
25
26 631 habitats; and (ii) deviations from the “perfect” power law are relatively minor and inconsistent.
27
28 632 Thus, for most purposes one can safely assume a constant z-value across the grain sizes studied
29
30 633 here. However, this is only true if species richness is recorded with the shoot presence method,
31
32 634 as for data recorded with the rooted presence method we found significant deviations from the
33
34 635 power law below 1 m², i.e. strongly increasing z-values. This finding matches the theory and
35
36 636 suggests that shoot presence recording is preferable when studying SARs, as this permits a
37
38 637 focus on ecological determinants of curve shapes by reducing distortion by mathematical
39 638 artifacts.

41 639 We consider SARs within the grain size range analyzed here to be mainly an expression of
42
43 640 granularity of species composition, which in turn is partly driven by granularity of the abiotic
44
45 641 environment, and partly by the growth form of the dominant species. If granule sizes vary over
46
47 642 a large range, constant z-values (no scale dependence of local z-value) should be expected,
48
49 643 while a prevalence of a particular granule size should lead to a peak of local z-values vs. grain
50
51 644 size. Scale dependence of local z-values appears to be mainly locally driven and highly
52
53 645 idiosyncratic. Of the few macroecological patterns that emerged, the responses to latitude
54
55 646 (possibly also related to land use), naturalness, and land use were most prominent. We propose
56
57 647 a mechanism explaining the effect of land use on decreasing peak z-value position, but this
58
59 648 should be tested experimentally. To explore the topic further, we also recommend conducting
60 649 simulation studies using artificial communities with varying granularity and species-abundance

distribution to understand more mechanistically how these parameters shape the details of SARs.

Acknowledgements

We would like to thank the hundreds of colleagues who obtained high-quality plant diversity data from across the Palaearctic and contributed them to GrassPlot.

Author contributions

J.De. conceived the idea of the study and led together with I.B., I.D. and R.P. the compilation and harmonisation of the data, which were contributed by most of the authors. J.Z. and F.G. conducted the statistical analyses with support from J.De., R.J., K.V.M. and S.W., while J.Z. and J.De. led the writing, with major inputs from F.G., S.B., J.M.A., and J.-A.G., I.D. and D.V. prepared the maps and all co-authors revised and approved the manuscript.

Data availability statement

The data used in this paper are derived from the collaborative vegetation-plot database GrassPlot (Dengler *et al.*, 2018; Biurrun *et al.*, 2019), version 2.09. They can be requested from GrassPlot with a project proposal following the GrassPlot Bylaws (see <https://edgg.org/databases/GrassPlot>).

References

- Arrhenius, O. (1921) Species and area. *Journal of Ecology*, **9**, 95–99. <https://www.jstor.org/stable/2255763>
- Biurrun, I., Burrascano, S., Dembicz, I., Guarino, R., Kapfer, J., Pielech, R. *et al.* (2019) GrassPlot v. 2.00: first update on the database of multi-scale plant diversity in Palaearctic grasslands. *Palaearctic Grasslands*, **44**, 26–47. <https://doi.org/10.21570/EDGG.PG.44.26-47>
- Bruelheide, H., Dengler, J., Jiménez-Alfaro, B., Purschke, O., Hennekens, S.M., Chytrý, M. *et al.* (2019) sPlot – A new tool for global vegetation analyses. *Journal of Vegetation Science*, **30**, 161–186. <https://doi.org/10.1111/jvs.12710>
- Cancellieri, L., Mancini, L.D., Sperandii, M.G. and Filibeck, G. (2017) In and out: Effects of shoot- vs. rooted-presence sampling methods on plant diversity measures in mountain grasslands. *Ecological Indicators*, **72**, 315–321. <https://doi.org/10.1016/j.ecolind.2016.08.029>

- 1
2
3
4 678 Chase, J.M., McGill, B.J., McGlinn, D.J., May, F., Blowes, S.A., Xiao, X. *et al.* (2018) Embracing
5
6 679 scale-dependence to achieve a deeper understanding of biodiversity and its change across
7
8 680 communities. *Ecology Letters*, **21**, 1737–1751. <https://doi.org/10.1111/ele.13151>
- 9
10 681 Connor, E.F. and McCoy, E.D. (1979) The statistics and biology of the species–area relationship.
11
12 682 *American Naturalist*, **113**, 791–833. <https://doi.org/10.1086/283438>
- 13
14 683 Crawley, M.J. and Harral, J.E. (2001) Scale dependence in plant biodiversity. *Science*, **291**, 864–
15
16 684 868. <https://doi.org/10.1126/science.291.5505.864>
- 17
18 685 Danielson, J.J. and Gesch, D.B. (2011) *Global multi-resolution terrain elevation data 2010*
19
20 686 *(GMTED2010)*. U.S. Geological Survey.
- 21
22 687 Dembicz, I., Velev, N., Boch, S., Janišová, M., Palpurina, S., Pedashenko, H. *et al.* (2021a) Drivers
23
24 688 of plant diversity in Bulgarian dry grasslands vary across spatial scales and functional-
25
26 689 taxonomic groups. *Journal of Vegetation Science*, **32**, e12935.
27
28 690 <https://doi.org/10.1111/jvs.12935>
- 29
30 691 Dembicz, I., Dengler, J., Steinbauer, M.J., Matthews, T.J., Bartha, S., Burrascano, S., *et al.*
31
32 692 (subm.) Patterns and drivers of fine-grain beta diversity in Palaeartic grassland vegetation.
33
34 693 *Journal of Vegetation Science*. (2nd round of review in the same Special Feature of JVS, likely
35
36 694 to be accepted before Zhang et al.)
- 37
38 695 Dengler, J., Bedall, P., Bruchmann, I., Hoefft, I. and Lang, A. (2004) Artenzahl-Areal-Beziehungen
39
40 696 in uckermärkischen Trockenrasen unter Berücksichtigung von Kleinstflächen – eine neue
41
42 697 Methode und erste Ergebnisse. *Kieler Notizen zur Pflanzenkunde in Schleswig-Holstein und*
43
44 698 *Hamburg*, **32**, 20–25.
- 45
46 699 Dengler, J. (2008) Pitfalls in small-scale species–area sampling and analysis. *Folia Geobotanica*,
47
48 700 **43**, 269–287.
- 49
50 701 Dengler, J. (2009) Which function describes the species–area relationship best? A review and
51
52 702 empirical evaluation. *Journal of Biogeography*, **36**, 728–744. [https://doi.org/10.1111/j.1365-
53
54 703 2699.2008.02038.x](https://doi.org/10.1111/j.1365-2699.2008.02038.x)
- 55
56 704 Dengler, J., Boch, S., Filibeck, G., Chiarucci, A., Dembicz, I., Guarino, R. *et al.* (2016) Assessing
57
58 705 plant diversity and composition in grasslands across spatial scales: The standardised EDGG
59
60 706 sampling methodology. *Bulletin of the Eurasian Grassland Group*, **32**, 13–30.
- 707
708 707 Dengler, J., Wagner, V., Dembicz, I., García–Mijangos, I., Naqinezhad, A., Boch, S. *et al.* (2018)
709
710 708 Grassplot – a database of multi–scale plant diversity in Palaeartic grasslands.
711
712 709 *Phytocoenologia*, **48**, 331–347. <https://doi.org/10.1127/phyto/2018/0267>

- 1
2
3
4 710 Dengler, J., Matthews, T.J., Steinbauer, M.J., Wolfrum, S., Boch, S., Chiarucci, A. *et al.* (2020)
5
6 711 Species–area relationships in continuous vegetation: Evidence from Palaeartic grasslands.
7
8 712 *Journal of Biogeography*, **47**, 72–86. <https://doi.org/10.1111/jbi.13697>
- 9
10 713 Drakare, S., Lennon, J.J. and Hillebrand, H. (2006) The imprint of the geographical, evolutionary
11
12 714 and ecological context on species–area relationships. *Ecology Letters*, **9**, 215–227.
13
14 715 <https://doi.org/10.1111/j.1461-0248.2005.00848.x>
- 15 716 Emiru, N. and Gebrekidan, H. (2013) Effect of land use changes and soil depth on soil organic
16
17 717 matter, total nitrogen and available phosphorus contents of soils in Senbat watershed,
18
19 718 western Ethiopia. *ARPN Journal of Agricultural and Biological Science*, **8**, 206–212.
- 20 719 EU-DEM v.1.1 (2020) European Digital Elevation Model (EU-DEM), version 1.1. Available at
21
22 720 <https://land.copernicus.eu/imageryin-situ/eu-dem/eu-dem-v1.1?tab=metadata> [Accessed 8
23
24 721 February 2020]
- 25
26 722 Fattorini, S., Borges, P.A., Dapporto, L. and Strona, G. (2017) What can the parameters of the
27
28 723 species–area relationship (SAR) tell us? Insights from Mediterranean islands. *Journal of*
29
30 724 *Biogeography*, **44**, 1018–1028. <https://doi.org/10.1111/jbi.12874>
- 31 725 Fridley, J.D., Peet, R.K., Wentworth, T.R. and White, P.S. (2005) Connecting fine- and broad-scale
32
33 726 species–area relationships of southeastern US flora. *Ecology*, **86**, 1172–1177.
34
35 727 <https://doi.org/10.1890/03-3187>
- 36
37 728 Gleason, H.A. (1922) On the relation between species and area. *Ecology*, **3**, 158–162.
38
39 729 <https://doi.org/10.2307/1929150>
- 40 730 Grime, J.P. (1977) Evidence for the existence of three primary strategies in plants and its
41
42 731 relevance to ecological and evolutionary theory. *American Naturalist*, **111**, 1169–1194.
43
44 732 <https://doi.org/10.1086/283244>
- 45
46 733 Grytnes, J.-A. (2000) Fine-scale vascular plant species richness in different alpine vegetation
47
48 734 types: relationship with biomass and cover. *Journal of Vegetation Science*, **11**, 87–92.
49
50 735 <https://doi.org/10.2307/3236779>
- 51 736 Güler, B., Jentsch, A., Bartha, S., Bloor, J.M.G., Campetella, G., Canullo, R. *et al.* (2016) How plot
52
53 737 shape and dispersion affect plant species richness counts: implications for sampling design
54
55 738 and rarefaction analyses. *Journal of Vegetation Science*, **27**, 692–703.
56
57 739 <https://doi.org/10.1111/jvs.12411>
- 58
59 740 Huisman, J., Olff, H. and Fresco, L.F.M. (1993) A hierarchical set of models for species response
60
741 analysis. *Journal of Vegetation Science*, **4**, 37–46. <https://doi.org/10.2307/3235732>

- 1
2
3
4 742 Huston, M.A. (2014) Disturbance, productivity, and species diversity: empirism vs. logic in
5
6 743 ecological theory. *Ecology*, **95**, 2382–2396. <https://doi.org/10.1890/13-1397.1>
- 7
8 744 Karger, D.N., Conrad, O., Böhner, J., Kawohl, T., Kreft, H., Soria-Auza, R.W. *et al.* (2017)
9
10 745 Climatologies at high resolution for the earth's land surface areas. *Scientific Data*, **4**, 170122.
11
12 746 <https://doi.org/10.1038/sdata.2017.122>
- 13
14 747 Kent, M. (2012) *Vegetation description and data analysis – a practical approach*, 2nd edition
15
16 748 Chichester, UK: Wiley-Blackwell.
- 17
18 749 Koleff, P., Gaston, K.J. and Lennon, J.J. (2003) Measuring β -diversity for presence-absence data.
19
20 750 *Journal of Animal Ecology*, **72**, 367–382. <https://doi.org/10.1046/j.1365-2656.2003.00710.x>
- 21
22 751 Kotliar, N.B. and Wiens, J.A. (1990) Multiple scales of patchiness and patch structure: a
23
24 752 hierarchical framework for the study of heterogeneity. *Oikos*, **59**, 253–260.
25
26 753 <https://doi.org/10.2307/3545542>
- 27
28 754 Kuzemko, A.A., Steinbauer, M.J., Becker, T., Didukh, Y.P., Dolnik, C., Jeschke, M. *et al.* (2016)
29
30 755 Patterns and drivers of phytodiversity in steppe grasslands of Central Podolia (Ukraine).
31
32 756 *Biodiversity and Conservation*, **25**, 1–18. <https://doi.org/10.1007/s10531-016-1060-7>
- 33
34 757 Lawton, J.H. (1999) Are there general laws in ecology? *Oikos*, **84**, 177–192.
35
36 758 <https://doi.org/10.2307/3546712>
- 37
38 759 MacArthur, R.H. and Wilson, E.O. (1967) *The theory of island biogeography*. Princeton:
39
40 760 Princeton University Press.
- 41
42 761 Mangeney, A., Roche, O., Hungr, O., Mangold, N., Faccanoni, G. and Lucas, A. (2010) Erosion
43
44 762 and mobility in granular collapse over sloping beds. *Journal of Geophysical Research*, **115**,
45
46 763 F03040. <https://doi.org/10.1029/2009JF001462>
- 47
48 764 Matthews, T.J., Guilhaumon, F., Triantis, K.A., Borregaard, M.K. and Whittaker, R.J. (2016) On
49
50 765 the form of species–area relationships in habitat islands and true islands. *Global Ecology and*
51
52 766 *Biogeography*, **25**, 847–858. <https://doi.org/10.1111/geb.12269>
- 53
54 767 Matthews, T.J., Rigal, F., Triantis, K.A. and Whittaker, R.J. (2019) A global model of island
55
56 768 species–area relationships. *Proceedings of the National Academy of Sciences of the USA*, **116**,
57
58 769 12337–12342. <https://doi.org/10.1073/pnas.1818190116>
- 59
60 770 McGill, B.J. (2019) The what, how and why of doing macroecology. *Global Ecology and*
771
Biogeography, **28**, 6–17. <https://doi.org/10.1111/geb.12855>

- 1
2
3
4 772 Oksanen, J. and Minchin, P.R. (2002) Continuum theory revisited: what shape are species
5 responses along ecological gradients? *Ecological Modelling*, **157**, 119–129.
6 773 [https://doi.org/10.1016/S0304-3800\(02\)00190-4](https://doi.org/10.1016/S0304-3800(02)00190-4)
7 774
8
9 775 O'Sullivan, J.D., Knell, R.J. and Rossberg, A.G. (2019) Metacommunity–scale biodiversity
10 regulation and the self–organised emergence of macroecological patterns. *Ecology Letters*,
11 776 **22**, 2168–2168. <https://doi.org/10.1111/ele.13294>
12 777
13
14 778 Patiño, J., Weigelt, P., Guilhaumon, F., Kreft, H., Triantis, K.A., Naranjo-Cigala, A. *et al.* (2014)
15 779 Differences in species–area relationships among the major lineages of land plants: a
16 macroecological perspective. *Global Ecology and Biogeography*, **23**, 1275–1283.
17 780 <https://doi.org/10.1111/geb.12230>
18 781
19
20 782 Plotkin, J.B., Potts, M.D., Yu, D.W., Bunyavejchewin, S., Condit, R., Foster, R. *et al.* (2000)
21 783 Predicting species diversity in tropical forests. *Proceedings of the National Academy of*
22 784 *Sciences of the USA*, **97**, 10850–10854. <https://doi.org/10.1073/pnas.97.20.10850>
23 785
24
25 786 Polyakova, M.A., Dembicz, I., Becker, T., Becker, U., Demina, O.N., Ermakov, N. *et al.* (2016)
26 787 Scale–and taxon–dependent patterns of plant diversity in steppes of Khakassia, South Siberia
27 788 (Russia). *Biodiversity and Conservation*, **25**, 2251–2273. <https://doi.org/10.1007/s10531-016-1093-y>
28 789
29
30 790 Qiao, X., Tang, Z., Shen, Z. and Fang, J. (2012) What causes geographical variation in the
31 791 species–area relationships? A test from forests in China. *Ecography*, **35**, 1110–1116.
32 792 <https://doi.org/10.1111/j.1600-0587.2011.06869.x>
33 793
34
35 794 Questad, E.J. and Foster, B.L. (2008) Coexistence through spatio-temporal heterogeneity and
36 795 species sorting in grassland plant communities. *Ecology Letters*, **11**, 717–726.
37 796 <https://doi.org/10.1111/j.1461-0248.2008.01186.x>
38 797
39
40 798 R Development Core Team (2016) R: A language and environment for statistical computing.
41 799 Vienna, AT: R Foundation for Statistical Computinga.
42 800
43
44 801 Roslin, T., Várkonyi, G., Koponen, M., Vikberg, V. and Nieminen, M. (2014) Species–area
45 802 relationships across four trophic levels – decreasing island size truncates food chains.
46 803 *Ecography*, **37**, 443–453. <https://doi.org/10.1111/j.1600-0587.2013.00218.x>
47 804
48
49 805 Sanaei, A., Ali, A., Chahouki, M.A.Z. and Jafari, M. (2018) Plant coverage is a potential ecological
50 806 indicator for species diversity and aboveground biomass in semi-steppe rangelands.
51 807 *Ecological Indicators*, **93**, 256–266. <https://doi.org/10.1016/j.ecolind.2018.05.011>
52 808
53
54
55
56
57
58
59
60

- 1
2
3
4 803 Schoener, T. (1976) The species–area relation within archipelagos: models and evidence from
5
6 804 island land birds. *Proceedings of the XVI International Ornithological Congress*, 6, 629–642.
7
8 805 Schrader, J., Moeljono, S., Keppel, G. and Kreft, H. (2019) Plants on small islands revisited:
9
10 806 The effects of spatial scale and habitat quality on the species–area relationship. *Ecography*,
11 807 **42**, 1405–1414. <https://doi.org/10.1111/ecog.04512>
12
13 808 Shmida, A. and Wilson, M.V. (1985) Biological determinants of species diversity. *Journal of*
14 809 *Biogeography*, **12**, 1–20. <https://doi.org/10.2307/2845026>
15
16 810 Sreekar, R., Katabuchi, M., Nakamura, A., Corlett, R.T., Slik, J.W.F., Fletcher, C. *et al.* (2018)
17 811 Spatial scale changes the relationship between beta diversity, species richness and latitude.
18 812 *Royal Society Open Science*, **5**, Article 181168. <https://doi.org/10.1098/rsos.181168>
19
20 813 Sugihara, G. (1980) Minimal community structure: an explanation of species abundance
21 814 patterns. *American Naturalist*, **116**, 770–787. <https://doi.org/10.1086/283669>
22
23 815 ter Braak, C.J.F. and Looman, C.W.N. (1986) Weighted averaging, logistic regression and the
24 816 Gaussian response model. *Vegetatio*, **65**, 3–11.
25
26 817 Tilman, D. (1994) Competition and biodiversity in spatially structured habitats. *Ecology*, **75**, 2–
27 818 16. <https://doi.org/10.2307/1939377>
28
29 819 Tjørve, E. (2003) Shapes and functions of species–area curves: a review of possible models.
30 820 *Journal of Biogeography*, **30**, 827–835. <https://doi.org/10.1046/j.1365-2699.2003.00877.x>
31
32 821 Tjørve, E. (2009) Shapes and functions of species–area curves (II): a review of new models and
33 822 parameterizations. *Journal of Biogeography*, **36**, 1435–1445.
34 823 <https://doi.org/10.1111/j.1365-2699.2009.02101.x>
35
36 824 Tjørve, E., Calf Tjørve, K.M., Šizlingová, E. and Šizling, A.L. (2018) Great theories of species
37 825 diversity in space and why they were forgotten: The beginnings of a spatial ecology and the
38 826 Nordic early 20th-century botanists. *Journal of Biogeography*, **45**, 530–540.
39 827 <https://doi.org/10.1111/jbi.13158>
40
41 828 Triantis, K.A., Guilhaumon, F. and Whittaker, R.J. (2012) The island species–area relationship:
42 829 biology and statistics. *Journal of Biogeography*, **39**, 215–231.
43 830 <https://doi.org/10.1111/j.1365-2699.2011.02652.x>
44
45 831 Turtureanu, P.D., Palpurina, S., Becker, T., Dolnik, C., Ruprecht, E., Sutcliffe, L.M. *et al.* (2014)
46 832 Scale–and taxon–dependent biodiversity patterns of dry grassland vegetation in
47 833 Transylvania. *Agriculture, Ecosystems & Environment*, **182**, 15–24.
48 834 <https://doi.org/10.1016/j.agee.2013.10.028>
49
50
51
52
53
54
55
56
57
58
59
60

- 1
2
3
4 835 van der Maarel, E. and Franklin, J. (Eds.) (2013) *Vegetation ecology*, 2nd edition. Chichester, UK:
5
6 836 Wiley-Blackwell.
7
8 837 Williams, M.R., Lamont, B.B. and Henstridge, J.D. (2009) Species–area functions revisited.
9
10 838 *Journal of Biogeography*, **36**, 1994–2004. <https://doi.org/10.1111/j.1365-2699.2009.02110.x>
11
12 839 Williamson, M. (2003) Species–area relationships at small scales in continuum vegetation.
13
14 840 *Journal of Ecology*, **91**, 904–907. <https://doi.org/10.1046/j.1365-2745.2003.00816.x>.
15
16 841 Wu, J. and Loucks O.L. (1995) From balance of nature to hierarchical patch dynamics: a
17
18 842 paradigm shift in ecology. *The Quarterly Review of Biology*, **70**, 439–464.
19
20 843 <https://www.journals.uchicago.edu/doi/10.1086/419172>
21
22 844

23 845 **Supporting Information**

24
25 846 Additional supporting information may be found online in the Supporting Information section.

26
27
28 847 Appendix S1. Methodological details

29
30 848 Appendix S2. Additional detailed results

31
32
33 849

For Review Only

34
35
36
37
38
39
40
41
42
43
44
45
46
47
48
49
50
51
52
53
54
55
56
57
58
59
60

Supporting Information to the paper Zhang, J. *et al.* Scale dependence of species-area relationships is widespread but generally weak in Palearctic grasslands *Journal of Vegetation Science*.

Appendix S1. Methodological details.

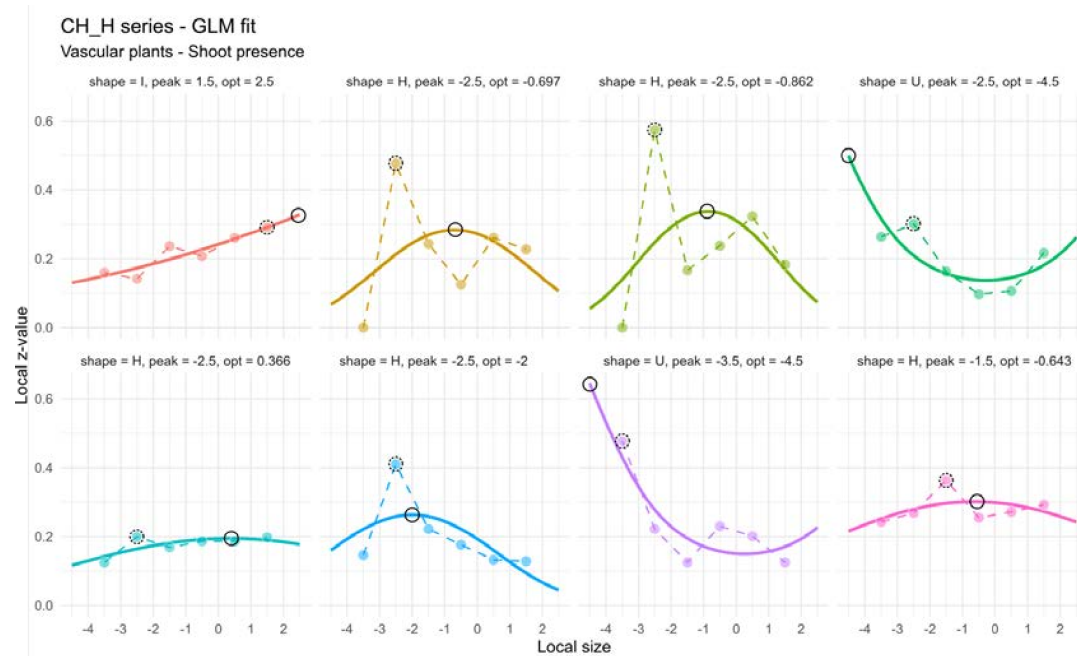


Figure S1.1. Actual local z-values and fitted Gaussian curves for the dataset CH_H series from GrassPlot (subalpine and alpine habitats in Grisons, Switzerland, sampled by J. Dengler and colleagues). The shape of each individual curve and the maximum z value are determined in the interval of the observed local scale ± 1 . H: hump-shaped (Gaussian); U: U-shaped (inverse Gaussian); I: monotonic increasing; peak (dotted circle): actual local scale of the maximum local z-value; opt (plain circle): local scale of the maximum fitted local z-value.

Table S1.1. The curve parameters with peak recognition for the eight nested-plot series in CH_H (see Fig. S1.1). Peak_act: actual local grain of the maximum observed local z-value; Peak_mod: local grain of the maximum fitted local z-value.

SeriesID	Shape	Peak_act	Peak_mod	b0	b1	b2	Opt	Tol	Max
CH_H_N001_100	I	1.5	2.5	-1.145	0.169	0.000	-203.636	NA	0.000
CH_H_N002_100	H	-2.5	-0.697	-0.984	-0.164	-0.118	-0.697	2.059	0.284
CH_H_N003_100	H	-2.5	-0.862	-0.797	-0.283	-0.164	-0.862	1.745	0.337
CH_H_N004_100	U	-2.5	-4.5	-1.828	0.059	0.103	-0.285	NA	0.137
CH_H_N005_100	H	-2.5	0.366	-1.424	0.019	-0.025	0.366	4.440	0.195
CH_H_N006_100	H	-2.5	-1.997	-1.431	-0.403	-0.101	-1.997	2.226	0.263
CH_H_N007_100	U	-3.5	-4.5	-1.733	-0.054	0.103	0.263	NA	0.149
CH_H_N008_100	H	-1.5	-0.643	-0.855	-0.039	-0.030	-0.643	4.077	0.301

Table S1.2. Predictor variables used to explain the position of the peak local z-value, grouped into four broad categories.

Predictor variables [with units]	Type	Explanation	Source(s)
1. Taxonomic group			
Taxonomic group	Categorical	Vascular plants, bryophytes, lichens, and complete vegetation (all groups sampled simultaneously)	GrassPlot (Dengler <i>et al.</i> , 2018)
2. Biogeographic characteristics			
Latitude [°]	Metric		GrassPlot (Dengler <i>et al.</i> , 2018)
Elevation [m a.s.l.]	Metric		GrassPlot (Dengler <i>et al.</i> , 2018)
Mean annual temperature [°C]	Metric	-	CHELSA (Karger <i>et al.</i> , 2017)
Mean annual precipitation [mm]	Metric	-	CHELSA (Karger <i>et al.</i> , 2017)
Temperature seasonality [°C]	Metric	Temperature variation over a given year (or averaged years) based on the standard deviation (variation) of monthly temperature averages	CHELSA (Karger <i>et al.</i> , 2017)
Precipitation seasonality [%]	Metric	Measure of the variation in monthly precipitation totals over the course of the year	CHELSA (Karger <i>et al.</i> , 2017)
3. Ecological (site) characteristics			
3.1 Productivity			
Soil pH	Metric	In upper soil layer, measured in H ₂ O	GrassPlot (Dengler <i>et al.</i> , 2018)
Soil depth mean [cm]	Metric	Mean of five random measurements within a plot	GrassPlot (Dengler <i>et al.</i> , 2018)
Vegetation cover [%]	Metric	Estimated in the field	GrassPlot (Dengler <i>et al.</i> , 2018)
Herb layer cover [%]	Metric	Estimated in the field	GrassPlot (Dengler <i>et al.</i> , 2018)
3.2 Disturbance			
Slope inclination [°]	Metric	Measured in the field	GrassPlot (Dengler <i>et al.</i> , 2018)
Litter cover [%]	Metric	Estimated in the field	GrassPlot (Dengler <i>et al.</i> , 2018)
Naturalness - at fine level	Categorical	no series for 1c – natural grasslands, overused): 1 – natural grasslands (1a – not managed, 1b – extensively managed); 2 – anthropogenic grasslands (2a – semi-natural, 2b – semi-intensified, 2c - intensified	GrassPlot (Dengler <i>et al.</i> , 2018)
Livestock grazing	Binary	Grazed vs. not grazed grassland	GrassPlot (Dengler <i>et al.</i> , 2018)
Mowing	Binary	Mown vs. not mown grassland	GrassPlot (Dengler <i>et al.</i> , 2018)
Burning	Binary	Burnt vs. unburnt grassland	GrassPlot (Dengler <i>et al.</i> , 2018)
Fertilization	Binary	Fertilized vs. unfertilized grassland	GrassPlot (Dengler <i>et al.</i> , 2018)
Managed	Binary	Managed vs. not managed	GrassPlot (Dengler <i>et al.</i> , 2018)
3.3 Heterogeneity			
Soil depth CV [cm]	Metric	Standard deviation of five random measurements	GrassPlot (Dengler <i>et al.</i> , 2018)
Rock and stone cover [%]	Metric	Estimated in the field as independent from vegetation cover and adding up to 100% with cover of gravel and fine soil	GrassPlot (Dengler <i>et al.</i> , 2018)

Predictor variables [with units]	Type	Explanation	Source(s)
Shrub layer cover [%]	Metric	Estimated in the field	GrassPlot (Dengler <i>et al.</i> , 2018)
4. Vegetation typology			
Biome	Categorical	Six biomes represented in the analyzed, among nine types distinguished in GrassPlot (as shown in Fig. S2.4) according to a recent classification by Bruelheide <i>et al.</i> (2019, based on Schultz, 2005 and Körner <i>et al.</i> , 2017), for details see Biurrun <i>et al.</i> (2019)	GrassPlot (Dengler <i>et al.</i> , 2018)
Vegetation group	Categorical	Six groups, for the details see Biurrun <i>et al.</i> 2019	GrassPlot (Dengler <i>et al.</i> , 2018)
Vegetation type	Categorical	20 vegetation types represented in the analysed data, among 22 types distinguished in GrassPlot (see Biurrun <i>et al.</i> , 2019)	GrassPlot (Dengler <i>et al.</i> , 2018)

References

- Biurrun, I., Burrascano, S., Dembiczy, I., Guarino, R., Kapfer, J., Pielech, R. *et al.* (2019) GrassPlot v. 2.00 – first update on the database of multi-scale plant diversity in Palaeartic grasslands. *Palaeartic Grasslands*, **44**, 26–47. <https://doi.org/10.21570/EDGG.PG.44.26-47>
- Bruelheide, H., Dengler, J., Jiménez-Alfaro, B., Purschke, O., Hennekens, S.M., Chytrý, M. *et al.* (2019) sPlot – a new tool for global vegetation analyses. *Journal of Vegetation Science*, **30**, 161–186. <https://doi.org/10.1111/jvs.12710>
- Dengler, J., Wagner, V., Dembiczy, I., García-Mijangos, I., Naqinezhad, A., Boch, S. *et al.* (2018) GrassPlot – a database of multi-scale plant diversity in Palaeartic grasslands. *Phytocoenologia*, **48**, 331–347.
- Karger, D.N., Conrad, O., Böhner, J., Kawohl, T., Kreft, H., Soria-Auza, R.W. *et al.* (2017) Climatologies at high resolution for the earth's land surface areas. *Scientific Data*, **4**, Article 170122. <https://doi.org/10.1038/sdata.2017.122>
- Körner, C., Jetz, W., Paulsen, J., Payne, D., Rudmann-Maurer, K. and Spehn, E.M. (2017) A global inventory of mountains for biogeographical applications. *Alpine Botany*, **127**, 1–15. <https://doi.org/10.1007/s00035-016-0182-6>
- Schultz, J. (2005) *The ecozones of the world. The ecological division of the geosphere*, 2nd edition. Berlin: Springer.

Table S1.3. Numbers of plots and series for all data and theoretically possible values of local $0 \leq z \leq 1$ used in the analysis. Number of plots, grain size transitions/pairs and nested plot series with at least seven grain sizes, local z -values were > 1 or < 0 .

Recording method	Shoot presence					Root presence					Total				
	Plot	grain size transitions/pairs	Number of Local $z < 0$	Number of Local $z > 1$	nested plot series with at least 7 grain sizes	Plot	grain size transitions/pairs	Number of Local $z < 0$	Number of Local $z > 1$	nested plot series with at least 7 grain sizes	Plot	grain size transitions/pairs	Number of Local $z < 0$	Number of Local $z > 1$	nested plot series with at least 7 grain sizes
Vascular plants	154942	22698	292	166	2114	21642	6137	13	27	275	177138	29276	317	196	2442
Bryophytes	11605	2651	6	5	500	4126	1423	50	25	119	15797	4109	57	30	622
Lichens	17896	1289	4	3	291	4126	694	5	10	71	22061	2000	10	13	364
Complete vegetation	11410	4179	9	2	636	4126	1610	6	15	130	15602	5845	15	17	772

Supporting Information to the paper Zhang, J. *et al.* Scale dependence of species-area relationships is widespread but generally weak in Palaeartic grasslands *Journal of Vegetation Science*.

Appendix S2. Additional detailed results.

Table S2.1. Shapes of fitted curves.

Taxonomic group	Total series	Shape	Number of series	Percent (%)
Complete vegetation	621	Hump-shaped (H)	396	64
		U-shaped (U)	133	21
		Decreasing (D)	79	13
		Increasing (I)	13	2
Vascular plants	1825	Hump-shaped (H)	1105	61
		U-shaped (U)	497	27
		Decreasing (D)	194	11
		Increasing (I)	29	1
Bryophytes	238	Hump-shaped (H)	118	50
		U-shaped (U)	102	42
		Decreasing (D)	9	4
		Increasing (I)	9	4
Lichens	78	Hump-shaped (H)	56	72
		U-shaped (U)	17	22
		Decreasing (D)	5	6
		Increasing (I)	0	0

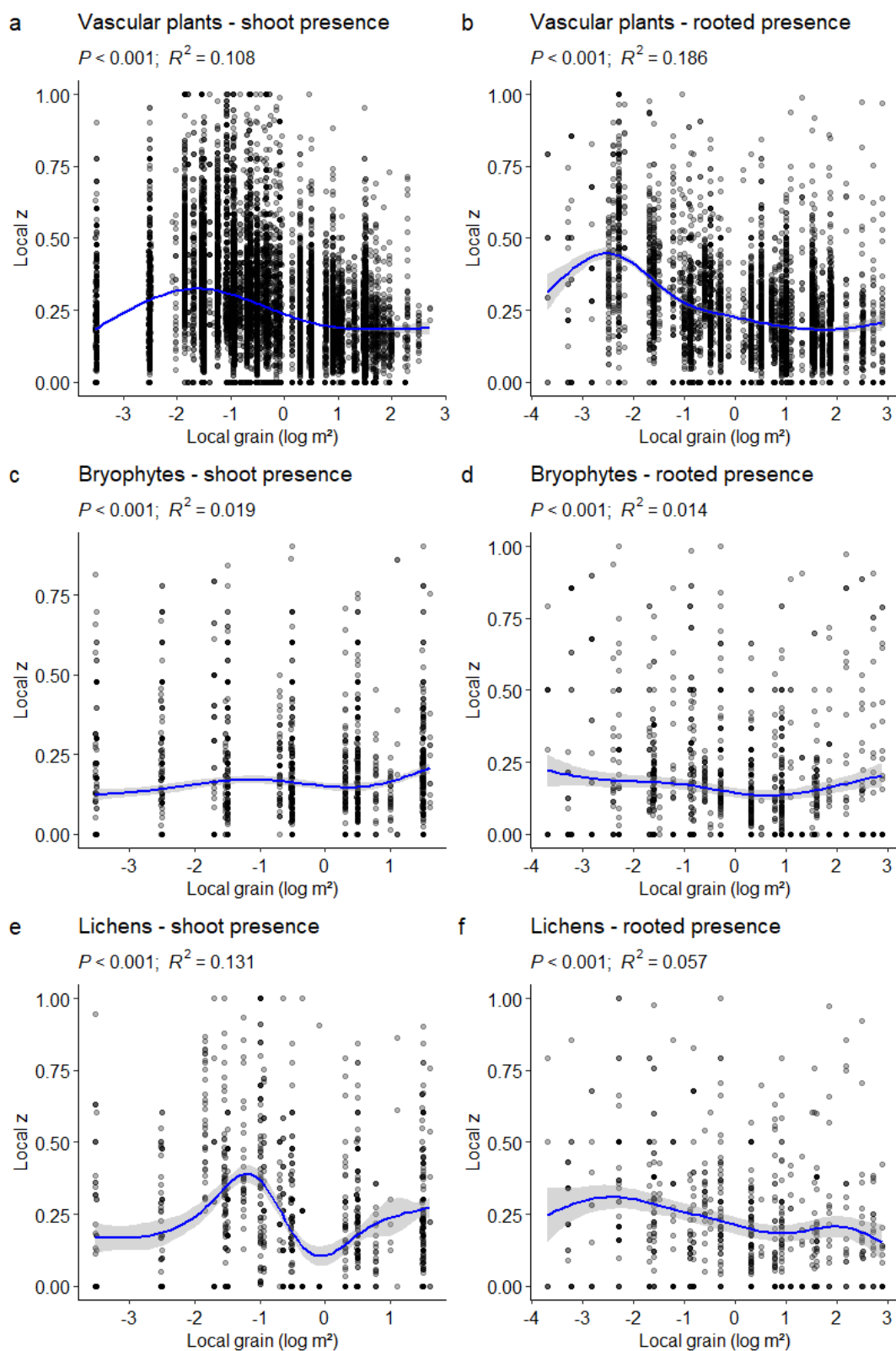


Figure S2.1. Generalized additive models (GAMs) of the effect of local grain on local z for (a, b) vascular plants, (c, d) bryophytes, and (e, f) lichens, with data obtained using two different ways of recording plants: (a, c, e) shoot presence and (b, d, f) rooted presence (excluding theoretically impossible values of local $z > 1$ or < 0).

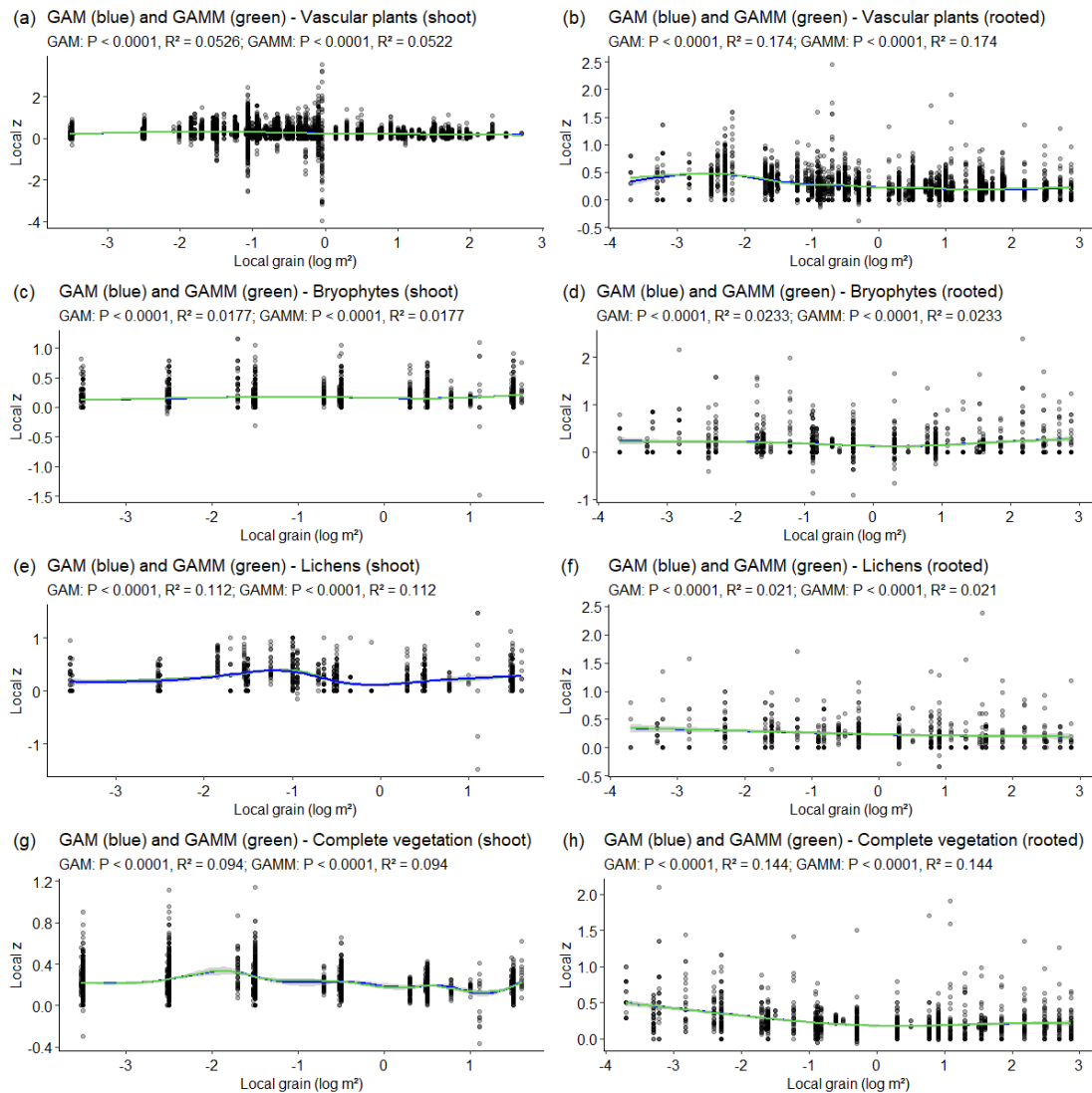


Figure S2.2. Generalized additive models (GAMs) and generalized additive mixed models (GAMMs) of the effect of local grain on local z for (a,b) vascular plants, (c,d) bryophytes, (e,f) lichens, and (g,h) with data obtained using two different ways of recording plants: (a,c,e,g) shoot presence and (b,d, f,h) root presence (with all data).

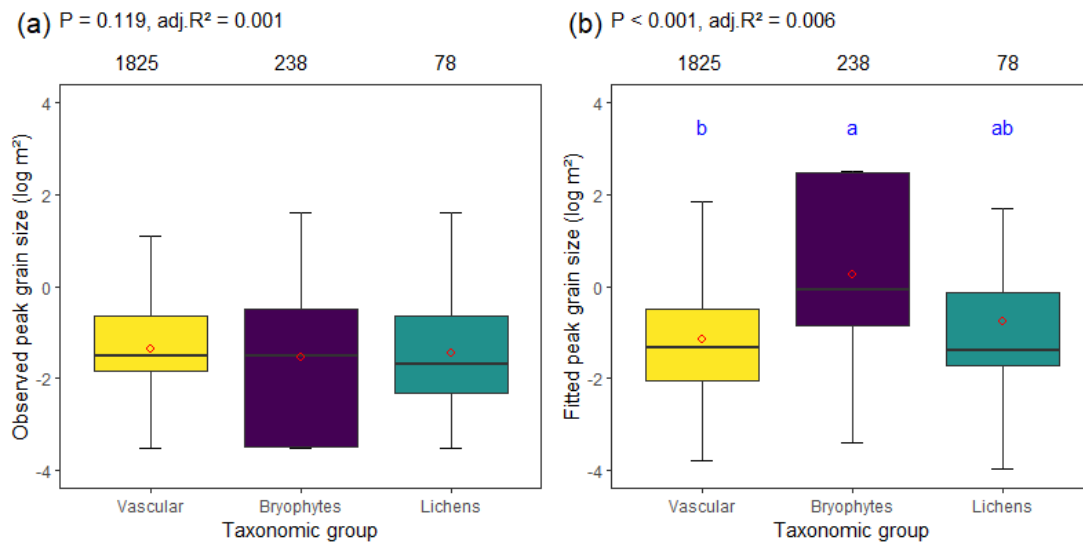


Figure S2.3. Differences in observed peak grain size (a) and fitted peak grain size (b) among taxonomic groups recorded by shoot presence. Blue lowercase letters indicate homogeneous groups ($P < 0.05$) according to Tukey's post-hoc tests.



Figure S2.4. Spatial distribution of the grain sizes of observed peak for vascular plants. The values are given as \log_{10} of area in m^2 . The colours of the background refer to the biomes distinguished in GrassPlot.

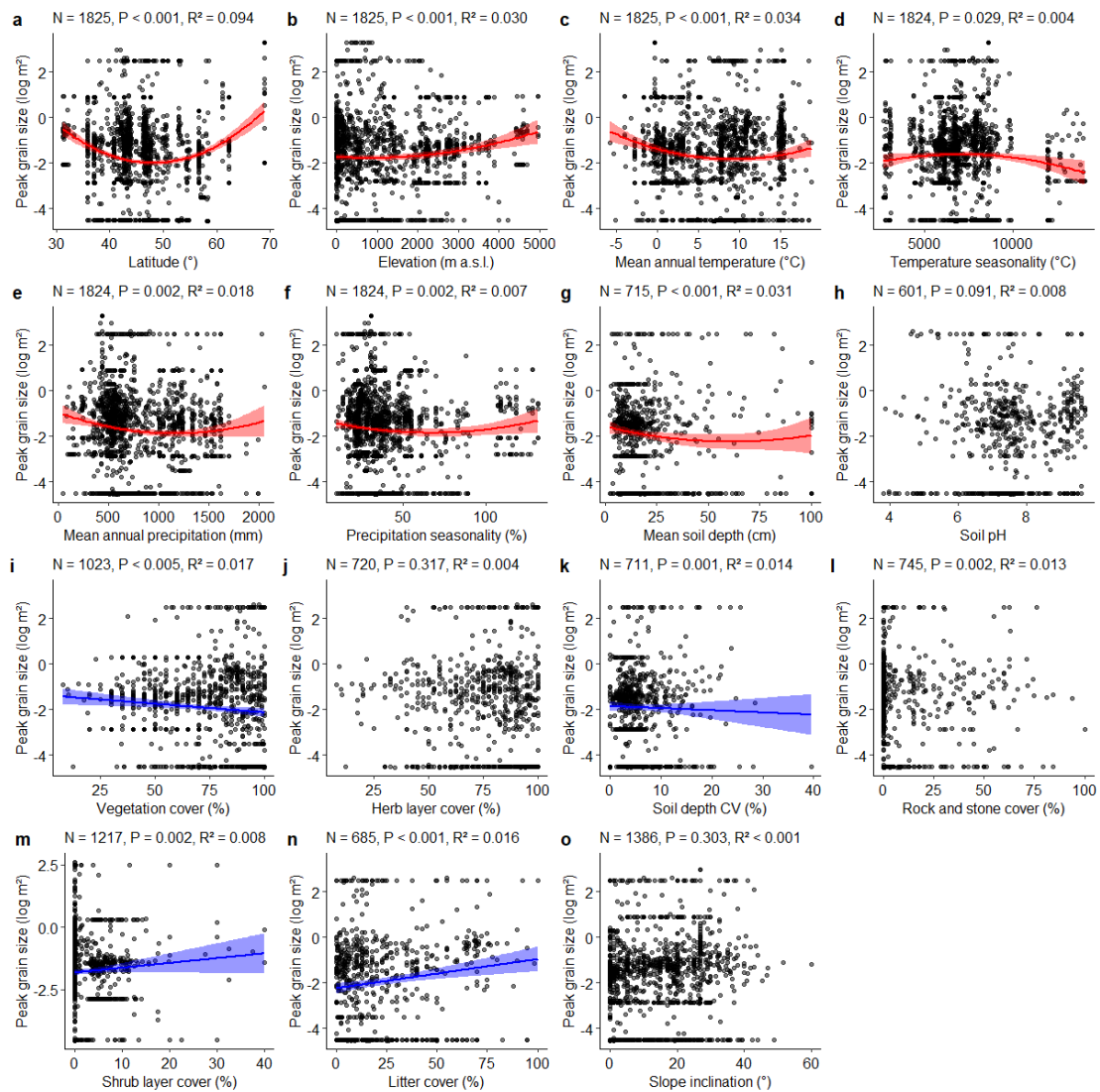


Figure S2.5. Differences in observed peak grain size (local grain size where the maximum local z occurred) of vascular plants ($R^2 < 0.02$) depending on predictor variables. Blue lines indicate significant linear relationships ($p < 0.05$) with confidence intervals, red lines represent quadratic relationships ($p < 0.05$) with confidence intervals.

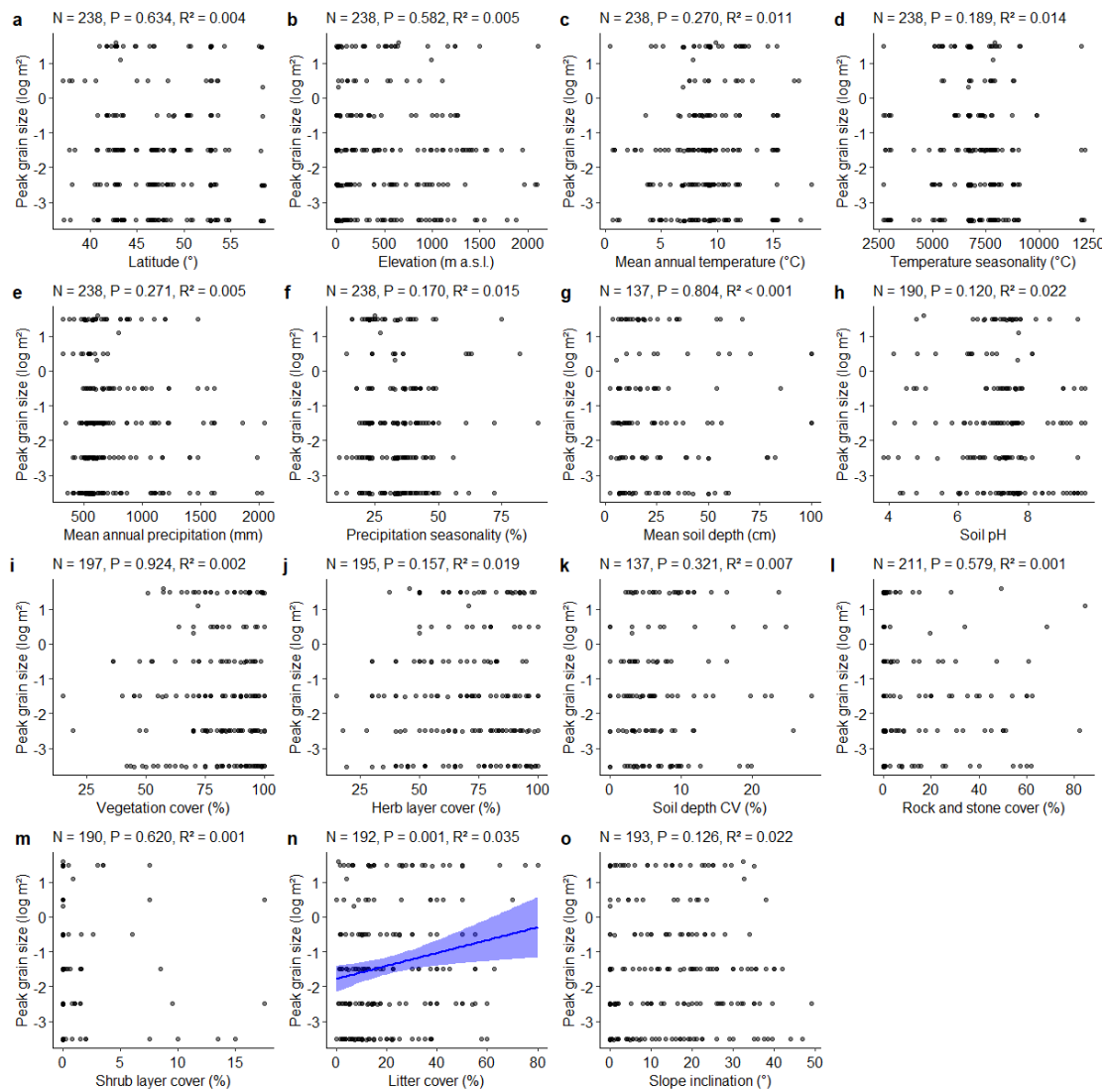


Figure S2.6. Differences in observed peak grain size (local grain size where the maximum local z occurred) of bryophytes depending on predictor variables. Blue lines indicate significant linear relationships ($p < 0.05$) with confidence intervals, red lines represent quadratic relationships ($p < 0.05$) with confidence intervals.

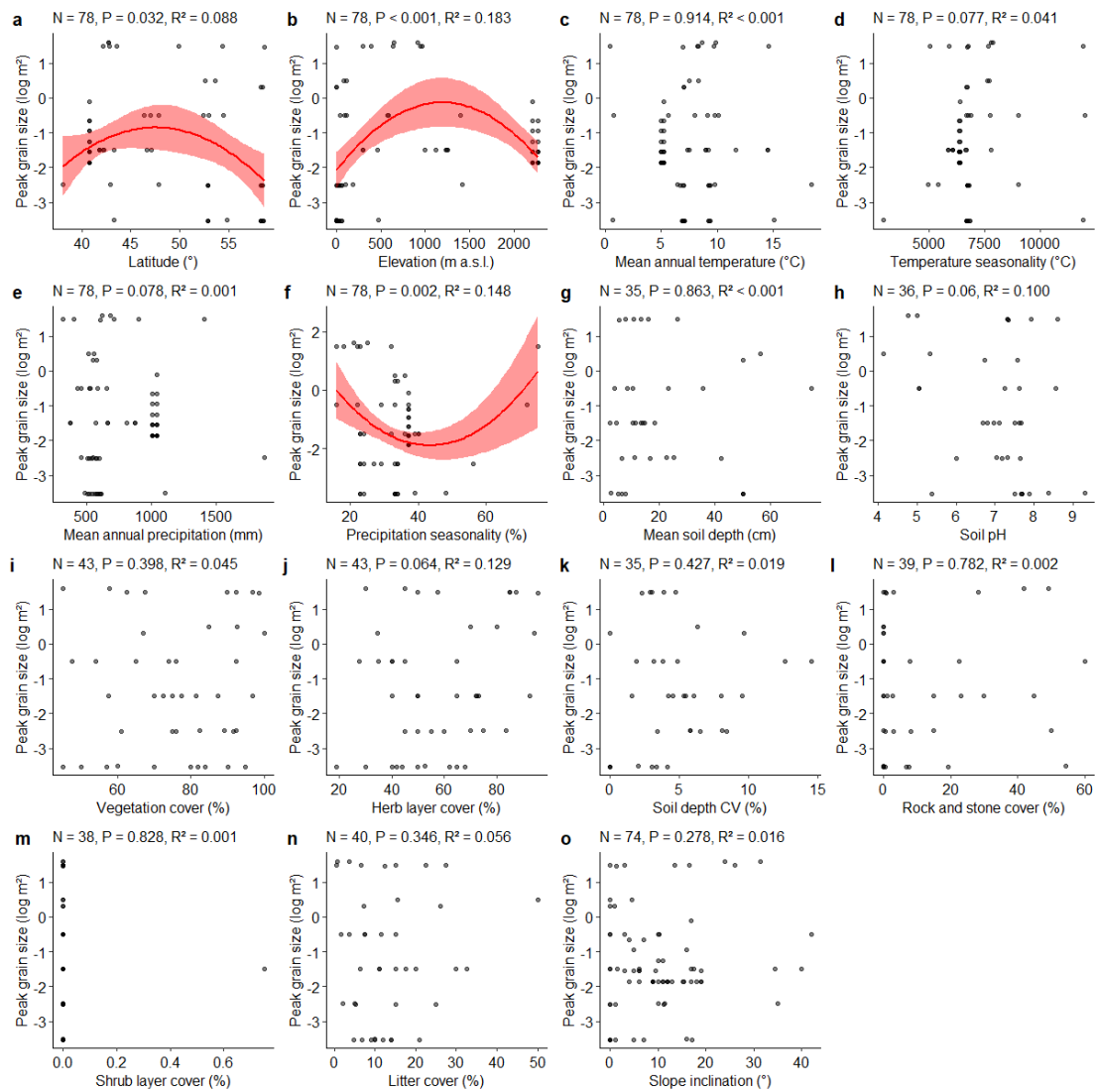


Figure S2.7. Differences in observed peak grain size (local grain size where the maximum local z occurred) of lichens depending on predictor variables. Blue lines indicate significant linear relationships ($p < 0.05$) with confidence intervals, Red lines represent quadratic relationships ($p < 0.05$) with confidence intervals.

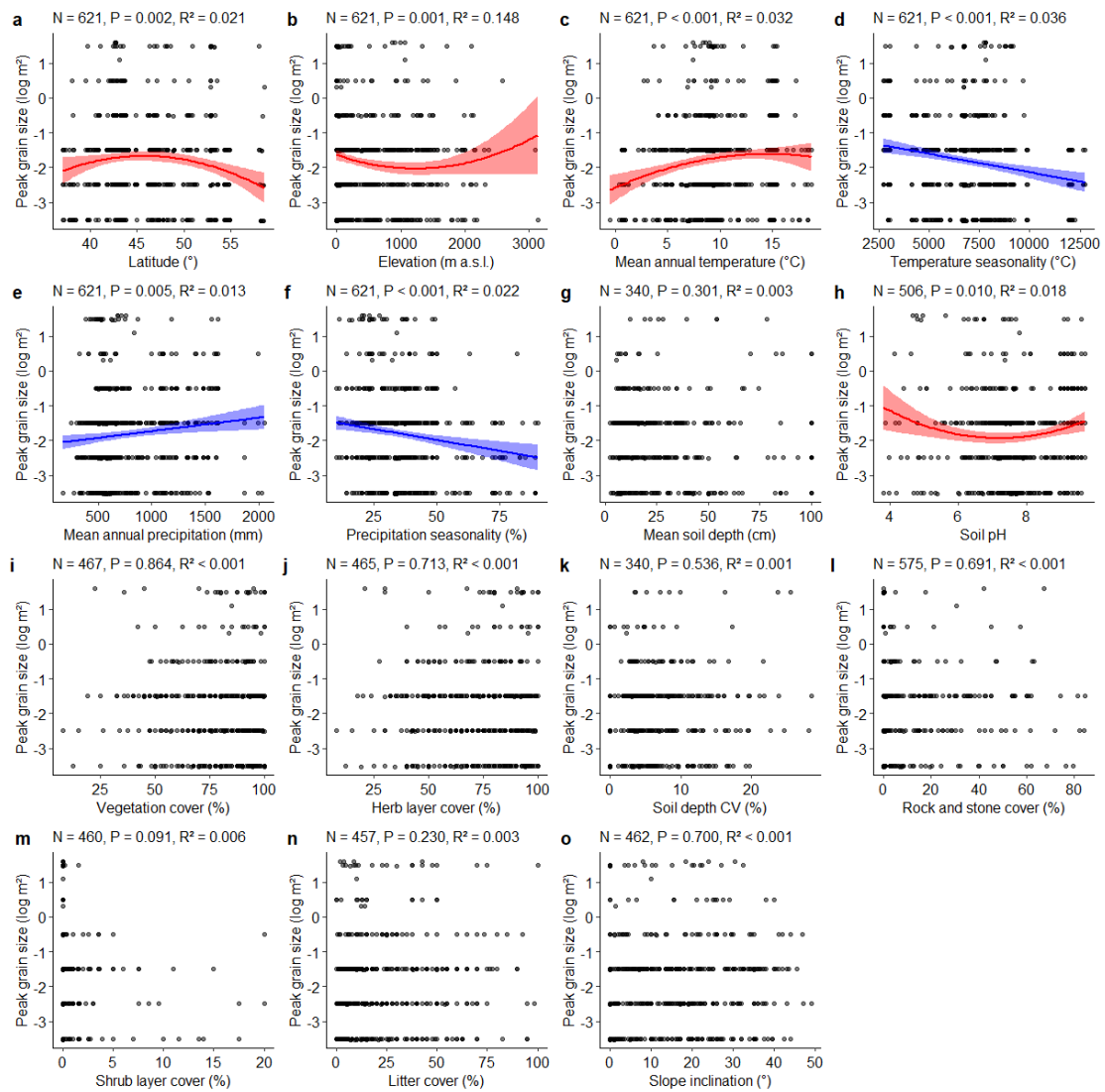


Figure S2.8. Differences in observed peak grain size (local grain size where the maximum local z occurred) of complete vegetation depending on predictor variables. Blue lines indicate significant linear relationships ($p < 0.05$) with confidence intervals; red lines represent quadratic relationships ($p < 0.05$) with confidence intervals.

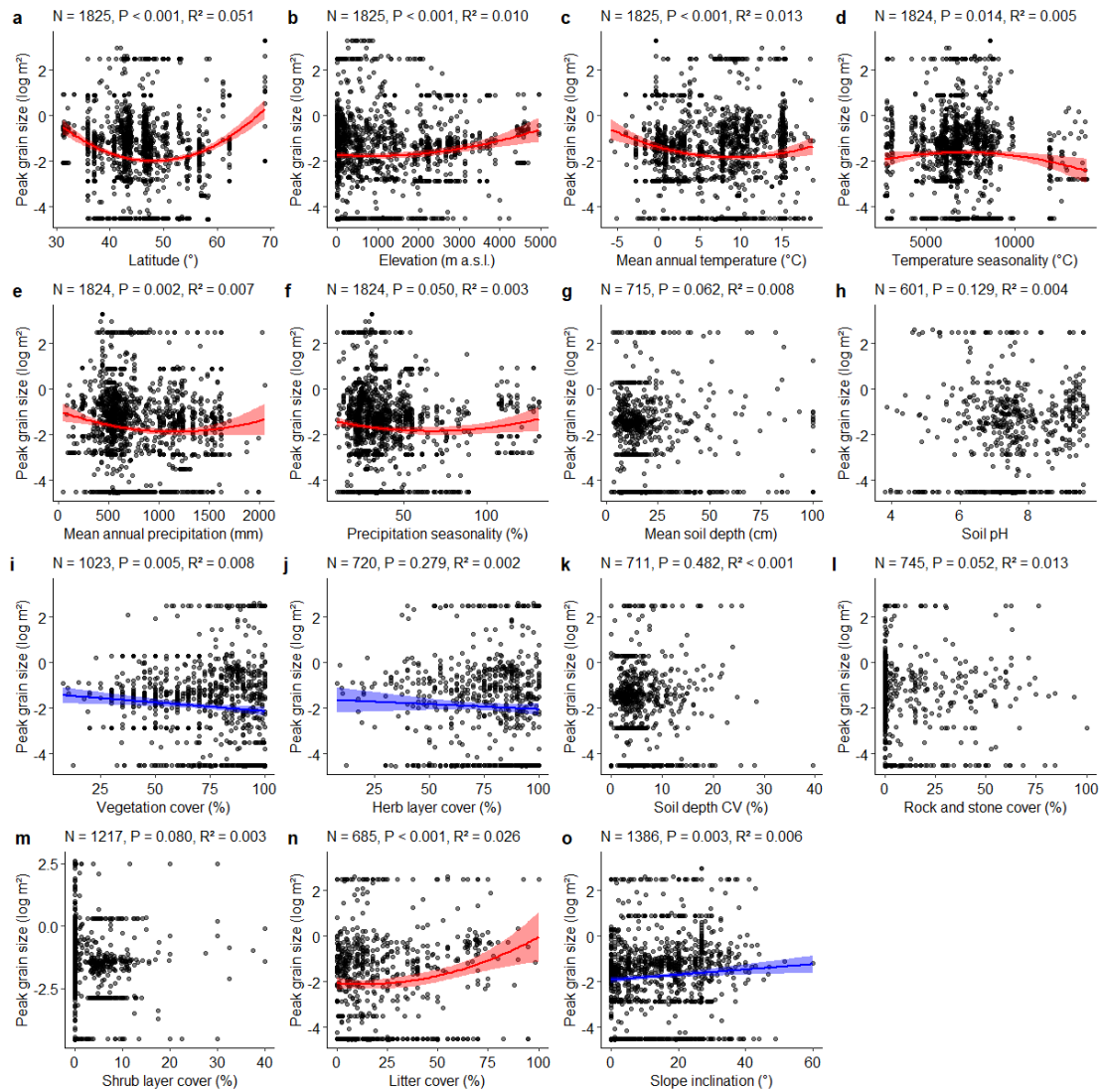


Figure S2.9. Differences in fitted peak grain size (local grain size where the maximum local z was predicted) for vascular plants depending on predictor variables. Blue lines indicate significant linear relationships ($p < 0.05$) with confidence intervals; red lines represent quadratic relationships ($p < 0.05$) with confidence intervals.

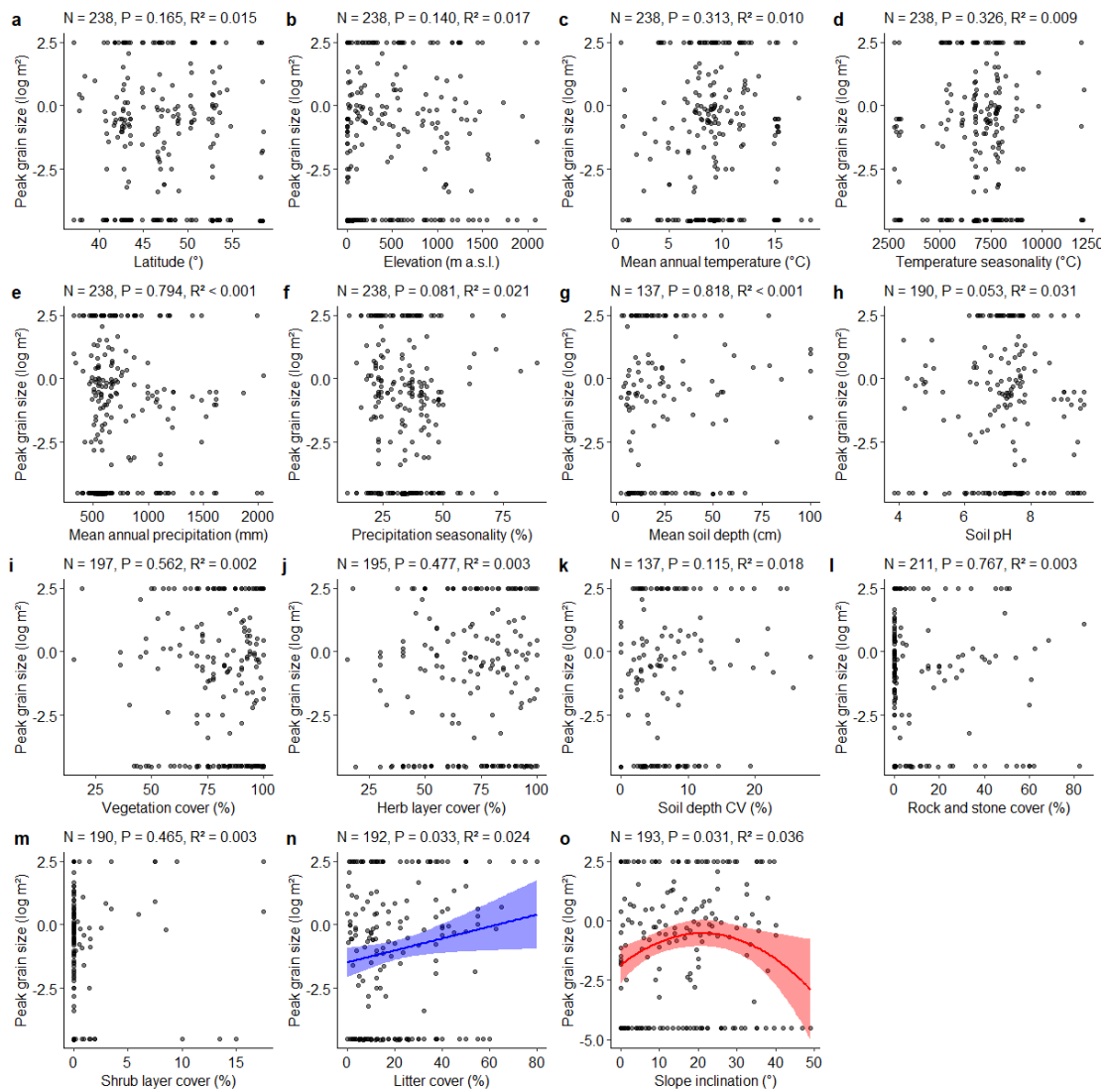


Figure S2.10. Differences in fitted peak grain size (local grain size where the maximum local z was predicted) for bryophytes depending on predictor variables. Blue lines indicate significant linear relationships ($p < 0.05$) with confidence intervals; red lines represent quadratic relationships ($p < 0.05$) with confidence intervals.

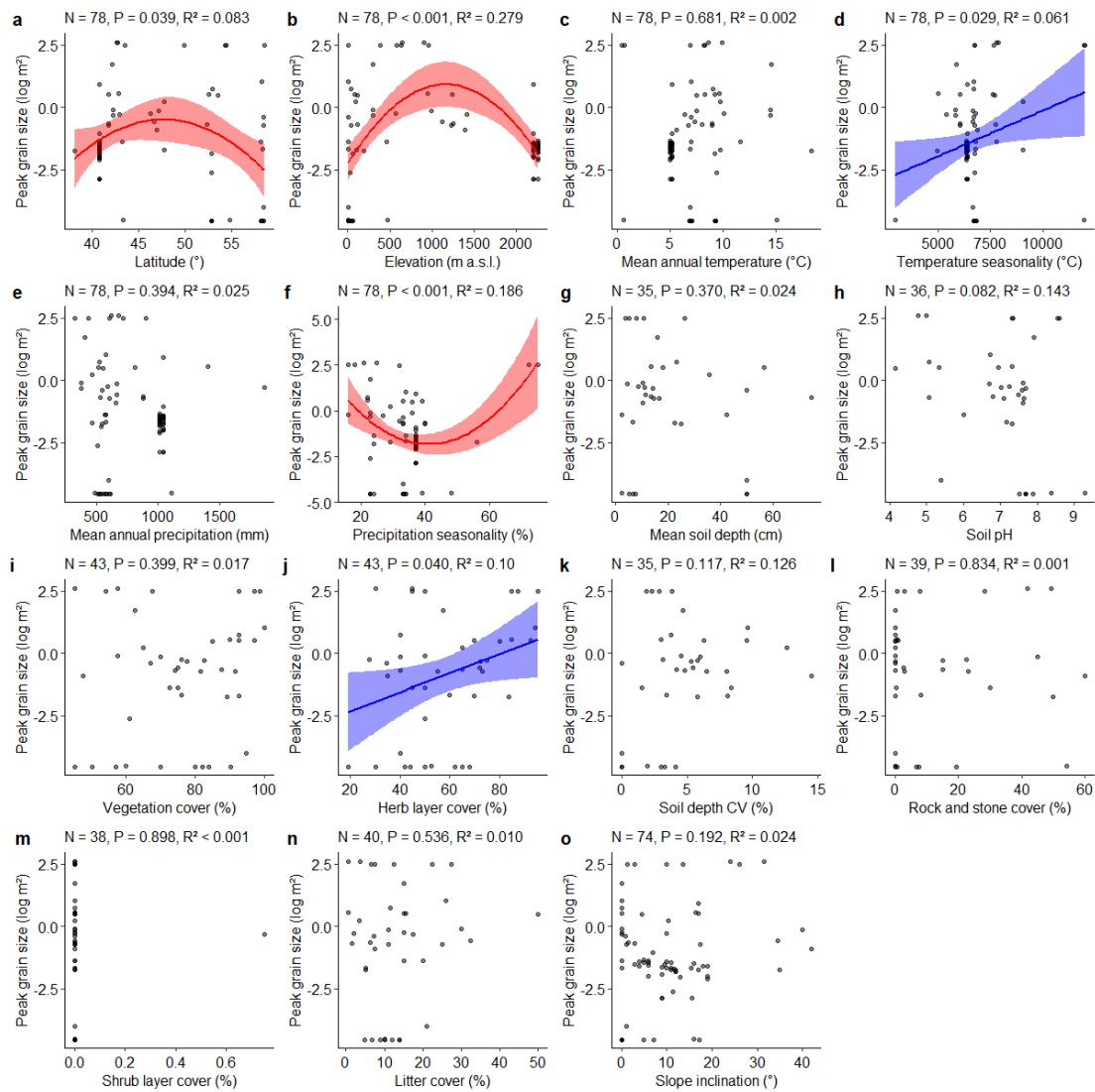


Figure S2.11. Differences in fitted peak grain size (local grain size where the maximum local z was predicted) for lichens depending on predictor variables. Blue lines indicate significant linear relationships ($p < 0.05$) with confidence intervals; red lines represent quadratic relationships ($p < 0.05$) with confidence intervals.

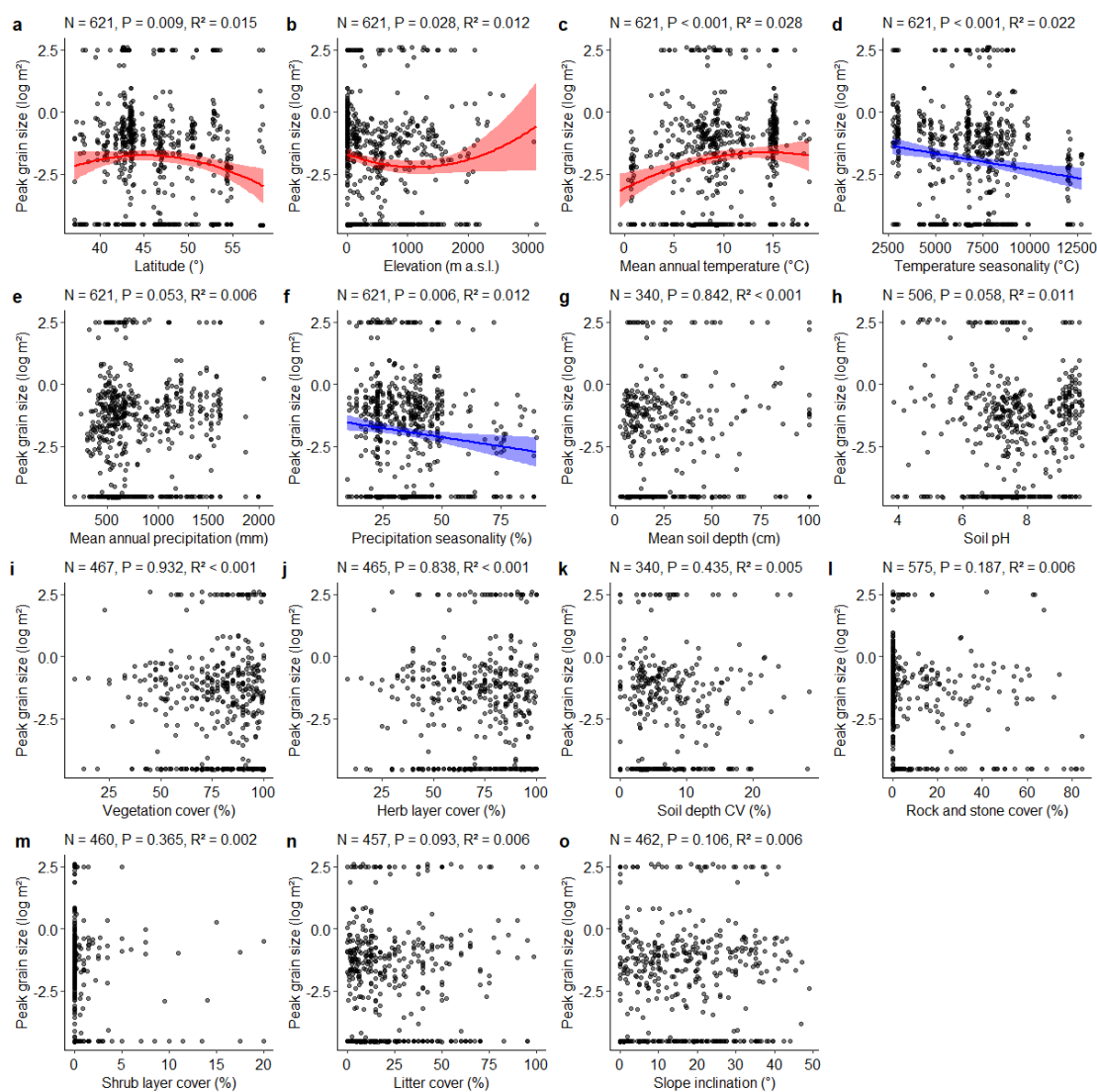


Figure S2.12. Differences in fitted peak grain size (local grain size where the maximum local z was predicted) for complete vegetation depending on predictor variables. Blue lines indicate significant linear relationships ($p < 0.05$) with confidence intervals; red lines represent quadratic relationships ($p < 0.05$) with confidence intervals.

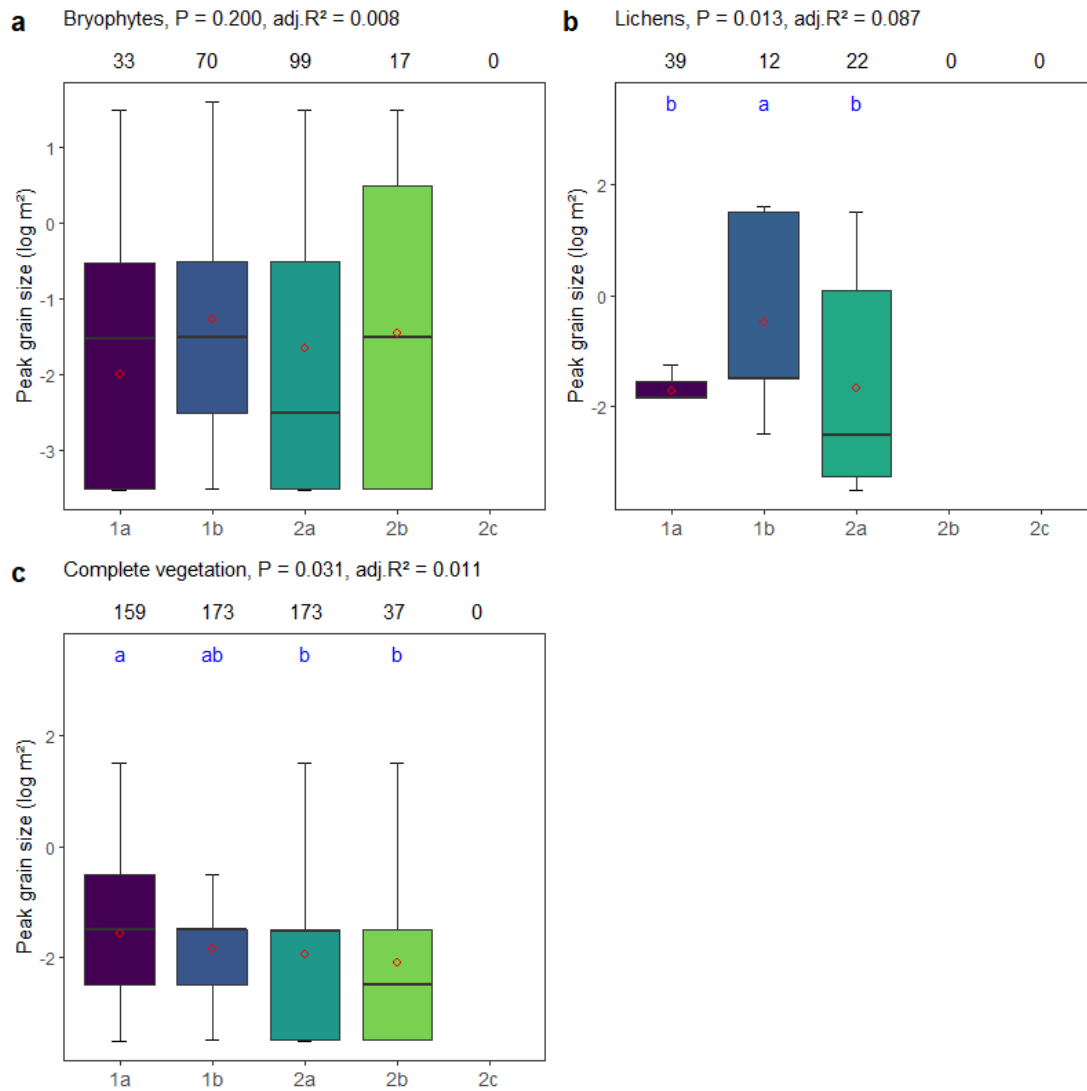


Figure S2.13. Comparison of observed peak grain size (local grain size where the maximum local z occurred) at the five levels of naturalness present in this study (no series for 1c – natural grasslands, overused): 1 – natural grasslands (1a – not managed, 1b – extensively managed); 2 – secondary grasslands (2a – semi-natural, 2b – semi-intensified, 2c – intensified). Blue lowercase letters indicate homogeneous groups ($P < 0.05$) as tested with Tukey's post-hoc test ANOVA, the figures on top indicate the sample size. Box and whisker plots represent the median and ± 1.5 IQR (interquartile range) while the red dots represent the mean values for each naturalness.

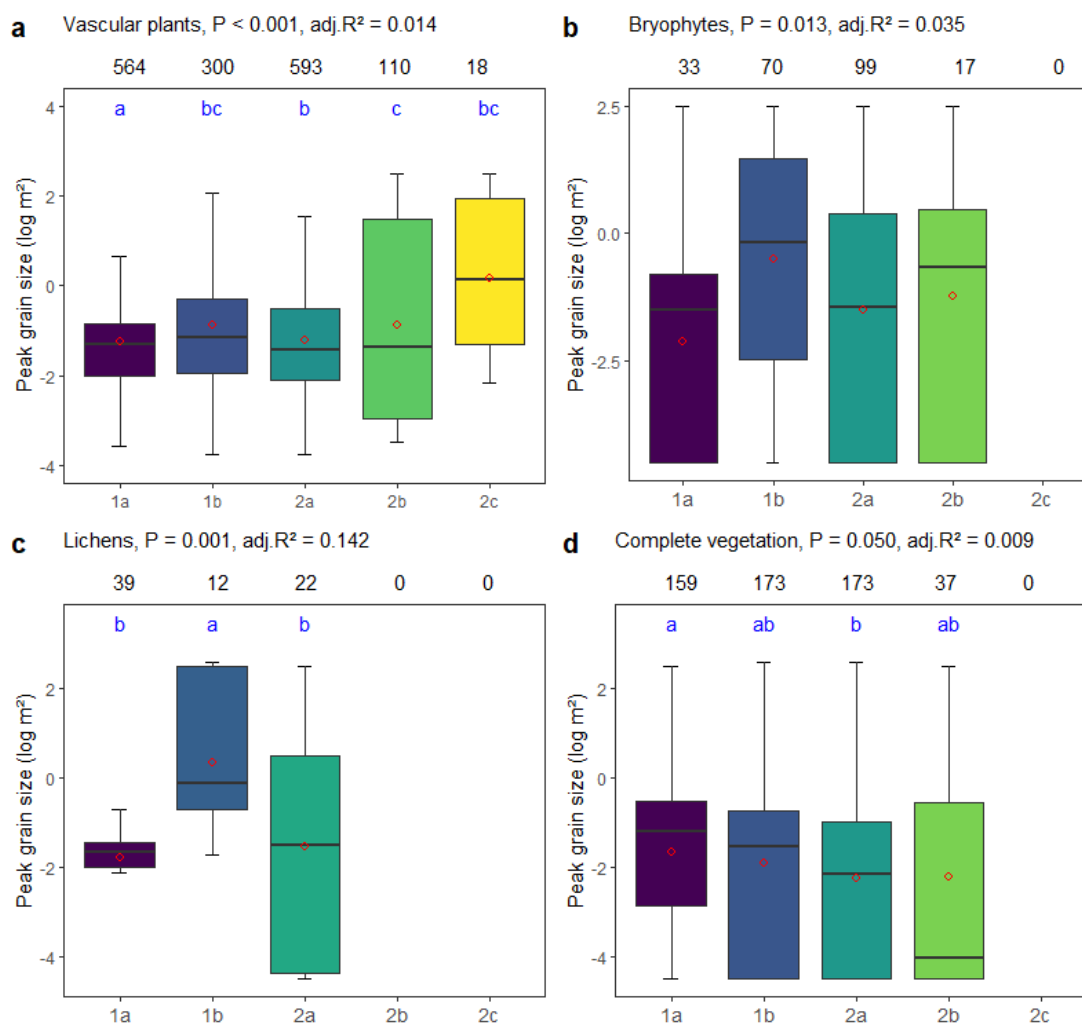


Figure S2.14. Comparison of fitted peak grain size (local grain size where the maximum local z was predicted) for a) vascular plants, b) bryophytes, c) lichens, d) complete vegetation in the five levels of naturalness considered in the study (no series for 1c – natural grasslands, overused): 1 – natural grasslands (1a – not managed, 1b – extensively managed); 2 – secondary grasslands (2a – semi-natural, 2b – semi-intensified, 2c – intensified). Blue lowercase letters indicate homogeneous groups ($p < 0.05$) as tested with Tukey's post-hoc test with ANOVA.

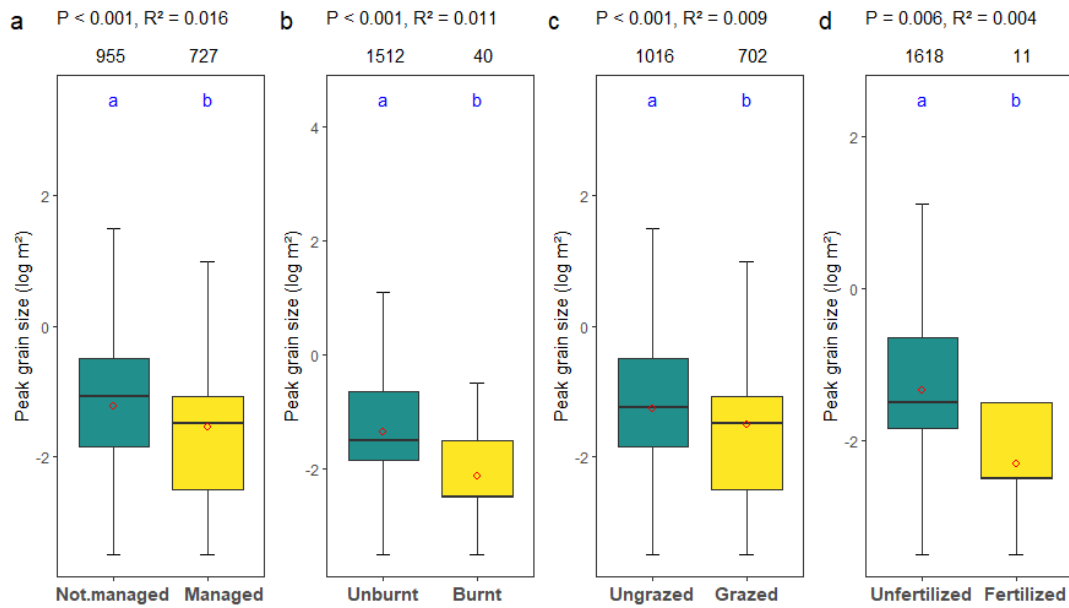


Figure S2.15. Comparison of effect of land use on observed peak grain size (local grain size where the maximum local z occurred) for vascular plants.

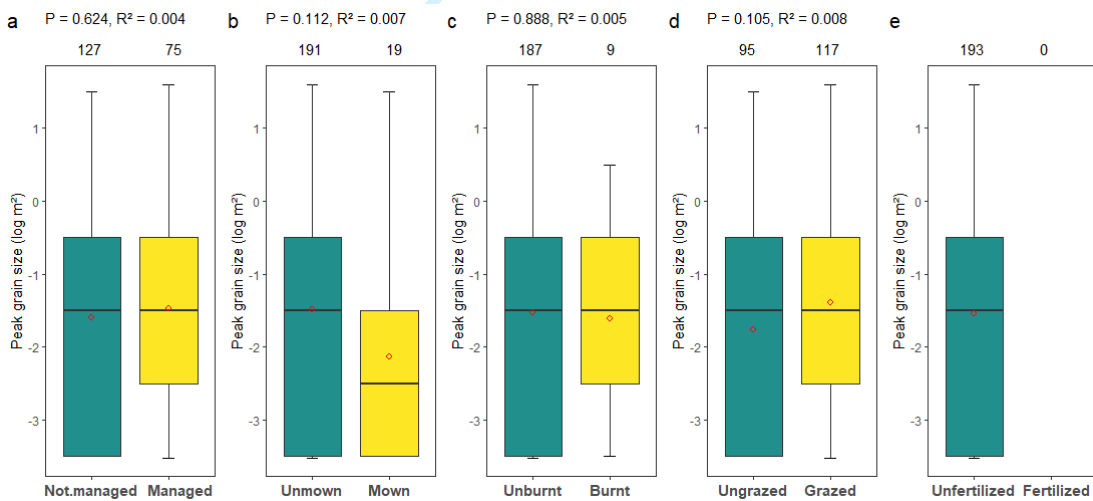


Figure S2.16. Comparison of effect of land use on observed peak grain size (local grain size where the maximum local z occurred) for bryophytes.

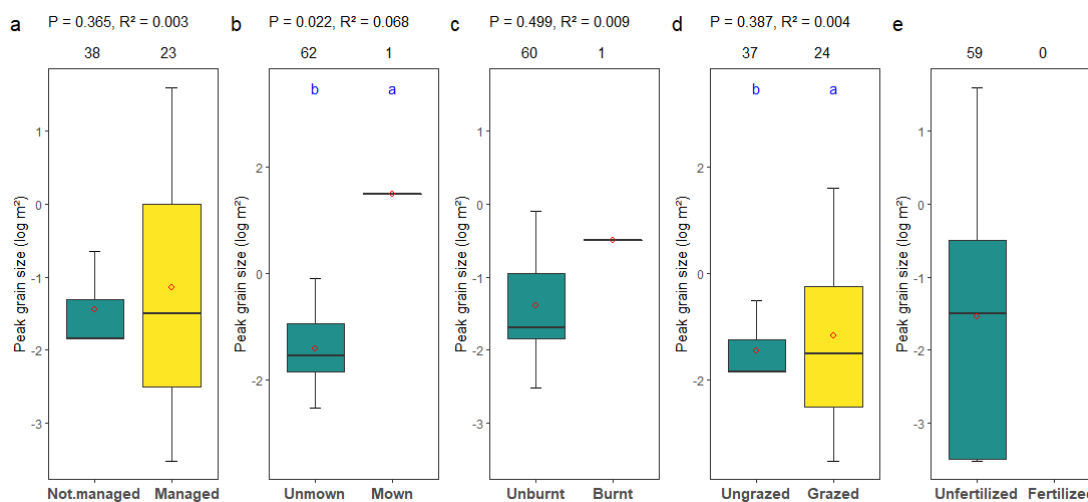


Figure S2.17. Comparison of effect of land use on observed peak grain size (local grain size where the maximum local z occurred) for lichens.

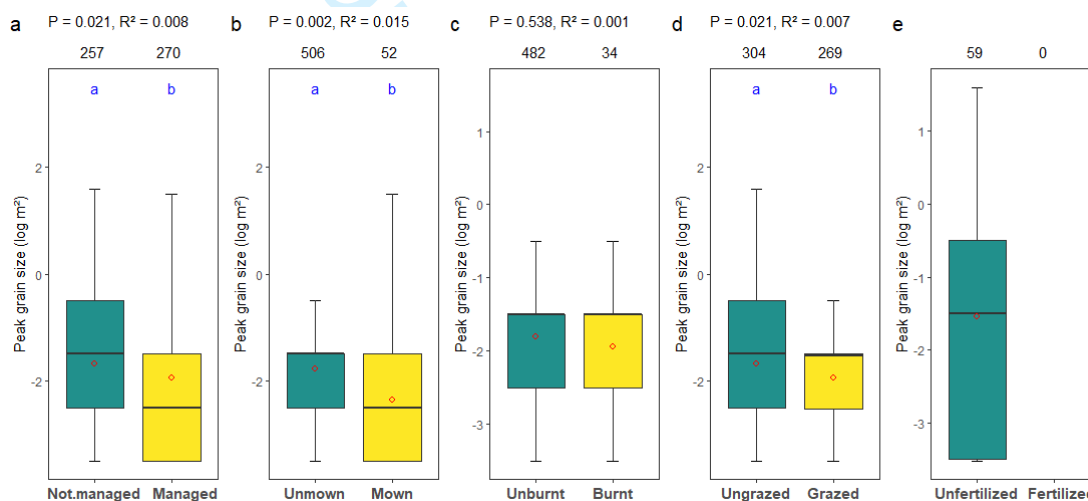


Figure S2.18. Comparison of effect of land use on observed peak grain size (local grain size where the maximum local z occurred) for complete vegetation.

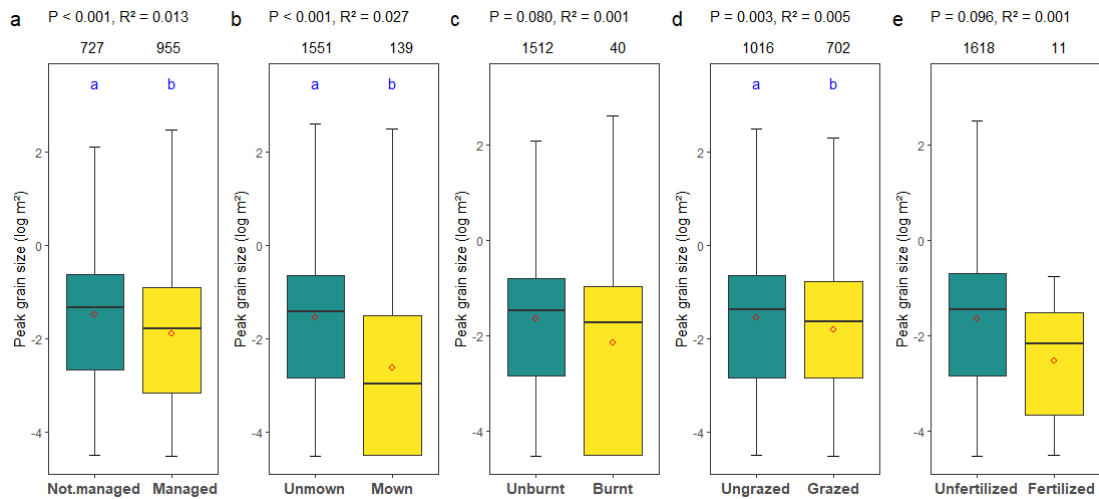


Figure S2.19. Comparison of effect of land use on fitted peak grain size (local grain size where the maximum local z was predicted) for vascular plants.

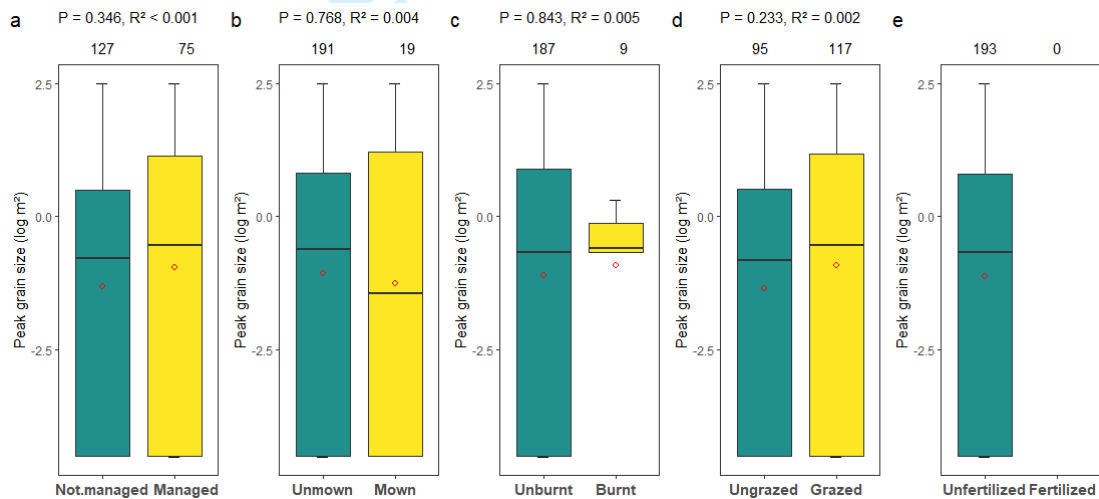


Figure S2.20. Comparison of effect of land use on fitted peak grain size (local grain size where the maximum local z was predicted) for bryophytes.

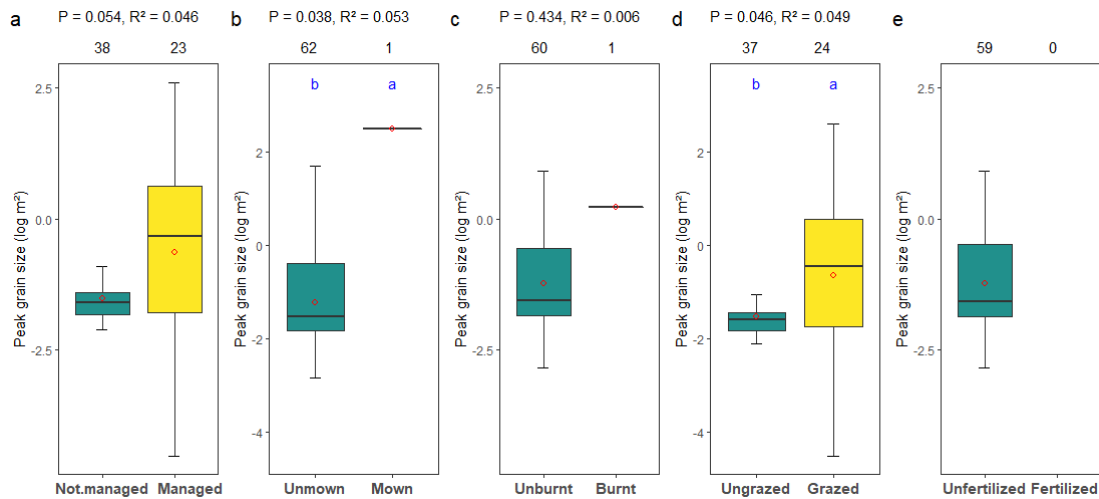


Figure S2.21. Comparison of effect of land use on fitted peak grain size (local grain size where the maximum local z was predicted) for lichens.

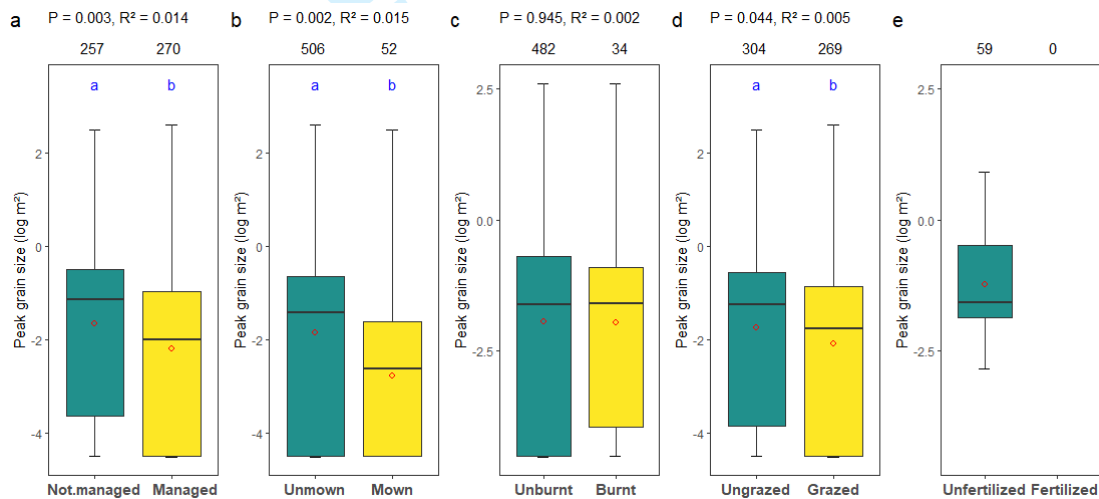


Figure S2.22. Comparison of effect of land use on fitted peak grain size (local grain size where the maximum local z was predicted) for complete vegetation.

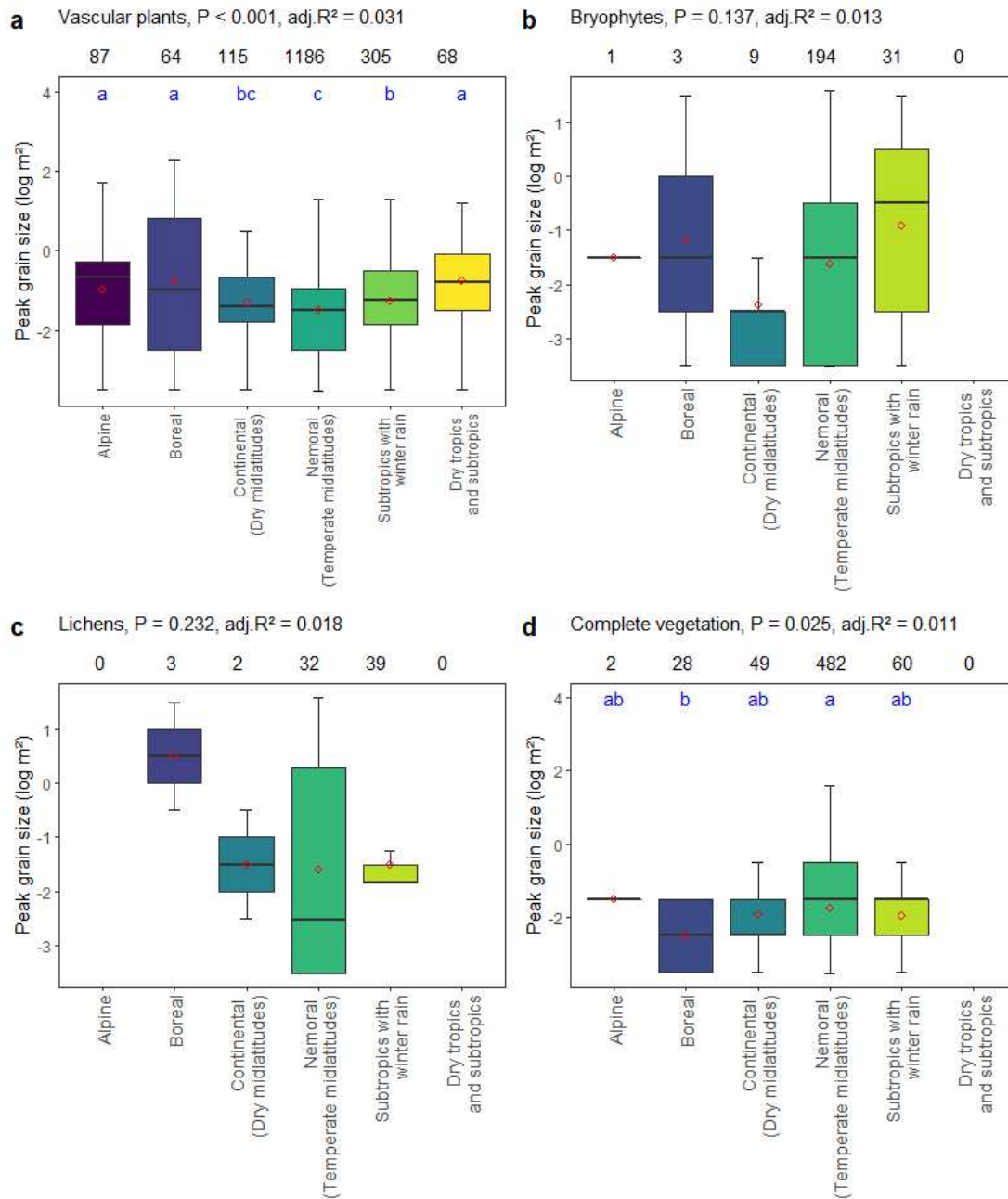


Figure S2.23. Comparison of observed peak grain size (local grain size where the maximum local z occurred) for a) vascular plants, b) bryophytes, c) lichens, d) complete vegetation between the six biomes considered in this study. A common blue lower-case letter between two boxes indicates homogeneous groups as tested with Tukey's post-hoc test with ANOVA ($P < 0.05$), the figures on top indicate the numbers of data. Box and whisker plots represent the median and quartiles while the red dots represent the mean values for each biome.

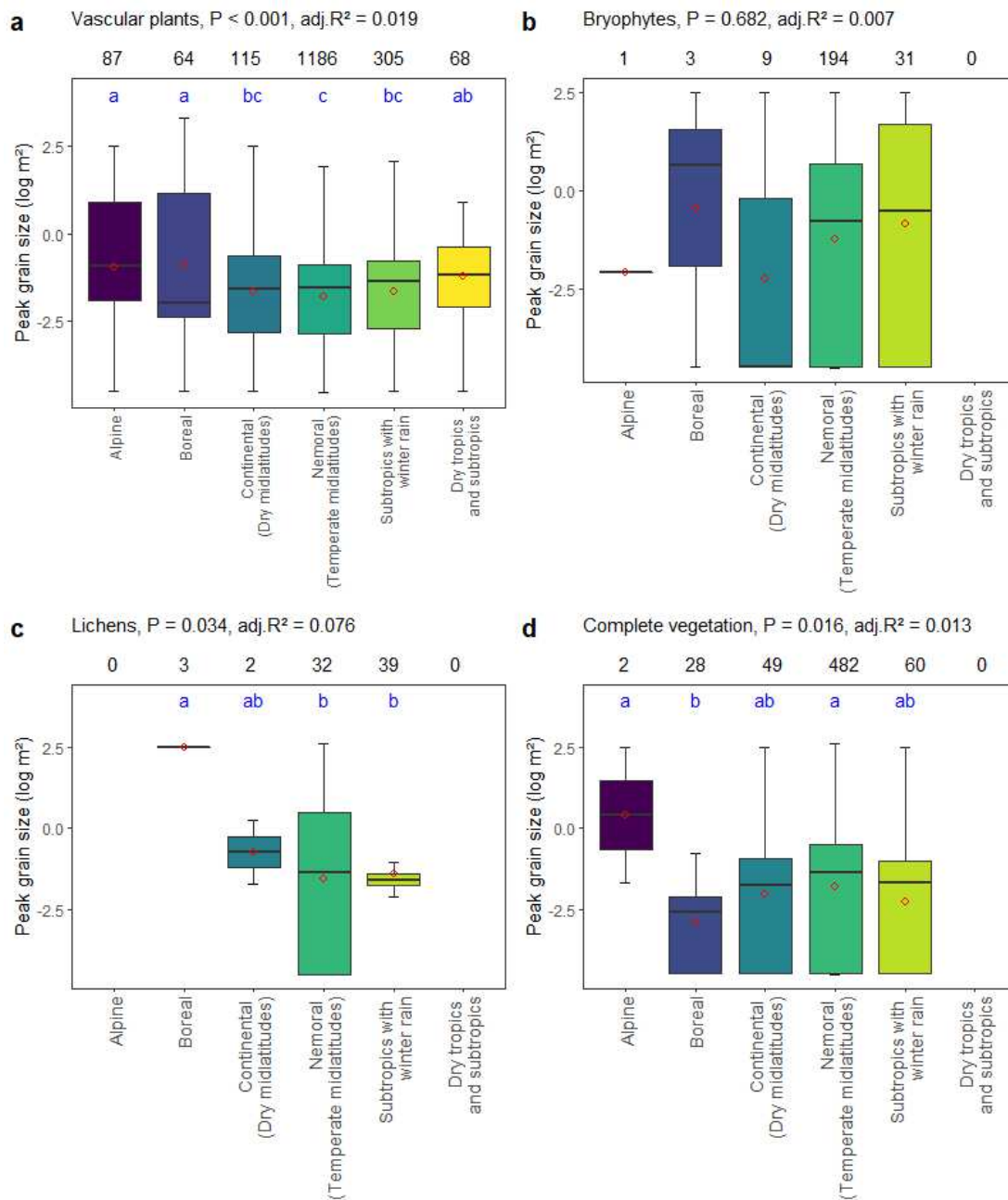


Figure S2.24. Comparison of fitted peak grain size (local grain size where the maximum local z was predicted) for a) vascular plants, b) bryophytes, c) lichens, d) complete vegetation between the six biomes considered in the study. A common blue lower-case letter between two boxes indicates homogeneous groups as tested with Tukey's post-hoc test with ANOVA ($P < 0.05$), the figures on top indicate the numbers of data. Box and whisker plots represent the median and quartiles while the red dots represent the mean values for each biome.

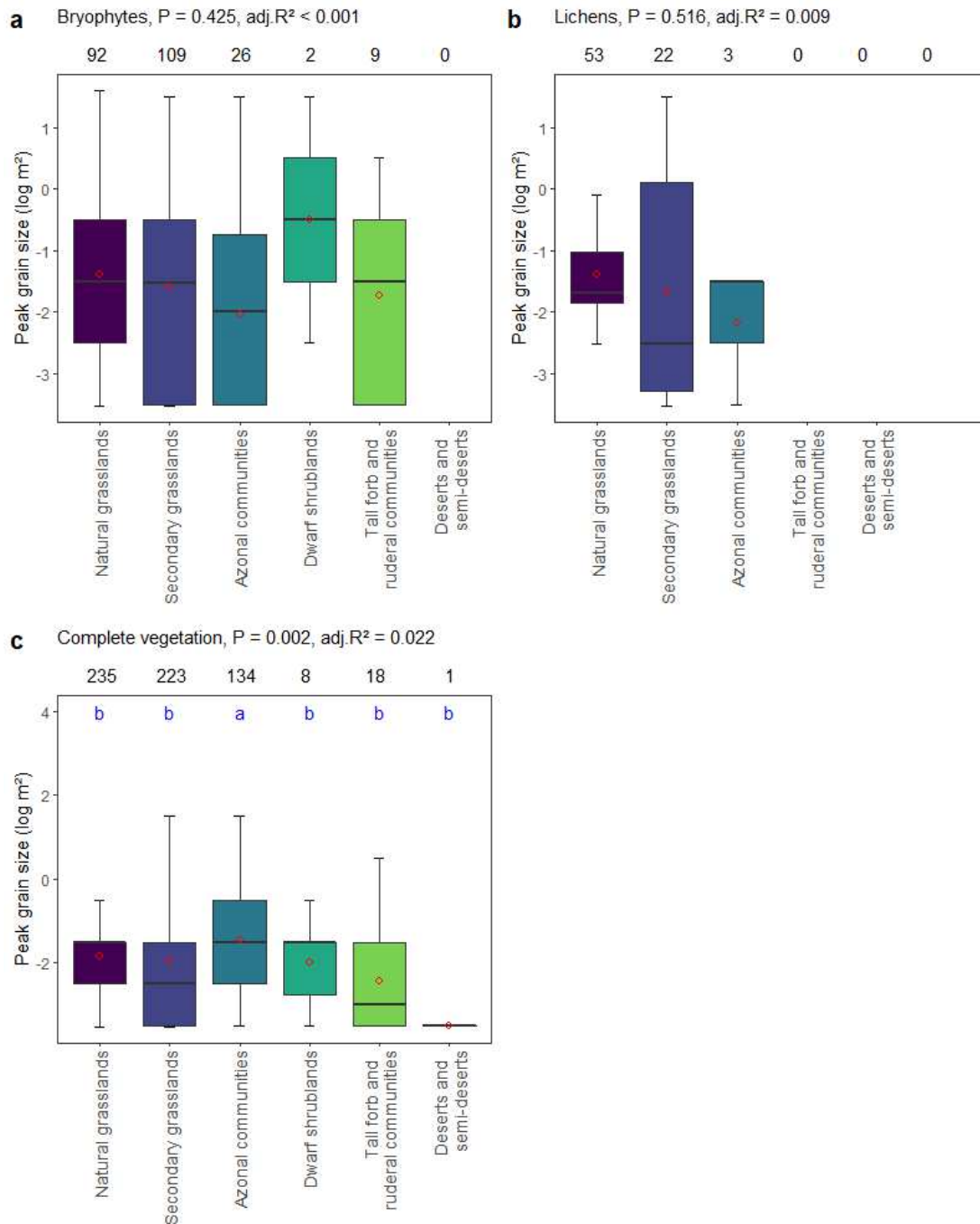


Figure S2.25. Comparison of observed peak grain size (local grain size where the maximum local z was predicted) for a) bryophytes, b) lichens, c) complete vegetation between the six vegetation types at coarse level considered in this study. A common blue lower-case letter between two boxes indicates homogeneous groups as tested with Tukey's post-hoc test with ANOVA ($p < 0.05$). Box and whisker plots represent the median and quartiles while the red dots represent the mean values for each vegetation type at coarse level.

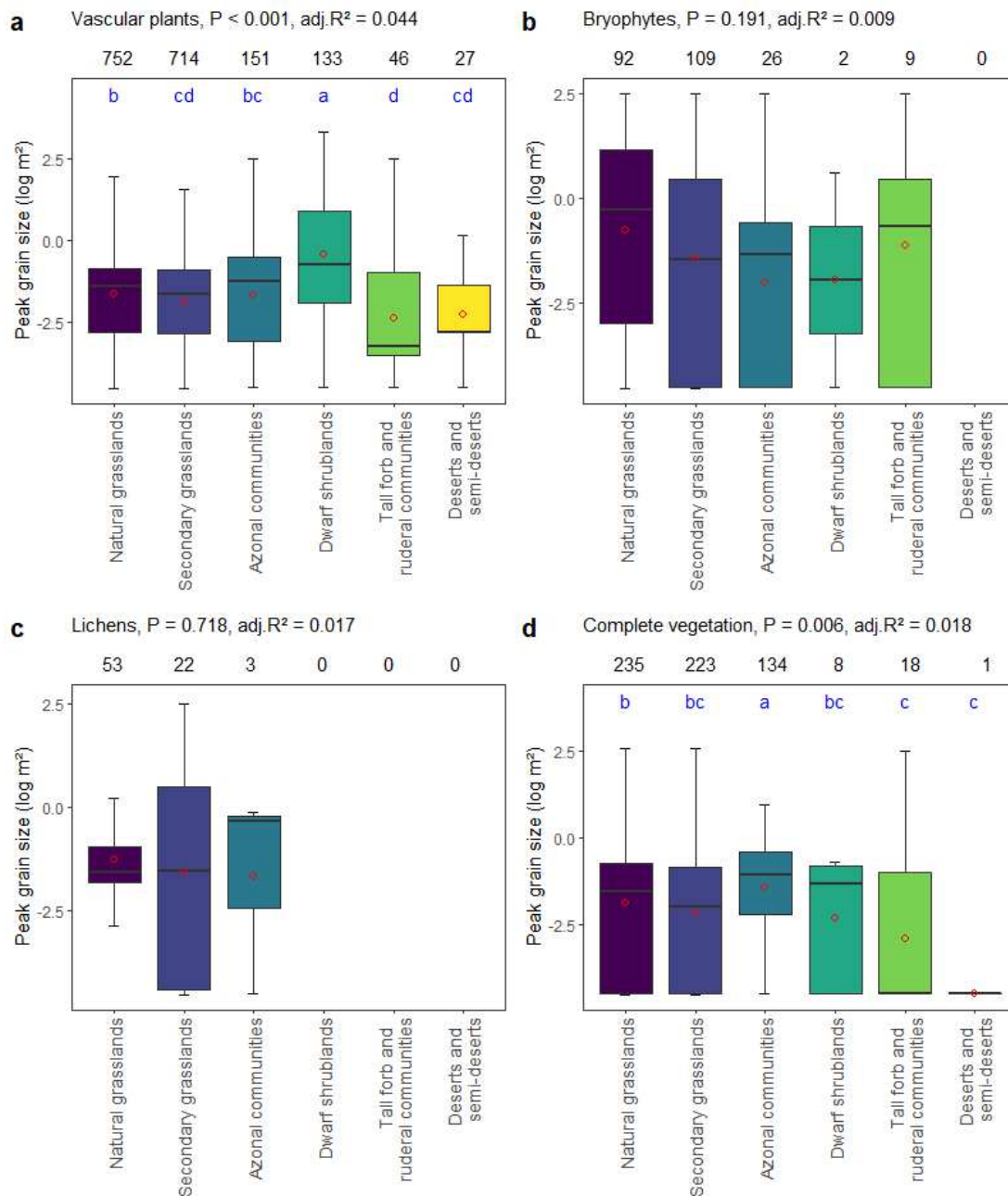


Figure S2.26. Comparison of fitted peak grain size (local grain size where the maximum local z was predicted) for a) vascular plants, b) bryophytes, c) lichens, d) complete vegetation between the six vegetation types at coarse level considered in this study. A common blue lower-case letter between two boxes indicates homogeneous groups as tested with Tukey's post-hoc test with ANOVA ($p < 0.05$). Box and whisker plots represent the median and quartiles while the red dots represent the mean values for each vegetation type at coarse level.

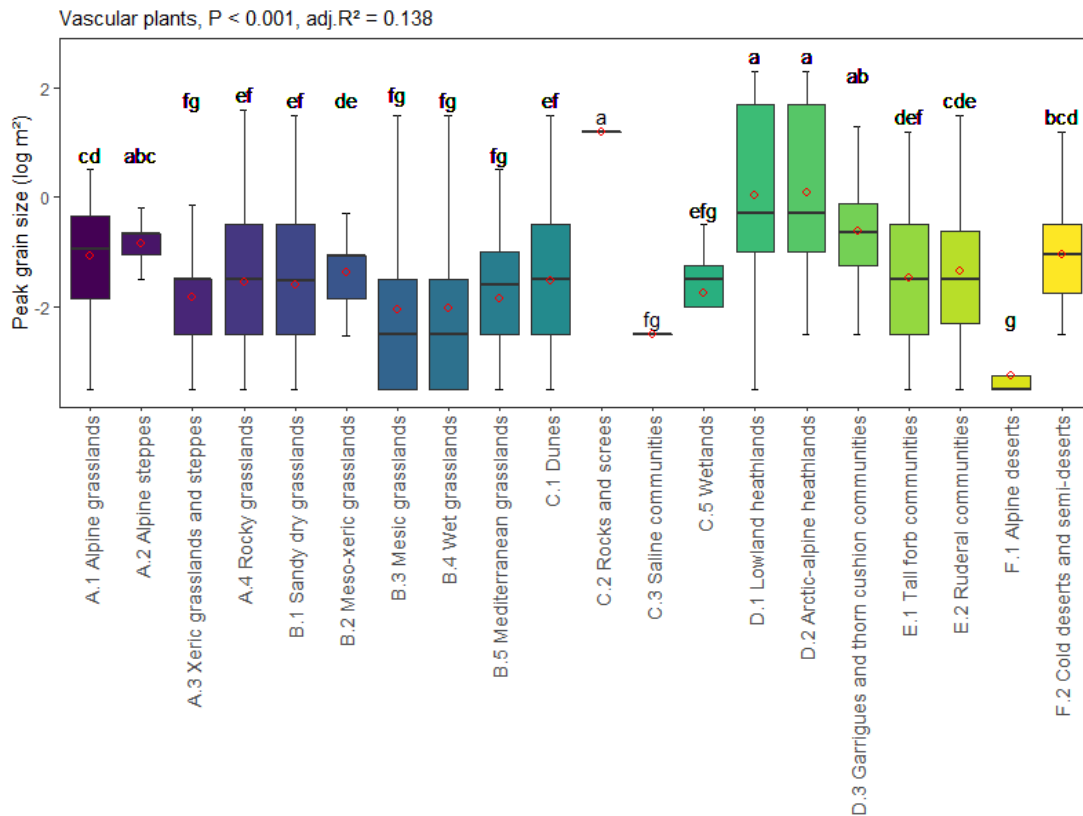


Figure S2.27. Comparison of observed peak grain size (local grain size where the maximum local z occurred) for vascular plants between the vegetation types at fine level considered in this study. A common lower-case letter between two boxes indicates homogeneous groups as tested with Tukey's post-hoc test with ANOVA ($p < .05$). Box and whisker plots represent the median and quartiles while the red dots represent the mean values for each vegetation type at fine levels.

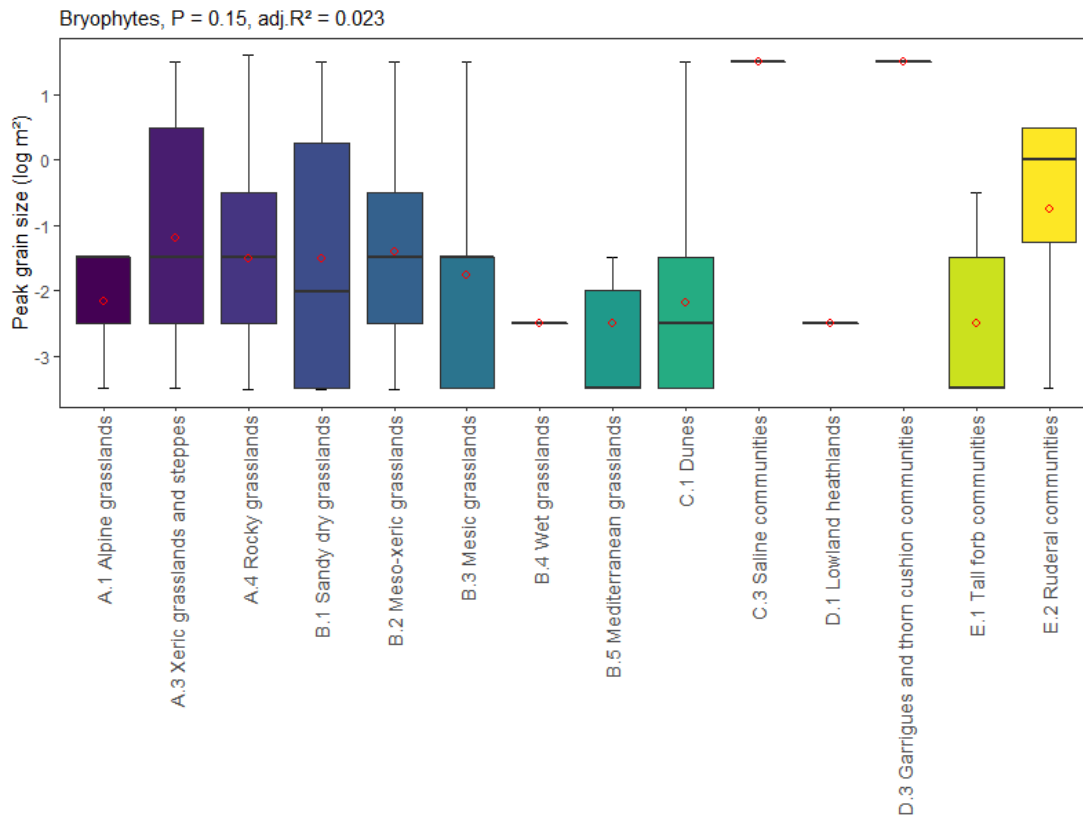


Figure S2.28. Comparison of observed peak grain size (local grain size where the maximum local z occurred) for bryophytes between the vegetation types at fine level considered in this study. Box and whisker plots represent the median and quartiles while the red dots represent the mean values for each vegetation type at fine levels.

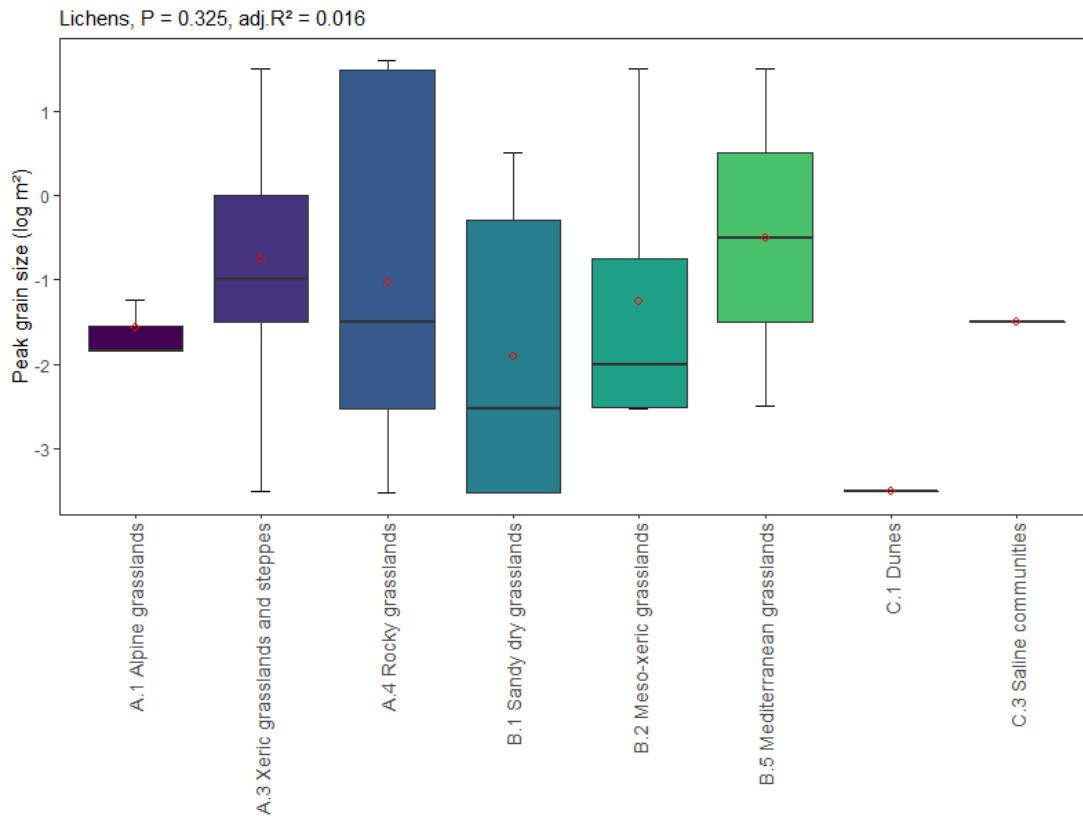


Figure S2.29. Comparison of observed peak grain size (local grain size where the maximum local z occurred) for lichens between the vegetation types at fine level considered in this study. Box-and-whisker plots represent the median and quartiles while the red dots represent the mean values for each vegetation type at fine levels.

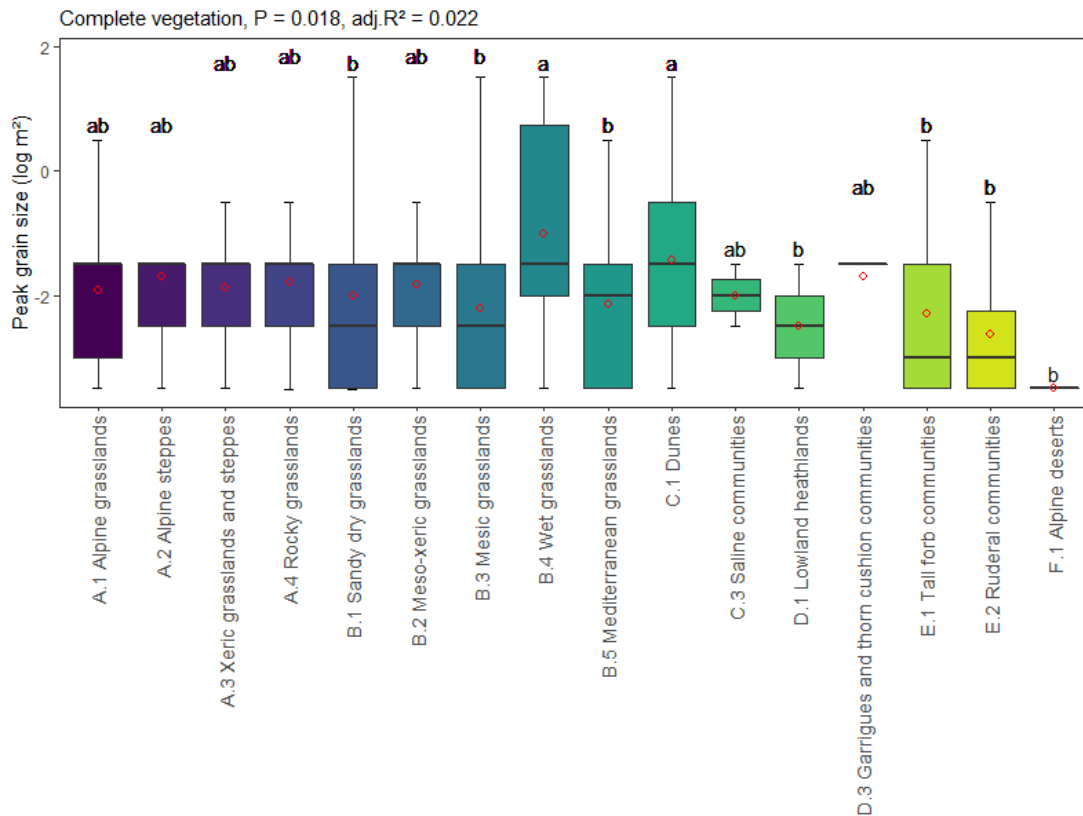


Figure S2.30. Comparison of observed peak grain size (local grain size where the maximum local z occurred) for complete vegetation between the vegetation types at fine level considered in this study. A common lower-case letter between two boxes indicates homogeneous groups as tested with Tukey's post-hoc test with ANOVA ($p < 0.05$). Box and whisker plots represent the median and quartiles while the red dots represent the mean values for each vegetation type at fine levels.

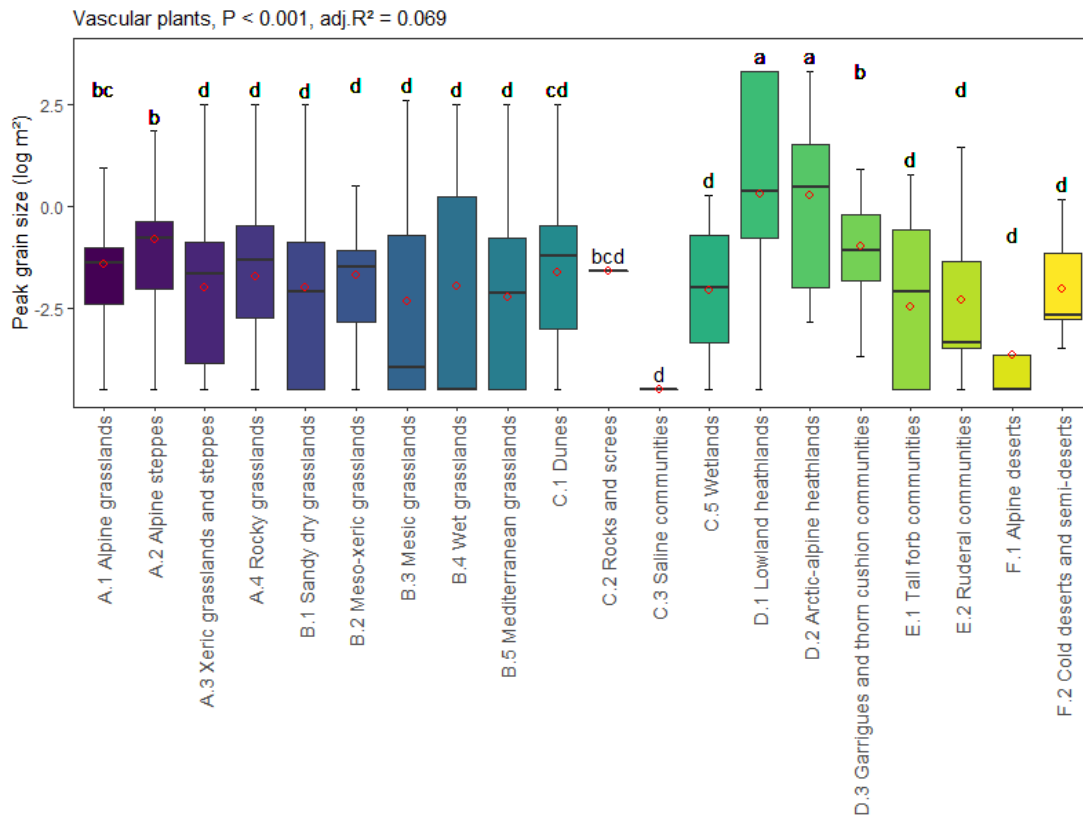


Figure S2.31. Comparison of fitted peak grain size (local grain size where the maximum local z was predicted) for vascular plants between the vegetation types at fine level considered in this study. A common lower-case letter between two boxes indicates homogeneous groups as tested with Tukey's post-hoc test with ANOVA ($p < 0.05$). Box and whisker plots represent the median and quartiles while the red dots represent the mean values for each vegetation type at fine levels.

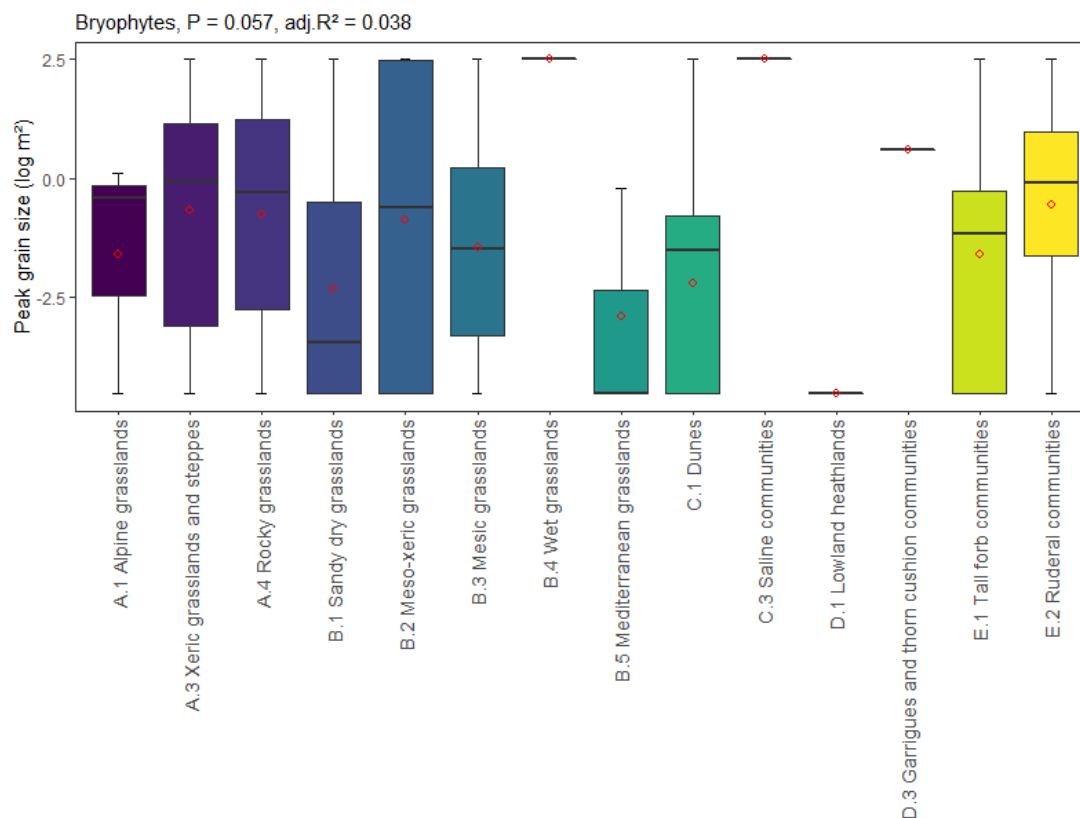


Figure S2.32. Comparison of fitted peak grain size (local grain size where the maximum local z was predicted) for bryophytes between the vegetation types at fine level considered in this study. Box and whisker plots represent the median and quartiles while the red dots represent the mean values for each vegetation type at fine levels.

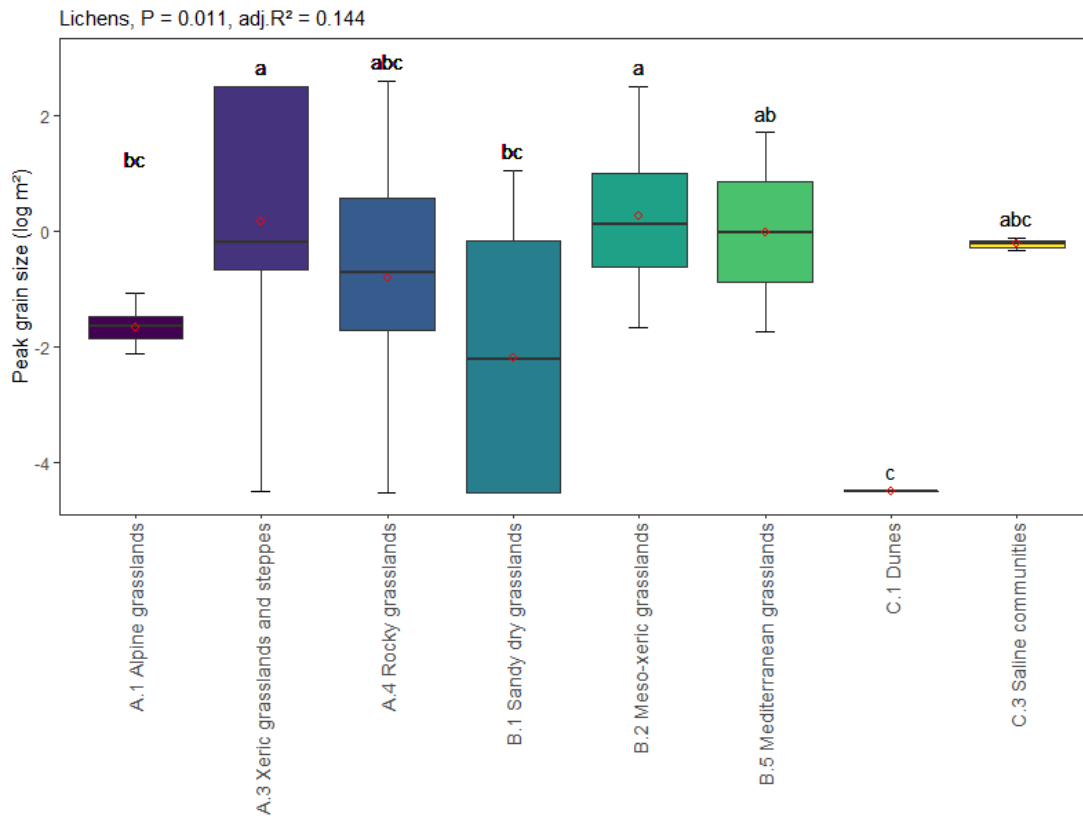


Figure S2.33. Comparison of fitted peak grain size (local grain size where the maximum local z was predicted) for lichens between the vegetation types at fine level considered in this study. A common lower-case letter between two boxes indicates homogeneous groups as tested with Tukey's post-hoc test with ANOVA ($p < 0.05$). Box and whisker plots represent the median and quartiles while the red dots represent the mean values for each vegetation type at fine levels.

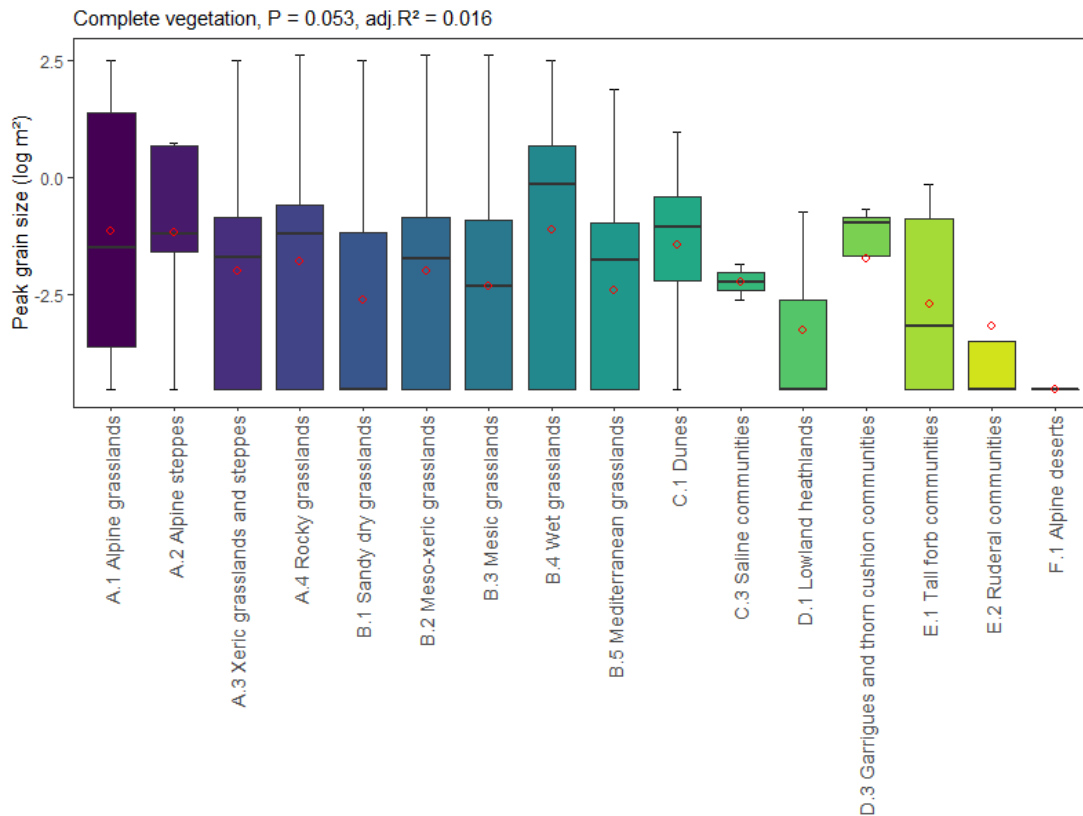


Figure S2.34. Comparison of fitted peak grain size (local grain size where the maximum local z was predicted) for complete vegetation between the vegetation types at fine level considered in this study. A common lower-case letter between two boxes indicates homogeneous groups as tested with Tukey's post-hoc test with ANOVA ($p < 0.05$). Box and whisker plots represent the median and quartiles while the red dots represent the mean values for each vegetation type at fine levels.

1
2
3
4
5
6
7
8
9
10
11
12
13
14
15
16
17
18
19
20
21
22
23
24
25
26
27
28
29
30
31
32
33
34
35
36
37
38
39
40
41
42
43
44
45
46
47
48
49
50
51
52
53
54
55
56
57
58
59
60

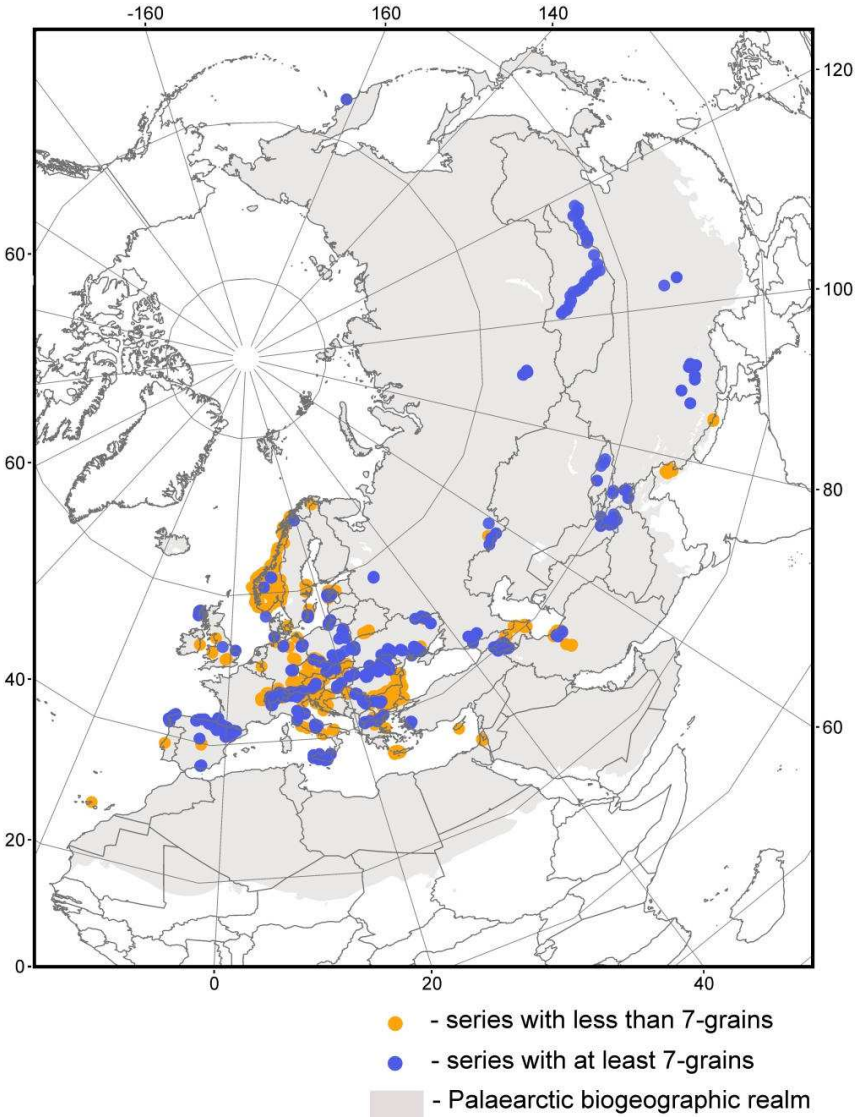
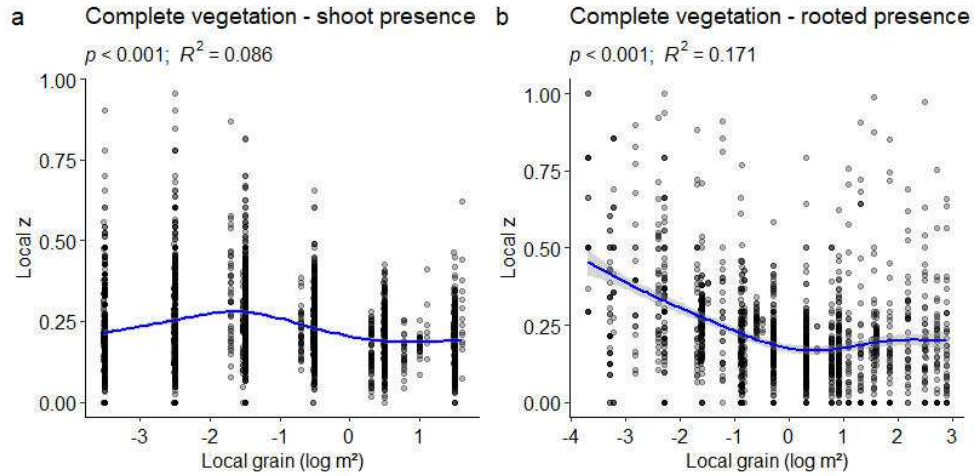


Figure 1. Spatial distribution of the 6,696 series in the Palearctic biogeographic realm that were analysed in this study.



23
24
25
26
27
28
29
30
31
32
33
34
35
36
37
38
39
40
41
42
43
44
45
46
47
48
49
50
51
52
53
54
55
56
57
58
59
60

Figure 2. Generalized additive models (GAMs) with 95% confidence intervals (pale blue) for the effect of local grain (on log scale) on local z-value for complete vegetation, in plot series using two different ways of recording species occurrence: a) shoot presence and b) rooted presence.

1
2
3
4
5
6
7
8
9
10
11
12
13
14
15
16
17
18
19
20
21
22
23
24
25
26
27
28
29
30
31
32
33
34
35
36
37
38
39
40
41
42
43
44
45
46
47
48
49
50
51
52
53
54
55
56
57
58
59
60

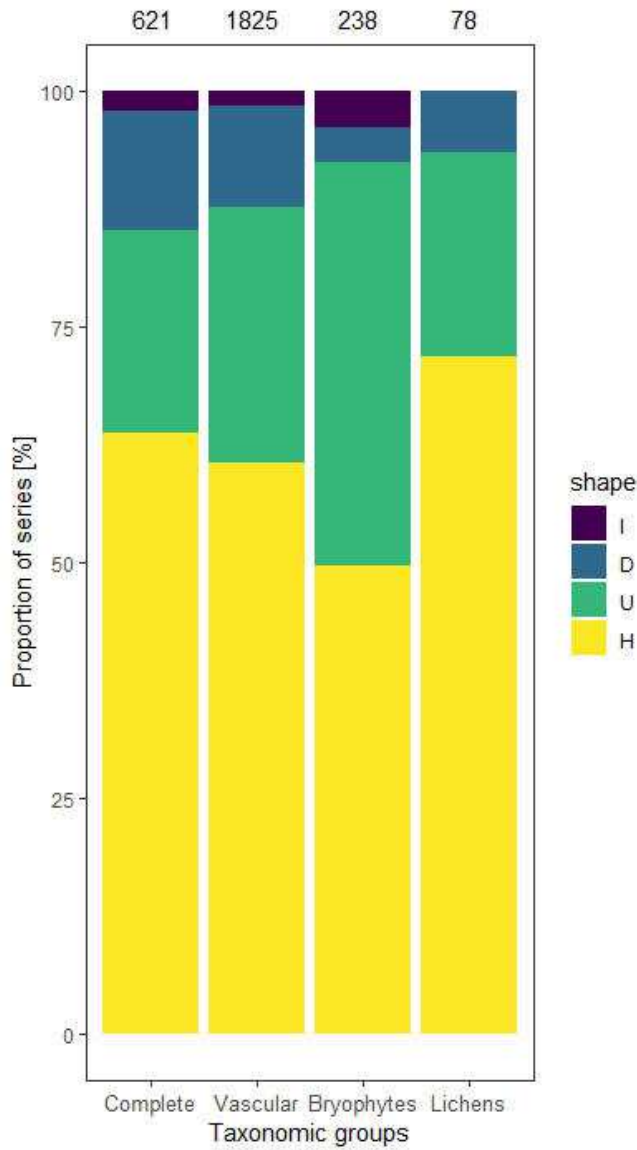


Figure 3. Comparison of the four shapes of fitted curves (hump-shaped (H), U-shaped (U), monotonic decreasing (D), and monotonic increasing (I)) for the complete vegetation and for the taxonomic groups vascular plants, bryophytes, and lichens (series with at least seven grain sizes). Values on top of bars are the number of nested-plot series analyzed.

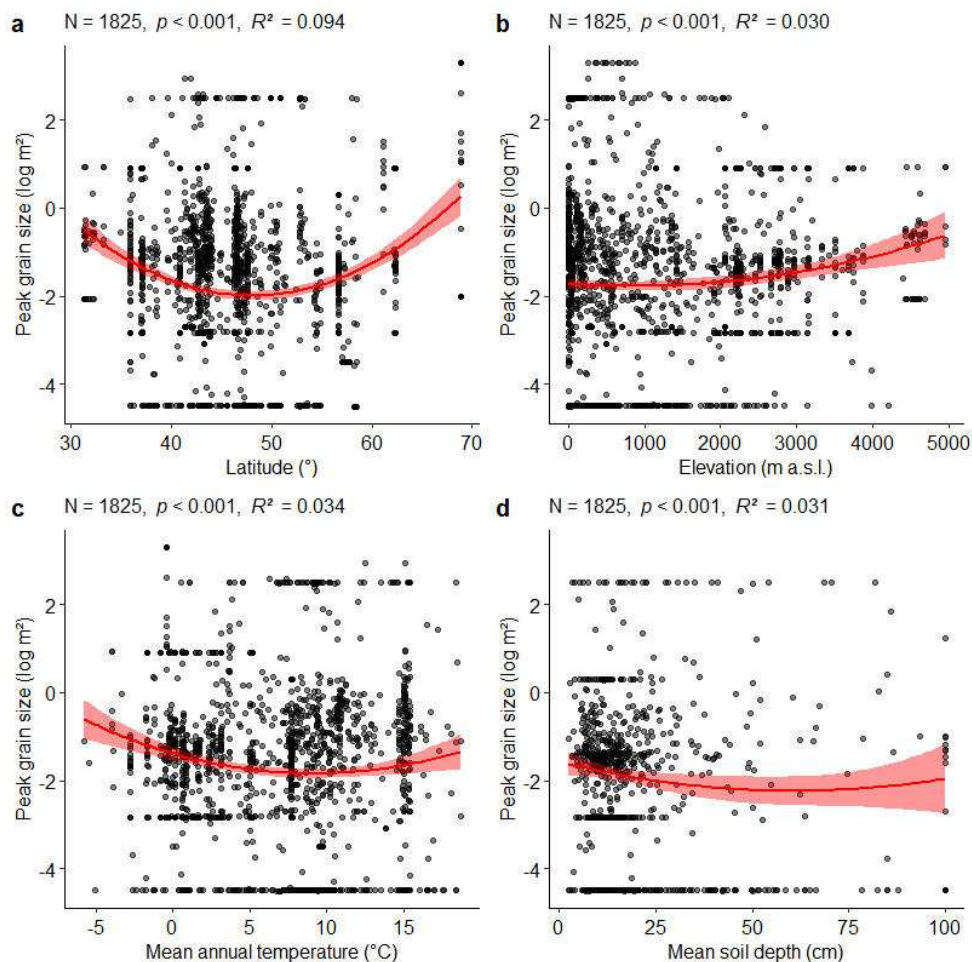


Figure 4. Differences in observed peak grain size (local grain size where the maximum local z occurred) of vascular plants depending on predictor variables. Red lines indicate quadratic relationships ($p < 0.05$) with confidence intervals.

1
2
3
4
5
6
7
8
9
10
11
12
13
14
15
16
17
18
19
20
21
22
23
24
25
26
27
28
29
30
31
32
33
34
35
36
37
38
39
40
41
42
43
44
45
46
47
48
49
50
51
52
53
54
55
56
57
58
59
60

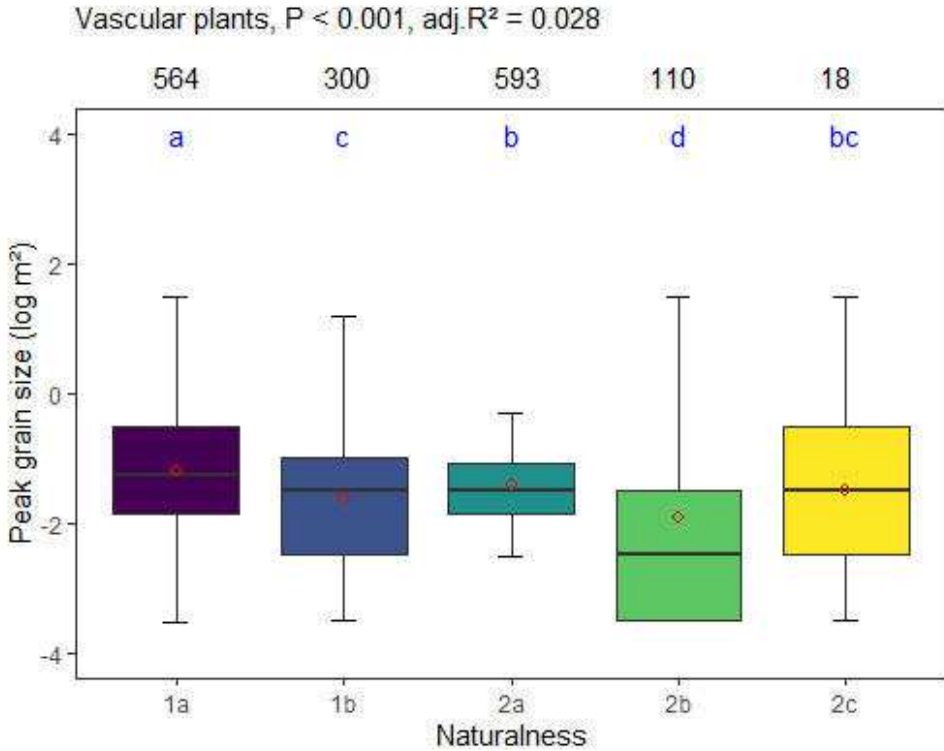


Figure 5. Differences of the observed peak grain size (local grain size where the maximum local z occurred) for vascular plants between the five levels of naturalness present in this study (no series for 1c – natural grasslands, overused): 1 – natural grasslands (1a – not managed, 1b – extensively managed); 2 – secondary grasslands (2a – semi-natural, 2b – semi-intensified, 2c – intensified) ($p < 0.001$; $R^2_{adj.} = 0.028$). Blue lowercase letters indicate homogeneous groups ($p < 0.05$) as tested with Tukey’s post-hoc test ANOVA, the figures on top indicate the numbers of data. Box and whisker plots represent the median and quartiles while the red dots represent the mean values.

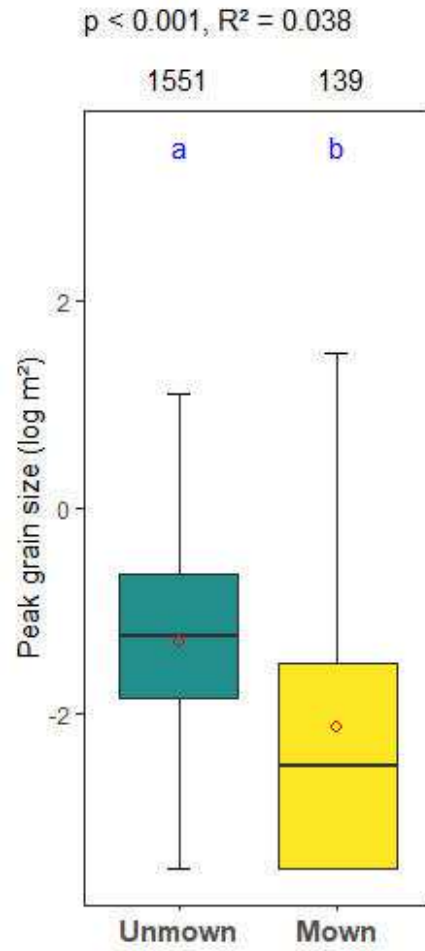


Figure 6. Effect of mowing on observed peak grain size (local grain size where the maximum local z occurred) for vascular plants ($p < 0.001$; $R^2 = 0.038$). Box and whisker plots represent the median and quartiles while the red dots represent the mean values for each management type.

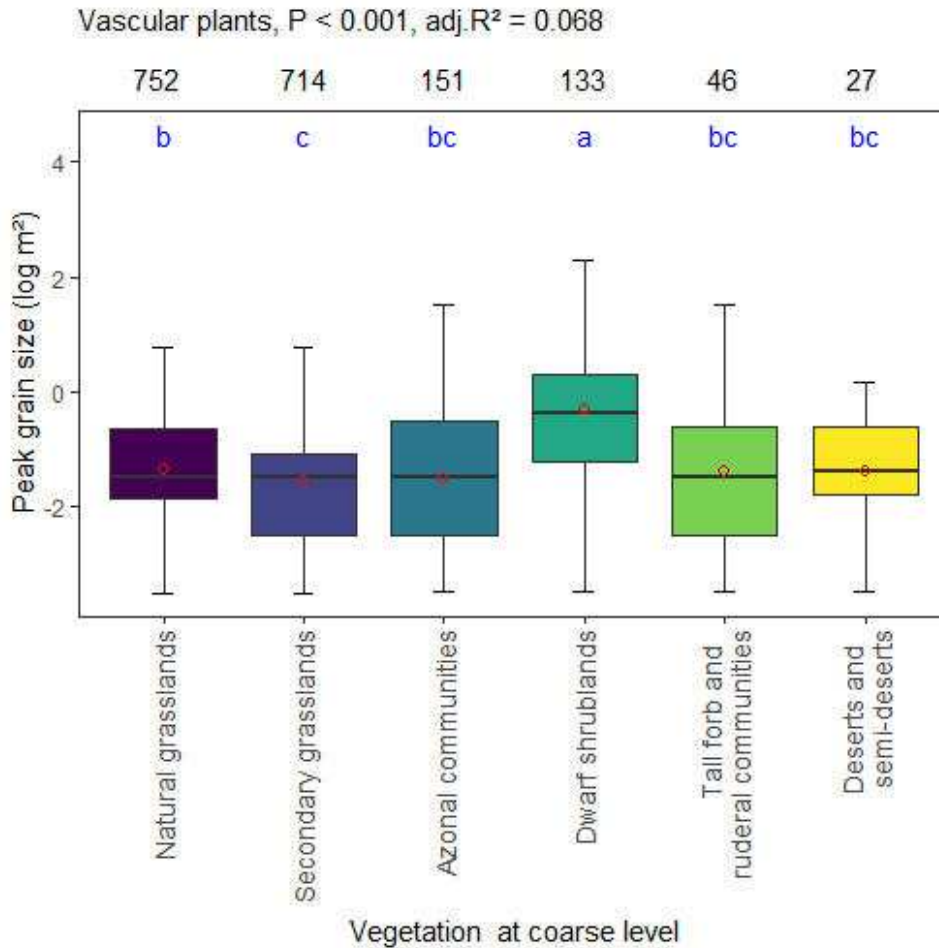


Figure 7. Differences in the observed peak grain size (local grain size where the maximum local z occurred) between the six main vegetation types for the vascular plants ($p < 0.001$, $R^2_{adj.} = 0.068$). A common blue lower-case letter between two boxes indicates homogeneous groups as tested with Tukey's post-hoc test with ANOVA ($p < 0.05$), the figures on top indicate the numbers of data. Box and whisker plots represent the median and quartiles while the red dots represent the mean values for each vegetation type at coarse level.